APOPTOSIS – A COMPARATIVE STUDY OF ITS ROLE ON THE TROPHOBLAST CELL IN NORMOTENSIVE AND HYPERTENSIVE PLACENTAL BED

ENBAVANI DORSAMY

Submitted in partial fulfillment of the requirements for the degree of

MASTER OF MEDICAL SCIENCE

In the

Department of Gynaecology and Obstetrics

Nelson R Mandela School of Medicine

University of Kwa-Zulu Natal

Durban

2006

DECLARATION

This study represents original work by the author and has not been submitted in any other form to another University. Where use was made of the work of others, it has been duly acknowledged in the text.

The research described in this dissertation was carried out in the Optics & Imaging Centre and the MRC Pregnancy Hypertension Research Unit, Nelson R Mandela School of Medicine, University of Kwa-Zulu Natal, Durban, South Africa under the supervision of Professors J Moodley and T. Naicker.

ENBAVANI DORSAMY

Dedication

For Uvan and My Mum,

The Two most important People in my Life,

This would not have been possible without your Love, Support and Encouragement

ACKNOWLEDGEMENTS

I wish to express my sincere thanks and gratitude to:

Professor J Moodley, for his supervision and constructive criticisms;

Prof T Naicker, for her excellent supervision, support, encouragement and her invaluable help with microscopy and formatting of the thesis;

Optics and Imaging Centre, Nelson R Mandela School of Medicine, where the work was carried out;

Vinogrin Dorsamy, for his assistance with image analysis and formatting of the thesis;

Mrs Tonya Esterhuizen, MRC, for help with statistical analysis of the data

To my family, especially my husband, Uvan, for his support and sacrifice of family time;

Finally, To God, for spiritual guidance to enable me to accomplish my goals.

ABSTRACT

Pregnancy complications, such as preeclampsia are associated with impaired trophoblast invasion. Although placental development depends on careful coordination of trophoblast proliferation and apoptosis, little is known about the equilibrium that exists between these two key processes that synchronise trophoblast invasion. The aim of this study was to determine whether an imbalance exists between trophoblast apoptosis (M30), and proliferation (Ki-67) in term placental beds of pre-eclamptic and normal pregnancies.

This retrospective study was conducted on true placental bed biopsies obtained from 12 normotensive and 12 hypertensive pregnant women at the Obstetric Unit of King Edward VIII Hospital, Durban, South Africa. Routine histopathology assessment of the biopsies was performed and using immunocytochemistry techniques, serial sections were immunolabelled with a Rabbit Anti-Human Ki67 antibody, monoclonal Mouse Anti-Human Cytokeratin 18 and its neo-epitope, a monoclonal M30, Cytodeath antibody.

Histologically, two populations of invasive extravillous trophoblast were identifiable within the myometrium in the normotensive group viz. interstitial and intramural trophoblast cells embedded within the spiral artery. In the preeclamptic group, the spiral arterioles did not demonstrate physiological conversion and were further compromised by a reduced lumen with endothelial vacuolation and smooth muscle hyperplasia.

The immunoexpression of anti-Ki67 for all trophoblast cell sub populations within the myometrium were non-reactive for both study groups. However, smooth muscle cells of the small caliber microvasculature signify a moderate degree of proliferation in both groups. Morphometric image analysis of the wall of the spiral artery in the normotensive group revealed a mean area of 311729 ± 51180μm^2 compared to 35795 ± 8045μm^2 and preeclamptic groups respectively ($p<0.0001$). Additionally, immunoexpression of anti-CK18 indicated intramural trophoblast invasion in the spiral artery of normotensive group was elevated compared to the pre-eclamptic group (13 ± 5% *vs* 0% respectively; $p<0.0001$). Comparative analyses of M30 distribution on corresponding serial sections were 2.5 ± 0.7% *vs* 0% in the normotensive and pre-eclamptic groups respectively ($p<0.0001$). The mean field area of the interstitial trophoblast invasion in the preeclamptic group was 2.87 ± 0.5% compared to 10.79 ± 4.2% in the normotensive group (0.000002). However the serial sections stained with M30 showed elevation of apoptotic invasive interstial trophoblast in the preeclamptic group compared to the normotensive group (1.9 ± 8% *vs* 0.8 ± 0.3%; $p=0.001$).

In conclusion, the expression pattern of Ki67 antigen in this study suggests that differentiation of invasive trophoblasts at term is coordinated with exit from the cell cycle. Increased apoptosis of interstitial trophoblast cells may be implicated in the aetiology of shallow invasion of trophoblasts in pre-eclampsia. The balance between trophoblast apoptosis and proliferation, in favour of increased apoptosis may represent a mechanism to control normal trophoblast invasion.

TABLE OF CONTENTS

	Page
DECLARATION	ii
DEDICATION	iii
ACKNOWLEDGEMENTS	iv
ABSTRACT	v
LIST OF ABBREVIATIONS	ix
LIST OF FIGURES	xi
LIST OF TABLES	xv
CHAPTER ONE: LITERATURE REVIEW	
1.0 Apoptosis	1
1.1 Mechanism of Apoptosis	4
1.1.1 Extrinsic factors	7
1.1.1.1 Death Receptors	7
1.1.1.2 Signaling by CD95/Fas	7
1.1.1.3 Induction of Apoptosis by TRAIL	11
1.1.2 Intrinsic factors	11
1.1.2.1 Role of Mitochondria in Apoptosis	11
1.1.2.2 Caspases	14
2.0 Hypertension in Pregnancy	17
2.1 Preeclampsia	18
2.1.1 Epidemiology in Preeclampsia	19
2.1.2 Risk factors for Preeclampsia	20
2.1.3 Genetic Risk Factors	20
2.1.4 Pathophysiology of Preeclampsia	21
2.2 Apoptosis in Preeclampsia	29
3.0 Normal Cell Cycle	30
3.1 Ki67	32
3.2 Cytokeratin 18	34
4.0 Summation and Aims	37

CHAPTER TWO: MATERIALS AND METHODS 38
2.1 Ethical Approval 38
2.2 Materials 38
2.3 Histology Preparation 39
2.3.1 Routine Staining techniques 39
2.4 Tissue Processing for Immunohistochemical Studies 43
2.4.1 Mouse anti-human cytokeratin antibody 43
2.4.1.1 Immunostaining schedule for anti-MNF 116 44
2.4.2 Immunohistochemical procedure for anti-Ki67 antibody 46
2.4.2.1 Rabbit Anti-Human Ki67 antibody 46
2.4.2.2 Immunostaining schedule for anti-Ki67 antibody 46
2.4.3 Cytokeratin 18 antibody isolation and specificity 49
2.4.3.1 Immunostaining schedule for anti-Cytokeratin 18 49
2.4.4 Clone M30, Cytodeath mouse IgG_{2b} antibody isolation and 51
2.4.4.1 Immunostaining schedule for anti-M30 antibody 51
2.4.5 Controls 52
2.5 Image analysis 54
2.5.1 Measurement Strategy 54

CHAPTER THREE: RESULTS 60
3.1 Patient Population 60
3.1.1 Demographics of Normotensive Group 60
3.1.2 Demographics of Preeclamptic Group 60
3.2 Histology of True Placental Bed Biopsies 63
3.2.1 Normotensive Group 63
3.2.2 Preeclamptic Group 70
3.3 CK18 and Ki67 Immunoreactivity 75
3.4 CK18 and M30 Immunoreactivity 86
3.4.1 Image analysis of anti-CK18 relative to M30 86

CHAPTER FOUR: DISCUSSION 97

REFERENCES 107

APPENDIX 127

LIST OF ABBREVIATIONS

AIF	Apoptotic Inducing Factor
Apaf 1	Apoptotic Protease Activating Factor 1
Bak	Bcl-2 antagonist/killer
Bax	BCL-2-Associated X Protein
BCL2	Apoptotic Proteins
BCL-XL	Anti-Apoptotic Proteins
Bid	Pro-Apoptotic Proteins
BP	Blood Pressure
BSA	Bovine Serum Albumin
Caspase	Cysteine Aspartate-Specific Proteases
CD95	Fatty Acid Synthetase Ligand
CK18	Cytokeratin 18
DAB	Diaminobenzidine
DBP	Diastolic Blood Pressure
DD	Death Domain
DED	Death Effector Domain
DISC	Death Inducing Signaling Complex
DNA	Deoxyribo-nucleic acid
DPX	1,3,-Diethyl-8-Phenylxanthine
DR	Death Receptor
DR 4	Death Receptor 4
DR 5	Death Receptor 5
EVG	Elastic Von Gieson
FADD	Fas- Associated Death Domain
Fas	Fatty Acid Synthetase
FasL	FAS associated Ligand
FLICE	Death Proteases - Caspase 8

G1-phase	Growth Phase 1
G2-phase	Growth Phase 2
G0-phase	Growth Phase 0
H&E	Haemotoxylin and Eosin
H_2O_2	Hydrogen Peroxide
HCL	Hydrochloric Acid
HRP-STREPAVIDIN	Horse-radish Peroxidase Strepavidin
Ki67	Proliferation Protein
M30	Antibody reacts with the CK18 Neo-epitope
MNF 116	Antibody that detects Cytokeratins
PAS	Periodic Acid Schiff
PBS	Phosphate Buffered Saline
PE	Preeclampsia
PT PORE	Permeability Transition Pore
S-phase	Synthesis phase
TBS	Tris Buffered Saline
TBSTT	Tris Buffered Saline- Tween/Triton
TNFα	Tumour Necrosis Factor alpha
TRADD	TNFRSF1A-associated via death domain
TRAIL	Tumour Necrosis Factorα Related Apoptosis Inducing Ligand
TRAIL-R1	Tumour Necrosis Factorα Related Apoptosis Inducing Ligand –Receptor 1
TRAIL-R2	Tumour Necrosis Factorα Related Apoptosis Inducing Ligand –Receptor 2
TRIS	Tris-[hydroxymethyl]-aminomethane
TUNEL	TerminI Uridine Triphosphate Nick-end Labelling

LIST OF FIGURES

		Page
Fig 1 :	Real-time microscopy images of trophoblast cells undergoing apoptosis in-vitro	3
Fig 2 :	Diagrammatic representation of the apoptotic pathways	5
Fig 3 :	Schematic illustration of intrinsic and extrinsic stimuli that induce apoptosis	6
Fig 4 :	Activation of apoptosis through CD95 / Fas	9
Fig 5 :	TNF receptor signaling	10
Fig 6 :	Role of Mitochondria in Apoptosis	13
Fig 7 :	Caspase Activation	15
Fig 8 :	Schematic representations of the intracellular components of the caspase cascade	16
Fig 9 :	Pathophysiology of Preeclampsia	24
Fig 10 :	Remodeling of Spiral Artery by Trophoblast	28
Fig 11 :	Cell cycle	31
Fig 12a-f :	Gallery of images of selected field for spiral artery analysis	58
Fig 13 :	Micrograph of spiral artery depicting segmented mask image overlayed on trophoblast cells in the myometrium	59
Fig 14 :	Micrograph showing physiologically converted myometrial spiral artery stained with H & E	65
Fig 15 :	Micrograph showing physiologically converted myometrial spiral artery stained with PAS	65
Fig 16 :	Micrograph showing physiologically converted myometrial spiral artery stained with EVG	66
Fig 17 :	Micrograph immunostained with anti-MNF 116 showing total physiological conversion of spiral artery	66
Fig 18 :	Micrograph illustrating cytoplasmic extensions	67

Fig 19 :	Micrograph immunostained with anti-MNF 116 depicting interstitial invasion of myometrium	67
Fig 20 :	Micrograph immunostained with anti-MNF 116 showing myometrial interstitial invasion by trophoblast cells.	68
Fig 21 :	High power micrograph of multinucleated giant cell within myometrium immunostained with anti-MNF 116.	68
Fig 22 :	Micrograph immunostained with anti-MNF 116 illustrating large arcuate artery occurring in preeclamptic group	69
Fig 23 :	Micrograph immunostained with anti-MNF 116 depicting cross reactivity of primary antibody	69
Fig 24 :	H & E stained section showing cluster of three myometrial spiral artery occurring within preeclamptic group	71
Fig 25 :	Micrograph illustrating small lumen of artery, vacuolation and perivascular aggregation of polymorphonuclear lymphocytes	71
Fig 26:	PAS stained section from pre-eclamptic group showing medial hyperplasia	72
Fig 27 :	EVG stained section of spiral artery in pre-eclamptic group	72
Fig 28 :	Micrograph immunostained with anti-MNF 116 showing perivascular localization of trophoblast cell	73
Fig 29 :	Micrograph immunostained with anti-MNF 116 from preeclamptic showing spiral artery with hyperplasia	73
Fig 30 :	Micrograph immunostained with anti-MNF 116 showing basal arteries	74
Fig 31 :	Micrograph immunostained with anti-MNF 116 illustrating myometrial interstitial trophoblast cells	74
Fig 32:	Physiologically converted spiral artery from placental bed of normotensive patient immunostained with anti-CK18	78
Fig 33 :	Serial section of Fig 32 immunostained with Ki67	78

Fig 34 :	Spiral artery with partial physiological conversion immunostained with anti-CK18.	79
Fig 35 :	Serial section of Figure 34 illustrating non-reactivity of trophoblast cells in spiral artery to anti-Ki67	79
Fig 36:	Cytokeratin positive section illustrating portion of physiologically converted spiral artery with Lumen	80
Fig 37 :	Serial section of Figure 36 illustrating non-reactivity of endovascular trophoblast immunostained for Ki67.	80
Fig 38 :	Cytokeratin positive section of non-physiologically converted artery from hypertensive patient	81
Fig 39 :	Deeper serial section of Figure 38 illustrating non-reactivity of anti-Ki67 within nonconverted spiral artery	81
Fig 40 :	Clusters of small spiral arteries immunostained with CK18. Interstitial trophoblast cells	82
Fig 41 :	Serial section of Figure 40 illustrating very mild reactivity of smooth muscle cells of spiral artery to anti-Ki67	82
Fig 42:	Section immunostained with anti-CK 18.	83
Fig 43:	Serial section of Figure 42 immunostained with anti-Ki67	83
Fig 44 :	Micrograph of myometrium immunostained with anti-CK 18	84
Fig 45 :	Serial section of Figure 44 showing non-reactive giant cells with moderate Ki67 immunoreactivity	84
Fig 46 :	Method control for CK18	85
Fig 47:	Method control for Ki67	85
Fig 48 :	Micrograph illustrating CK18 immunoreactivity within trophoblast cells	89
Fig 49 :	Serial section of Figure 48 immunostained with anti-M30	89
Fig 50 :	Micrograph of cross sections through loops of spiral arteries.	90
Fig 51 :	Mild to moderate immunoreaction product within trophoblast cells	90

LIST OF TABLES

			Page
Table I	:	Procedure for H & E staining	40
Table II	:	Procedure for PAS staining	41
Table III	:	Procedure for von Gieson elastic staining	42
Table IV	:	Procedure for immunohistochemical localisation of anti-MNF 116	45
Table V	:	Procedure for immunohistochemical localisation of anti-Ki67 antibody	48
Table VI	:	Procedure for immunohistochemical localisation of Cytokeratin 18 antibody	50
Table VII	:	Procedure for immunohistochemical localisation of M30 antibody	53
Table VIII	:	Steps formulated in the macro utilised for image analysis of antibody distribution	57
Table IX	:	Clinical Classification of Two Groups of Patients in the study	62
Table X	:	Cytokeratin 18 *vs* Ki67 Immunoreactivity within placental bed of normotensive and hypertensive pregnant women	77
Table XI	:	Cytokeratin 18 *vs* M30 Immunoreactivity within placental bed of normotensive and hypertensive pregnant women	88
Table XII:		Mean area of spiral artery parameters in placental bed biopsies	95
Table XIII:		Image analysis of CK 18 *vs* M30 immunoexpression	96

Fig 52 :	Myometrial interstitial trophoblast cells immunoreactive to anti-CK18 from the normotensive group	91
Fig 53:	Serial section of Fig 52 depicting myometrium immunostained with anti-M30	91
Fig 54:	Micrograph of non physiologically converted spiral artery	92
Fig 55 :	Section of non-physiologically converted spiral artery immunostained for anti-M30.	92
Fig 56 :	Micrograph illustrating interstitial trophoblast population immunoreactivity CK 18 from the preeclamptic group	93
Fig 57 :	Serial section of Figure 56 illustrating interstitial trophoblast and giant cell within myometrium	93
Fig 58:	Method control for M30	94
Fig 59:	Histogram depicting area occupied by spiral artery, lumen and arterial wall	95
Fig 60:	Histogram illustrating anti-CK and M30 immunoreactivity within interstitiitial trophoblast in both study groups.	96

CHAPTER 1

INTRODUCTION

1.0 Apoptosis

The term apoptosis comes from the ancient Greek word meaning "*the falling of petals from a flower or of leaves from a tree in autumn*". Apoptosis is an evolutionarily conserved, genetically regulated active process characterised by profound distinct changes in the cellular architecture leading to self destruction of cells (Kerr *et al.*, 1972).

It is the process of programmed cell death or cell suicide and is a normal component of the development and health of multicellular organisms (Kerr *et al.*, 1972). Cells undergo apoptosis as a form of creating a balance between the withdrawal of positive signals needed for continued cell survival and the receipt of negative signals threatening the cell.

There are two ways in which this process occurs:

a. death by injury - as can be seen in cases of trauma and mechanical damage.

b. death by "suicide" – a process in which cells play an active role in their own death (Kerr *et al.*, 1972).

A number of distinctive biochemical and morphological alterations occur within the cell undergoing apoptosis.

In trophoblast cells, apoptosis occurs throughout pregnancy and is an essential counterbalance to cellular proliferation. A family of proteins known as caspases are activated to cleave cellular substrates required for the normal functioning of the cells and nuclear proteins (Strasser *et al.*, 2000).

This causes morphological changes to occur in the cell, as is depicted by time-lapse microscopy images of a trophoblast cell undergoing apoptosis (Fig. 1A-D). Following the cleavage of lamins and actin filaments, the cytoplasm shrinks (Fig 1A). This is followed by nuclear condensation due to the breakdown of chromatin and nuclear structural proteins, the nuclei take on a "horse-shoe" like appearance (Fig 1B). Cells continue to shrink, packaging themselves into a form that allows for easy clearance by macrophages (Fig 1C). Apoptotic cells often undergo plasma membrane changes that trigger the macrophage response. One such change is the translocation of phosphatidylserine from the inner membrane of the cell to the outer surface. Blebbing of the membrane may be observed (Fig 1D) often towards the end of the apoptotic cycle. Small vesicles called apoptotic bodies may also sometimes be noted (Fig 1D).

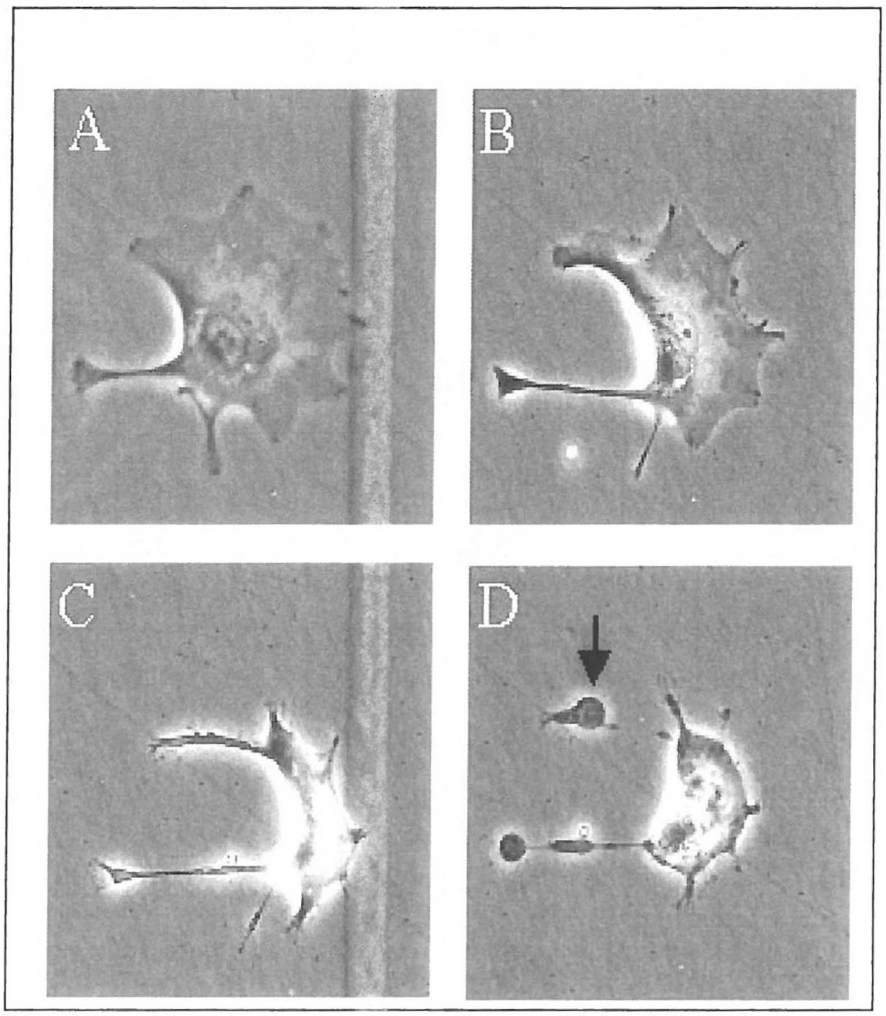

Fig 1: Real-time microscopy images of trophoblast cells undergoing apoptosis in-vitro

A: Cytoplasm shrinkage B: Nuclear condensation

C: Cell Shrinkage D: Presence of apoptotic bodies

(Reproductive and Cardiovascular Disease Research Group, 2005)

1.1 Mechanisms of Apoptosis

In recent years, the molecular machinery responsible for apoptosis has been elucidated revealing a family of intracellular proteases which are directly or indirectly responsible for the morphological and biochemical changes that characterise this phenomenon (Barret *et al.*, 2001; Reed *et al.*, 2000).

There are two major pathways that induce apoptosis (Fig 2):

(a) extrinsic pathway

(b) intrinsic mitochondrial pathway (Strasser *et al.*,2000)

Induction of apoptosis may occur by external or internal stimuli. The sensitivity of cells to these stimuli may vary depending on a number of factors such as the expression of pro- and anti-apoptotic proteins, the severity of the stimulus and the stage of the cell cycle. Some of the major stimuli that can induce apoptosis include (Fig 3):

a) Binding of death inducing ligands to cell surface receptors (1).

b) Cellular stress such as exposure to radiation (2) or chemicals

c) Viral infection (3) initiates apoptosis via intrinsic signals.

d) Cytotoxic T-lymphocytes induction by granzyme in the presence of damaged or virus infected cells (4).

e) Growth factor deprivation or oxidative stress. Apoptosis initiated by intrinsic signals generally involves the mitochondria (5).

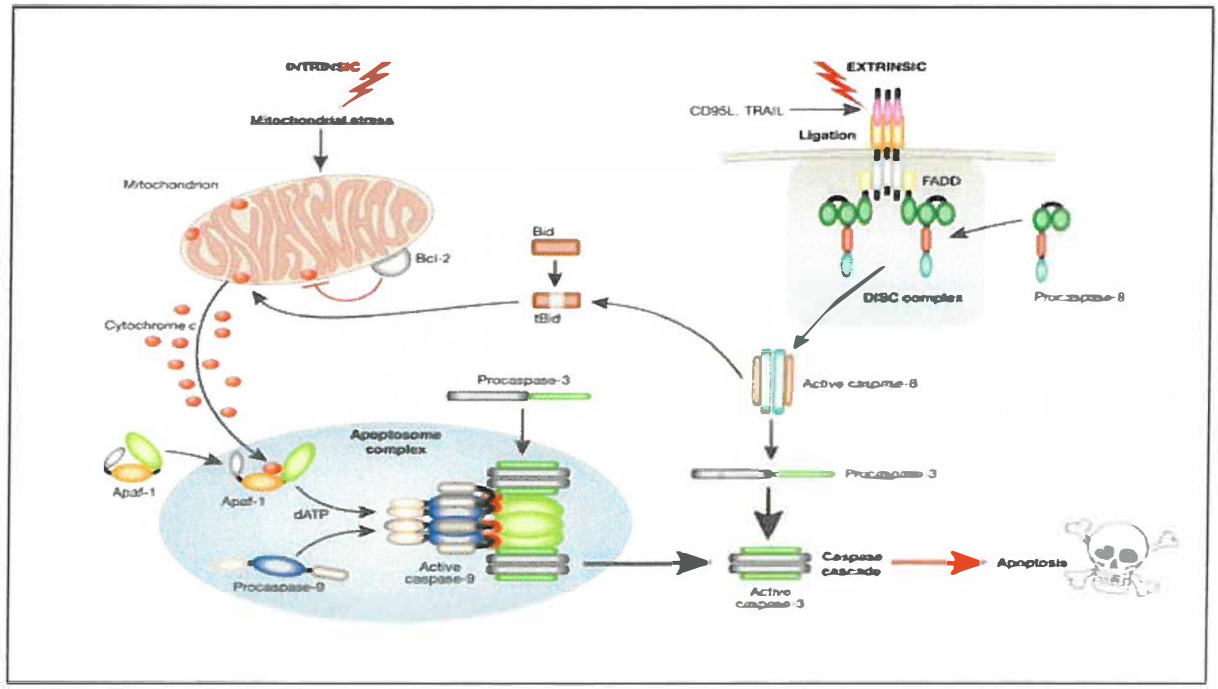

Fig 2: Two major apoptotic pathways are illustrated: intrinsic and extrinsic activated via death receptor activation and the other by stress-inducing stimuli, respectively. Triggering of cell surface death receptors of the tumour necrosis factor (TNF) receptor superfamily (CD95 and TNF-related apoptosis-inducing ligand (TRAIL)-R1/-R2), results in rapid activation of the initiator caspase 8 after its recruitment to a trimerised receptor-ligand complex (DISC) through the adaptor molecule Fas-associated death domain protein (FADD). In the intrinsic pathway, stress-induced apoptosis results in perturbation of mitochondria and the ensuing release cytochrome *c* from the inter-mitochondrial membrane space. The release of cytochrome *c* is regulated in part by Bcl2 family members, with anti-apoptotic (Bcl2/ Bcl-X_L/Mcl1) and pro-apoptotic (Bax, Bak and tBid) members inhibiting or promoting the release, respectively. Cytochrome *c* then binds to apoptotic protease-activating factor 1 (Apaf1), resulting in the formation of the Apaf1–caspase 9 apoptosome complex and activation of the initiator caspase 9. This then activates the effector caspases 3, 6 and 7, which are responsible for the cleavage of important cellular substrates resulting in the classical biochemical and morphological changes associated with the apoptotic phenotype (Adams, 2003; Danial & Korsmeyer, 2004).

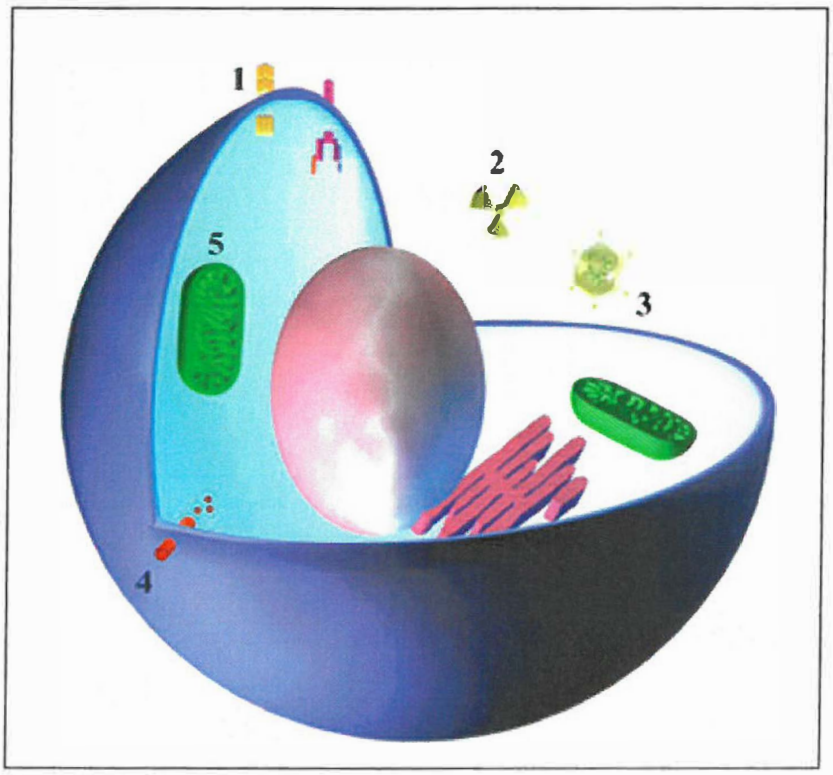

Fig 3: Schematic illustration of intrinsic and extrinsic stimuli that induce apoptosis (Reproductive and Cardiovascular Disease Research Group, 2005):

1 Binding of death inducing ligands to cell surface receptors

2 Cellular stress such as exposure to radiation or chemicals

3 Viral infection initiates apoptosis via intrinsic signals.

4 Cytotoxic T-lymphocytes induction by granzyme in the presence of damaged or virus infected cells.

5 Growth factor deprivation or oxidative stress, apoptosis initiated by intrinsic signals generally involves the mitochondria.

1.1.1. Extrinsic Factors

1.1.1.1 Death receptors

Death receptors (DR) are cell surface receptors that belong to the tumor necrosis factor gene (TNF) family. These receptors signal specific ligands to induce apoptosis. This mechanism of apoptosis induction is very rapid as the caspase cascade is activated within seconds of ligand binding (Krammer *et al*, 2000). The death receptors are CD95 (or Fas), TNF receptor-1 (TNFR1) and the TNF-related apoptosis inducing ligand (TRAIL) receptors DR4 and DR5 (Ashkenazi *et al*., 2002).

1.1.1.2. Signaling by CD95 / Fas

The ligand for CD95 (CD95L or FasL) is a trimer that on association with the receptor promotes receptor-trimerisation which in turn results in intracellular clustering of parts of the receptor called death domains (DD) (Fig 4) (Krammer *et al.*, 2000). This allows an adapter protein called Fas-associated death domain (FADD) to associate with the receptor through an interaction between homologous death domains on the receptor and on FADD. FADD also contains a death effector domain (DED).

The death effector domain allows binding of pro-caspase 8 to the CD95-FADD complex. Pro-caspase 8 (also known as FLICE) associates with FADD through its own death effector domain, and upon recruitment by FADD is immediately cleaved to produce caspase 8.

This then triggers activation of execution caspases such as caspase 9 that cleave multiple cellular death substrates resulting in inevitable apoptosis (Krammer *et al.*, 2000).

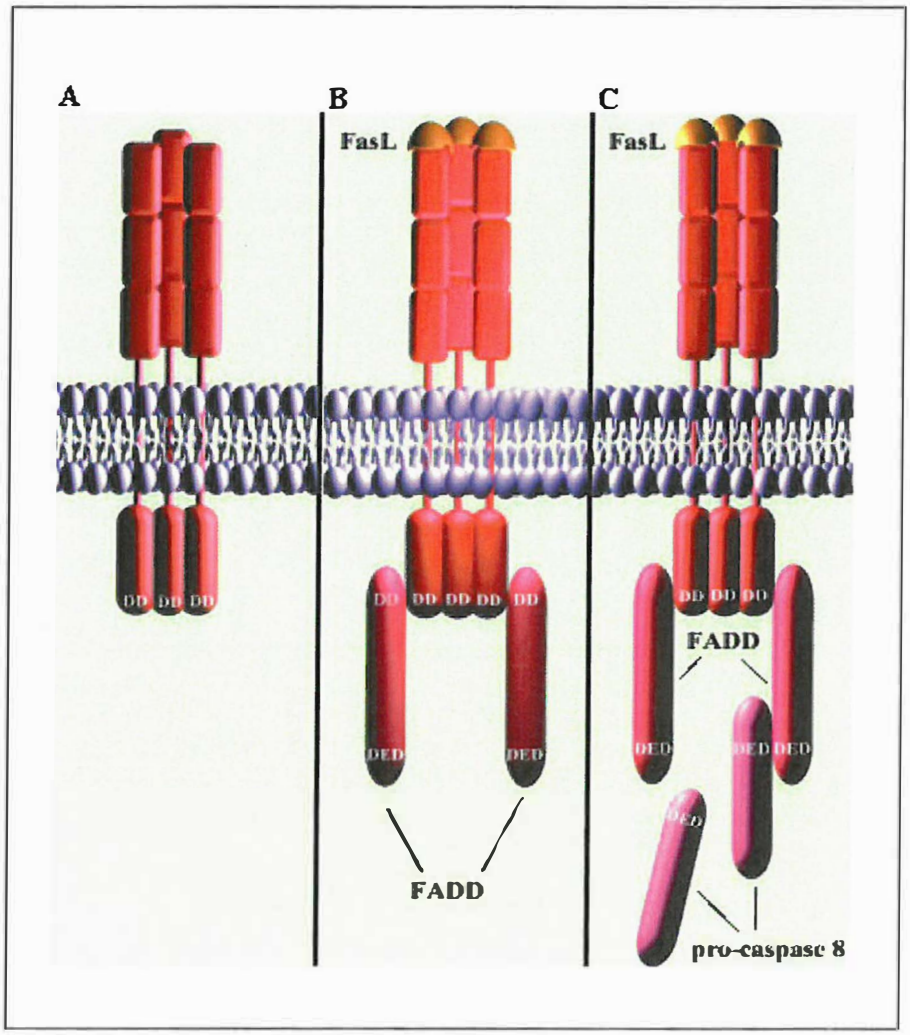

Fig 4: Activation of apoptosis through CD95 / Fas Receptor trimerisation of CD95 with death domains allows FADD to associate with the death domains. FADD also houses DED which allows binding of pro-caspase 8 to the CD 95-FADD complex. FADD is immediately cleaved to produce Caspase 8. This in turn triggers activation of execution caspases resulting in inevitable apoptosis (Reproductive and Cardiovascular Disease Research Group, 2005).

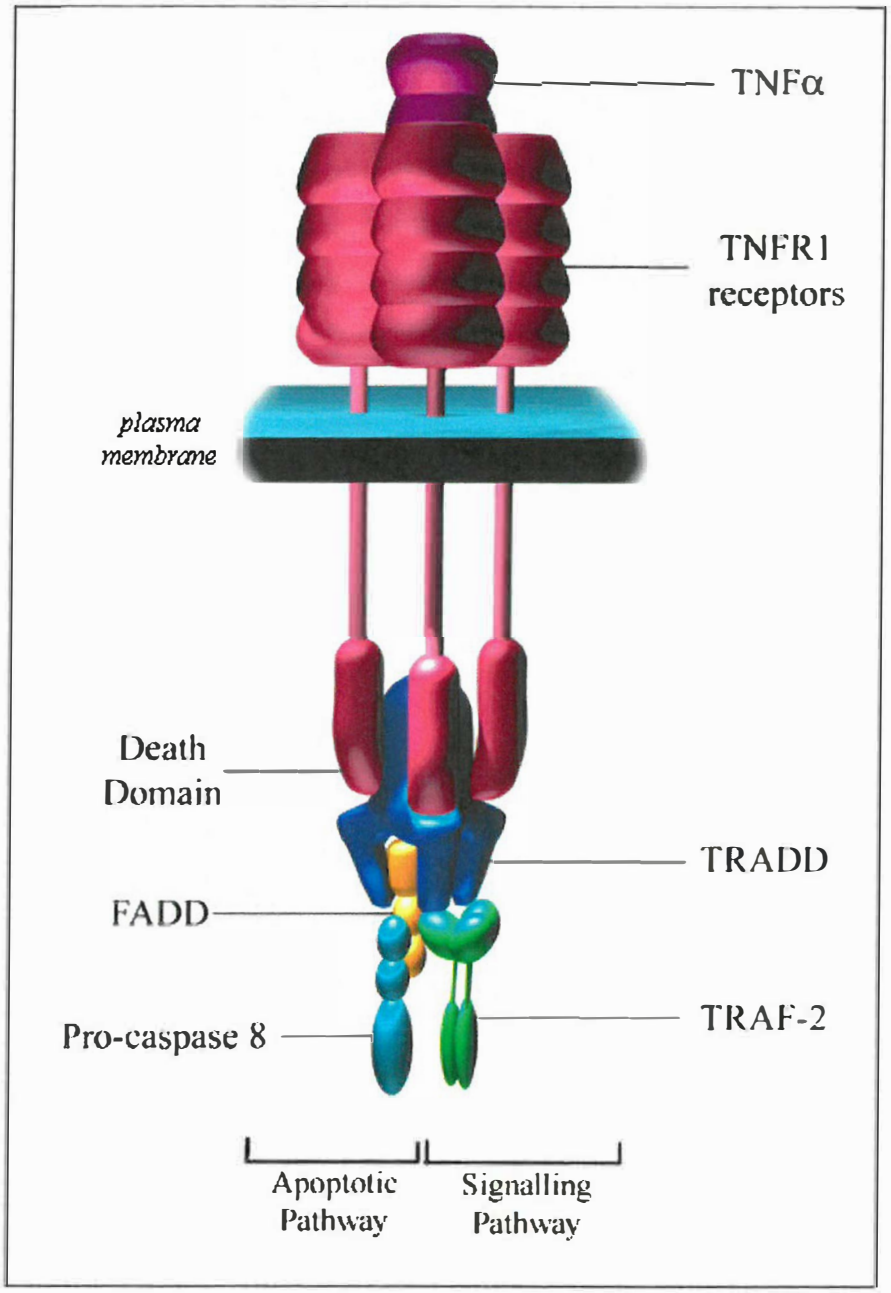

Fig 5: TNF receptor signaling (Reproductive and Cardiovascular Disease Research Group, 2005)

1.1.1.3 Induction of apoptosis by TNF∝ Related Apoptosis-Inducing Ligand (TRAIL)

Binding of TRAIL to its receptors DR4 or DR5 triggers rapid apoptosis in many cells. The DR4 and DR5 receptors contain death domains in their intracellular domain, but as yet no adaptor molecule (such as FADD or TRADD) has been identified that associates with the receptor to initiate apoptosis (Suliman *et al.*, 2001) (Fig 5).

1.1.2 Intrinsic Factors

1.1.2.1 Role of Mitochondria in Apoptosis

Mitochondria have the ability to promote apoptosis through the release of cytochrome C (Liu *et al.*, 1996). Mitochondrial permeability and release of cytochrome C is regulated by a family of proteins called Bcl-2. There are both anti-apoptotic and pro-apoptotic Bcl-2 proteins found in the mitochondria (Chittenden *et al.*, 1995). The pro-apoptotic proteins, Bad, Bid, Bax and Bim, reside in the cytosol but translocate to mitochondria following death signaling, where they promote the release of cytochrome C. Anti-apoptotic proteins Bcl-2 and Bcl-xL reside in the outer mitochondrial wall and inhibit cytochrome C release (Kroemer *et al.*, 1997). Since Bax, and other Bcl-2 proteins, show structural similarities with pore-forming proteins, it has been suggested that Bax can form a transmembrane pore across the outer mitochondrial membrane, leading to loss of membrane potential and efflux of cytochrome C and AIF (apoptosis inducing factor) (Susin *et al.*, 1999).

Bcl-2 and Bcl-XL may prevent this pore formation (Gross *et al.*, 1999). Heterodimerisation of Bax or Bad with Bcl-2 or Bcl-XL is thought to inhibit their protective effects (Fig 6).

In addition, Bax and Bad can also promote the formation of the large diameter PT pore (Green and Kroemer, 2004), with subsequent loss of cytochrome C and initiation of apoptosis (Crompton *et al.*, 1999).

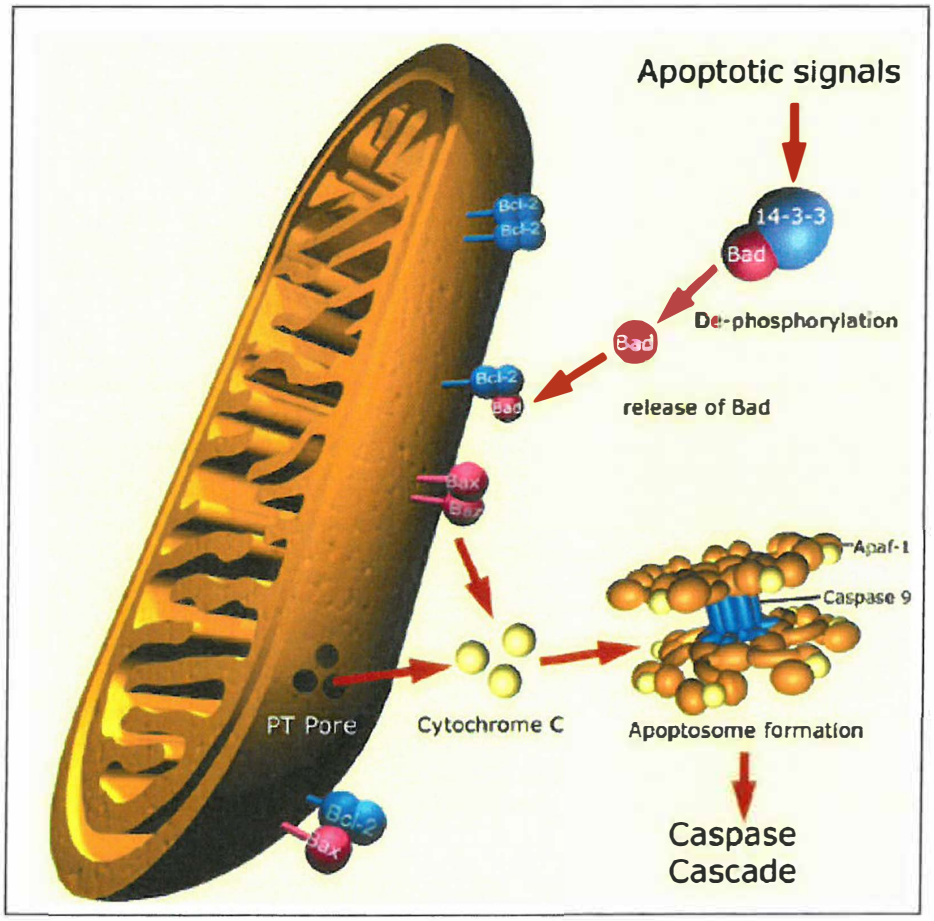

Fig 6: Role of Mitochondria in Apoptosis; Pro- and Anti – apoptotic Bcl-2 proteins regulate the release of cytochrome c in the mitochondria. Proteins either translocate from the cytosol to the mitochondria following death signalling or forming a transmembrane pore leading to the loss of membrane potential and the efflux of cytochrome c and AIF (Nitric Oxide research group, 2005).

1.1.2.2 Caspases

Caspases (cysteinyl aspartate-specific proteases), a group of cysteine proteases, are one of the main effectors of apoptosis. These enzymes cleave specific proteins at aspartate residues. Two main pathways activate Caspases: the death receptor pathway and the mitochondrial pathway (Salvesen and Dixit, 1997).

The caspases exist within the cell as inactive pro-forms or zymogens. These zymogens can be cleaved to form active enzymes following the induction of apoptosis. At least 14 caspase isoforms have been identified which are broadly categorised into initiators, effectors and inflammatory caspases. Induction of apoptosis activates initiator (caspase 8 or 10) and effector caspases (caspase 3 or 6) in cascade. This cascade results in the cleavage of the key cellular proteins that leads to the typical morphological changes observed in cells undergoing apoptosis. The mitochondria are also key regulators of the caspase cascade and apoptosis. Release of cytochrome C from mitochondria can lead to the activation of caspase 9, and then of caspase 3 (Shi, 2002). This effect is mediated through the formation of an apoptosome (Fig 7), a multi-protein complex consisting of cytochrome C, Apaf-1, pro-caspase 9 and ATP (Waterhouse *et al.*, 2002; Fig 8).

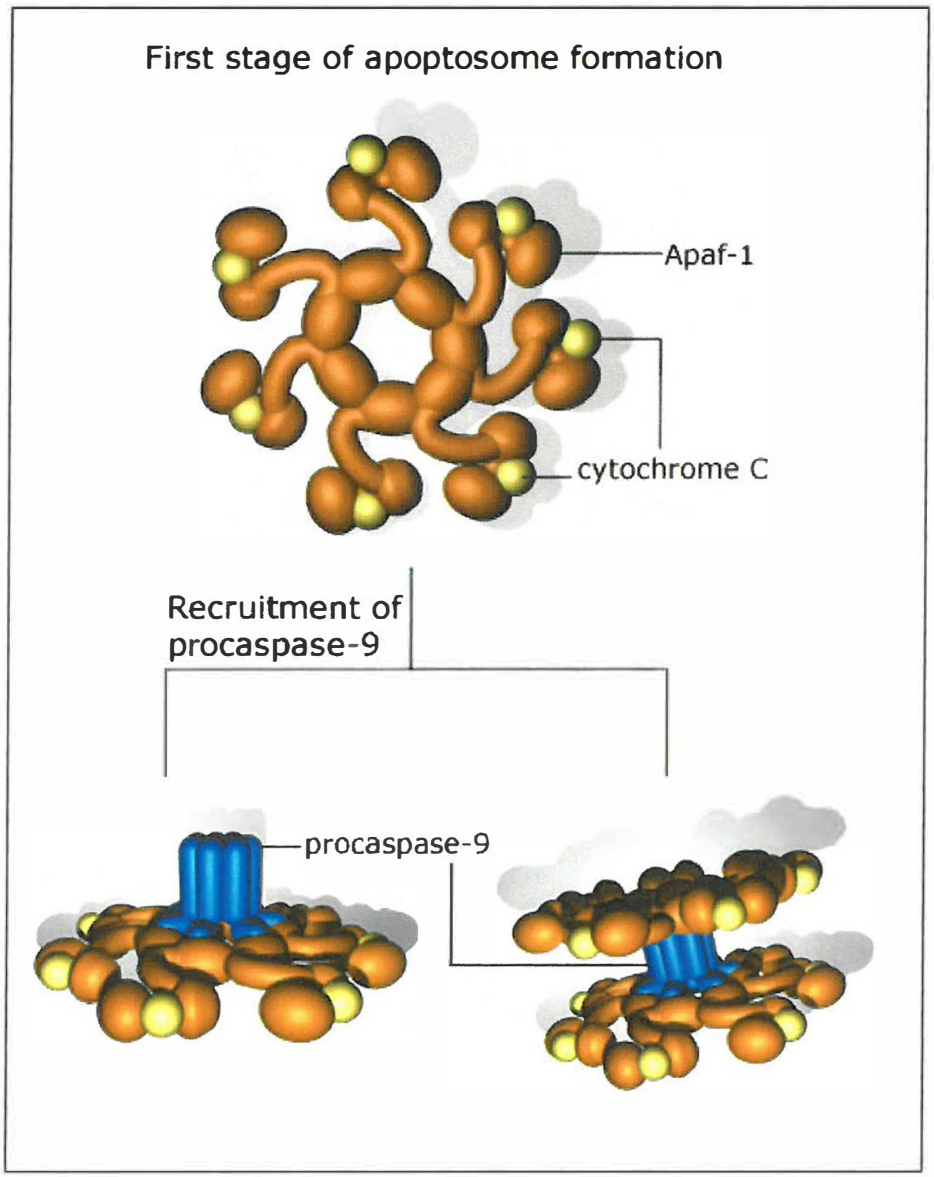

Fig 7: Caspase Activation (Reproductive and Cardiovascular Disease Research Group, 2005)

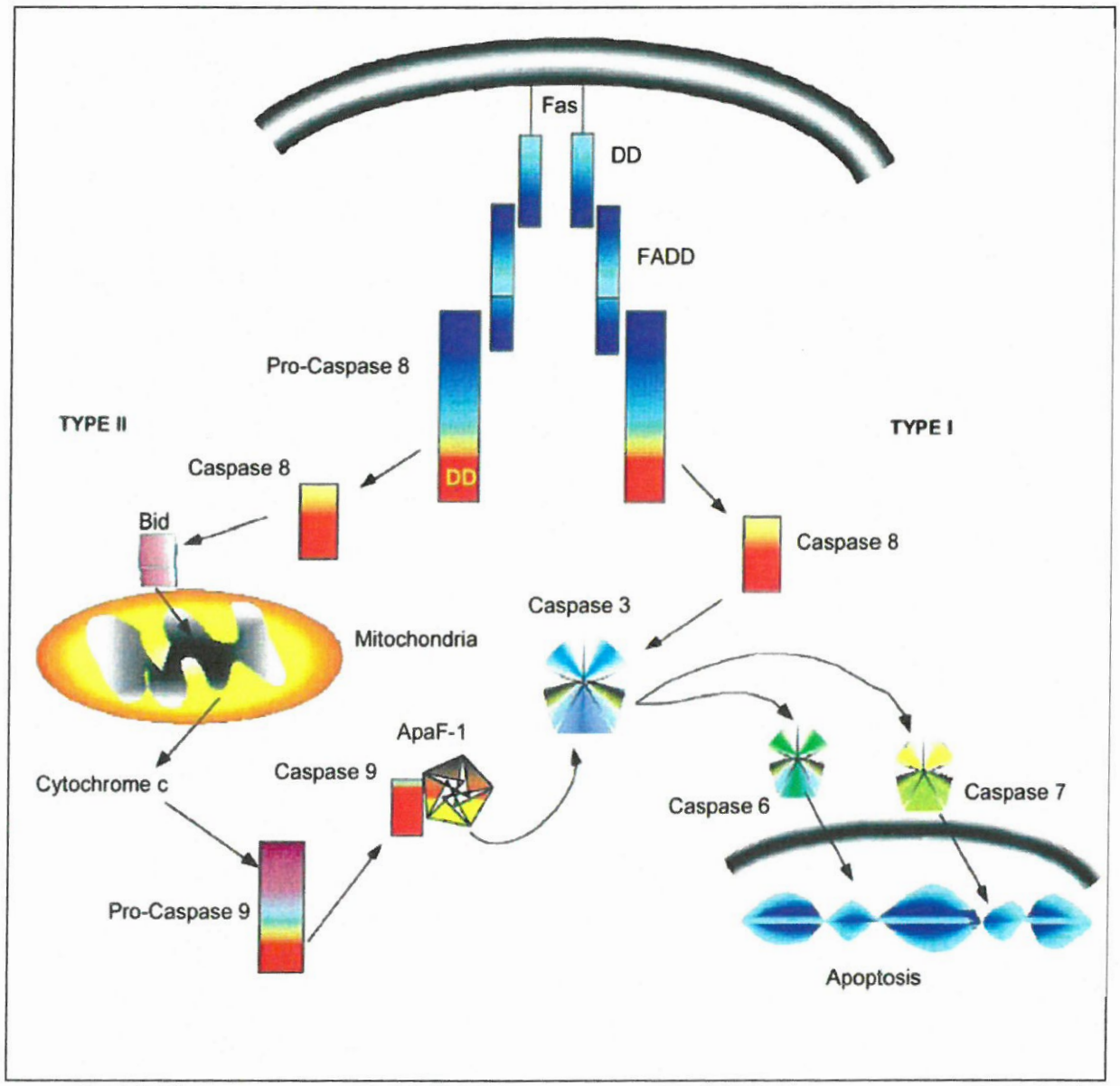

Fig 8: Schematic representations of the intracellular components of the caspase cascade (Mor *et al.*, 2002)

2.1 Preeclampsia (PE)

Preeclampsia, a multisystem disorder unique to pregnancy is characterised clinically by increased blood pressure accompanied by proteinuria, edema, or both (Perloff, 1998).

Either of the following criteria suffice for the diagnosis of hypertension in this situation: (1) systolic blood pressure increases of 30mm Hg or greater or (2) diastolic blood pressure increases of 15mm Hg or greater from early values (average of values before 20 weeks' gestation). If prior blood pressure is not known, readings of 140/90 mm Hg or greater after 20 weeks' gestation are considered sufficiently elevated to satisfy the blood pressure criteria of preeclampsia. Note, however, that many young pregnant women will show blood pressure increases required for the diagnosis of preeclampsia without their pressure increasing to 140/90 mm Hg (Report of the National High Blood Pressure Education Program Working Group on High Blood Pressure in Pregnancy, 2000).

Proteinuria is defined as the excretion of 0.3 g or greater in a 24-hour specimen (Davey *et al.*, 1988). This will usually correlate with 30 mg/dl ("1+ dipstick") or greater in a random urine determination. Proteinuria usually presents as a late clinical sign in the course of preeclampsia; although it is nonspecific, its appearance greatly bolsters the diagnosis of preeclampsia (Higgins and Swiet, 2001)

Women with hypertension can be classified into four main categories:

- Gestational hypertension. This is hypertension occurring for the first time after 20th week of pregnancy.
- Preeclampsia is defined as hypertension in pregnancy asssociated with proteinuria of > 0.3 g/day in 24-hour urine collection.
- Chronic or preexisting hypertension which pre-dates preeclampsia or is diagnosed prior to the 20th week of gestation
- Superimposed preeclampsia. This is high blood pressure and proteinuria superimposed on the preexisting hypertension or renal disease

All women with hypertensive disorders in pregnancies should be assessed 6 -1 2 weeks following delivery, in order to reclassify their condition. In gestational hypertension and preeclampsia all abnormalities should have returned to pre-pregnancy levels (Moodley, personal communication).

2.1.1 Epidemiology of Preeclampsia

At risk are mainly primigravidae and women with renal diseases, diabetes mellitus, pre-existing hypertension and microvascular disorders (Ness *et al.*, 2003). Eighty-five percent of preeclamptic cases occur in primigravid women with seldom re-occurrence in subsequent pregnancies (Robillard *et al.*, 1994). However, with a change in partner, the risk with multiparous women increases. If there is a family history of hypertension there is a risk of PE in a first-degree relative (Saftlas *et al.*, 2003). Preeclampsia is more common in black women compared to other racial

groups. This is due to the higher prevalence of underlying chronic hypertension (Klonoff-Cohen *et al.*, 1989). Worldwide, preeclampsia affects women mostly at the two extremes of reproductive age (<18yrs or >35yrs) (Fisher *et al.*, 1981).

2.1.2 Risk Factors for Preeclampsia

A recent review suggests that a previous history of preeclampsia, multiple pregnancy, nulliparity, pre-existing diabetes, high BMI before pregnancy, maternal age >40 years, renal disease, hypertension, >10 years since previous pregnancy and presence of antiphospholipid antibodies all increase a woman's risk of developing preeclampsia (Duckitt and Harrington, 2005). Increases in risk of more than nine fold, sevenfold and threefold, respectively, were documented for antiphospholipid antibodies, previous history of preeclampsia and diabetes.

Other risk factors for preeclampsia are insulin resistance in concert with obesity and thrombophilia (Walker, 2000; Wolf *et al.*, 2002; Kupferminc *et al.*, 1999). In developing countries, protein-calorie undernutrition has been identified as an important risk factor (Brewer, 1976).

2.1.3 Genetic Risk factors

The precise role of genetic factors in the development of preeclampsia is unclear, and no specific contributory gene has been identified. The inheritance pattern of the disease has been described as Mendelian (autosomal recessive and autosomal dominant with incomplete penetrance), polygenic/multifactorial and mitochondrial (Ward *et al.*, 1993).

Studies have indicated an association between preeclampsia and polymorphisms of genes that control blood pressure, coagulation or oxygen-free-radical metabolism — such as renin, angiotensinogen, endothelial nitric oxide synthase, factor V Leiden, methyltetrahydrofolate or lipoprotein lipase (Villar and Belizan, 2000; Arngrimsson *et al.*, 1997; Dizon-Townson *et al.*, 1996; Sohda *et al.*, 1997). Linkage analysis has identified three potential loci linked to susceptibility to preeclampsia: 2p13, 2p25 and 9p13 (Laivuori *et al.*, 2003; Lachmeijer *et al.*, 2001; Moses *et al.*, 2000). A fourth locus for preeclampsia was subsequently identified on 10q22. Maximal allele sharing between pre-eclamptic sisters at this locus was observed for maternal-derived but not paternal-derived alleles, indicating matrilineal inheritance (Oudejans *et al.*, 2004).

In a large study by the British Genetics of Preeclampsia Consortium, 657 women affected by preeclampsia and their families were genotyped at sites of 28 single-nucleotide polymorphisms in several genes, including those involved in angiotensin activity and oxidative stress (GOPEC Consortium, 2005). None of the genetic variants tested were found to confer a high risk of disease development, indicating that alterations of angiotensin activity and oxidative stress are not prime causes of preeclampsia.

2.1.4 Pathophysiology of Preeclampsia

The cause of PE remains unknown but has been associated with placental dysfunction which initiates systemic vasospasm, ischemia and thrombosis that eventually damages maternal organs (Brown *et al.*, 1991). There is maternal endothelial cell

damage due to the release of substances from a poorly perfused placenta (Brown *et al.*, 1991). This creates an increased responsiveness to a variety of endogenous substances. Renal necrosis leads to decreased glomerular filtration and there is an increase in renal blood flow as opposed to normal pregnancy. There is also an increase in urinary protein excretion. Liver injury from hepatocellular necrosis leads to elevation of liver enzymes with subsequent abdominal pain (Gallery and Brown, 1987). Cardiovascular and hematologic manifestations include increased cardiac output, lower intravascular volume and thrombocytopenia. Neurologic dysfunction with other signs defines eclampsia (Smith, 1993).

Eclampsia is the most serious complication of hypertensive disorders of pregnancy. It ranges from 0.5% to 0.8% of pregnancies (Sahin, 2003). Seizures, cerebral hemorrhage, edema vasospasm and thrombosis can all occur. Cerebral hemorrhage is the leading cause of maternal death from eclampsia (Royburt *et al.*, 1991).

When vasospasm affects the uteroplacental bed, the fetus becomes growth restricted accompanied by an increased risk of stillbirth and neonatal death. The incidence of intrauterine fetal growth restriction related to PE ranges from 30-80% (Helewa *et al.*, 1997).

There is increased cardiac output which is the fundamental haemodynamic derangement in PE (Easterling *et al.*, 1990). The capillary beds are damaged by exposure to elevated pressures and flow. This is due to maximal compensatory vasodilation which is caused by hyperperfusion. Endothelial cells lose their normal response to physiological changes and demonstrate new responses, leading ultimately

to diffuse vasospasm, alteration in coagulability, and increased permeability (de Groot *et al.*, 1993). Blood concentrations of a number of substances manufactured or regulated by endothelial cells have been found to be altered suggesting that these substances may mediate the observed pathophysiological changes. Other pathological features of preeclampsia are acute atherosis and persistent intraluminal endovascular trophoblast cells. Acute atherosis is characterised by fibrinoid necrosis of the vessel wall with a perivascular mononuclear cell infiltrate and lipid-laden macrophages. Acute atherosis labels for lipoprotein-a, which is thrombogenic and atherogenic, and it is not surprising therefore that thrombosis is often seen within these uteroplacental arteries (Fig 9) (Meekins *et al.*, 1994)

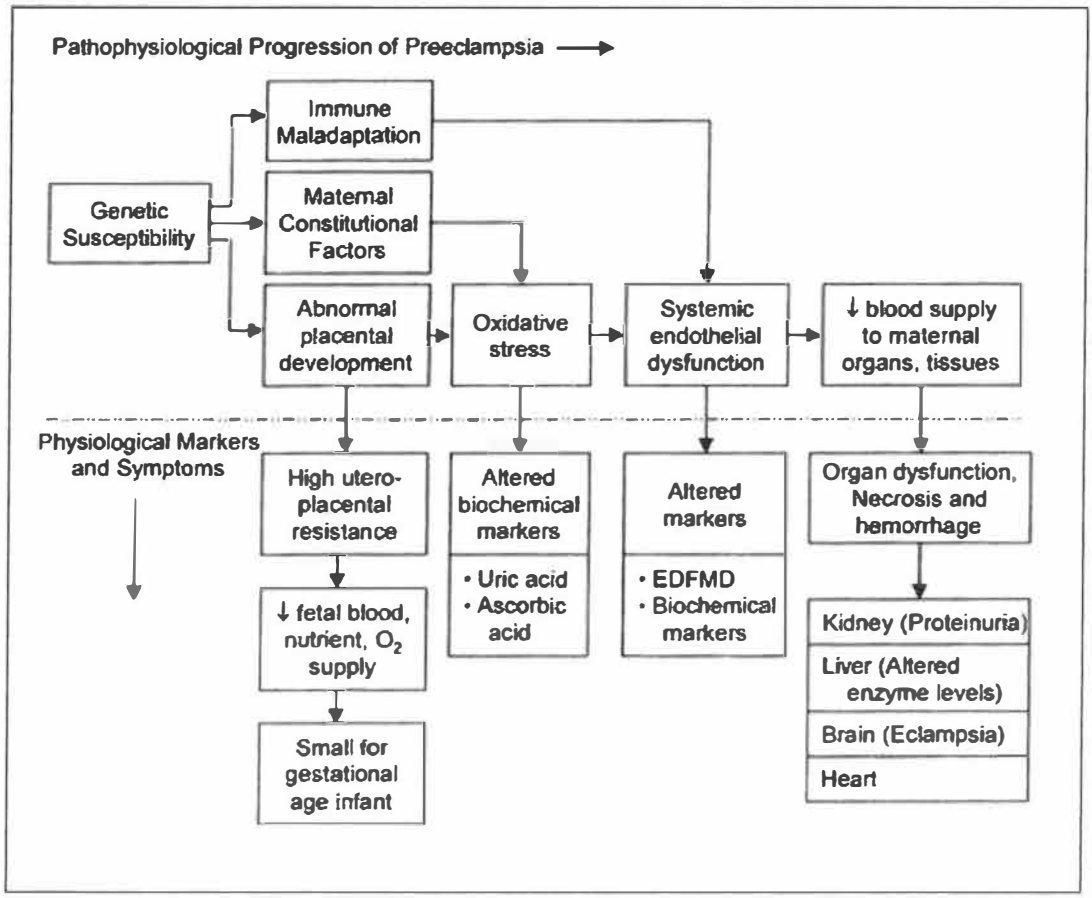

Fig 9: Pathophysiology of Preeclampsia (Medscape, 2005)

The placenta has been suggested to be the primary cause of PE, since delivery of the placenta resolves the signs and symptoms of PE (de Groot *et al.*, 1993). In addition, women with molar pregnancies, which are characterised by placental tissue in the absence of a fetus frequently, develop PE (Slattery *et al.*, 1993). From this it is concluded that placental dysfunction may possibly be the primary trigger responsible for both the pathophysiology and pathogenesis of preeclampsia. Supporting the pathogenic role of placental ischaemia, preeclampsia is more common in conditions where placental oxygen demand is increased (as in multiple pregnancies) or those with decreased oxygen transfer due to preexisting vascular alterations. The latter would explain the high incidence of preeclampsia in primigravidas whose uterine vasculature is less developed than those of multiparas or women with microvascular alterations secondary to chronic hypertension or diabetes (Redman, 1991).

For a pregnancy to proceed normally, the early blastocyst must adhere to and invade the uterine endometrium so that maternal blood can effectively bathe the placental cotyledons (Red-Horse *et al.*, 2004). Trophoblast cells derived from the basal plate and the tips of the anchoring villi infiltrate into the decidua and inner myometrium in a timed sequence (Pijnenborg *et al*, 1980). Two populations of invasive extravillous trophoblasts have been identified viz. interstitial and endovascular trophoblasts. Interstitial trophoblasts invade the decidual stroma and reach the myometrium. At the end of their invasion path, these cells fuse to form multinuclear giant cells (Lyall, 2002).

In another pathway, the trophoblast cell migrates into the lumen of the spiral arteries, invades, and replaces the endothelium, internal elastic lamina, and musculoelastic media of these arteries. The vascular change extends from the intervillous space to the inner third of the myometrium (Robertson *et al.*, 1986; Pijnenborg, 1996). This process is usually completed by 20 weeks of gestation. These muscular arteries are converted to a low resistance high capacitance system, with a 4 to 6 fold increase in arterial diameter, hence meeting the oxygen and nutrient demands of the growing foetus. This transformation of the artery by the trophoblast cell is called a *"physiological change"*. The time and sequence of events in the remodelling of these arteries is portrayed in Figure 10 (Brosens *et al.*, 1972).

In preeclampsia, early in pregnancy, the migration of trophoblast cells in the maternal tissues is compromised resulting in a lack of physiological vascular changes. Placental derangement begins with the impaired extravillous trophoblast invasion of the spiral arteries with the consequent failure of vascular dilation and remodeling and hence placental ischaemia (Brosens *et al.*, 1972; Ghidini *et al.*, 1997). Intraluminal migration of the trophoblast cell in spiral arteries is limited to the decidua (Khong *et al.*, 1986; Pijnenborg *et al.*, 1991; Zuspan, 1988; Redman, 1991). The arteries fail to dilate adequately and the spiral arteries retain responsiveness to vasoconstrictors. Arteries dilate to only 40% of the diameter occurring in normal pregnancy with a resultant underperfusion of the developing placenta (Roberts and Redman, 1993).

Consequently, abnormal trophoblast invasion, with resultant lower intervillous blood flow would place the fetus at risk of oxygen and nutrient deprivation (McParland *et*

al., 1988; Kingdom *et al.*, 1997). From this, it is plausible to hypothesise that up-regulation of apoptosis contributes to the characteristic defective placentation of preeclampsia.

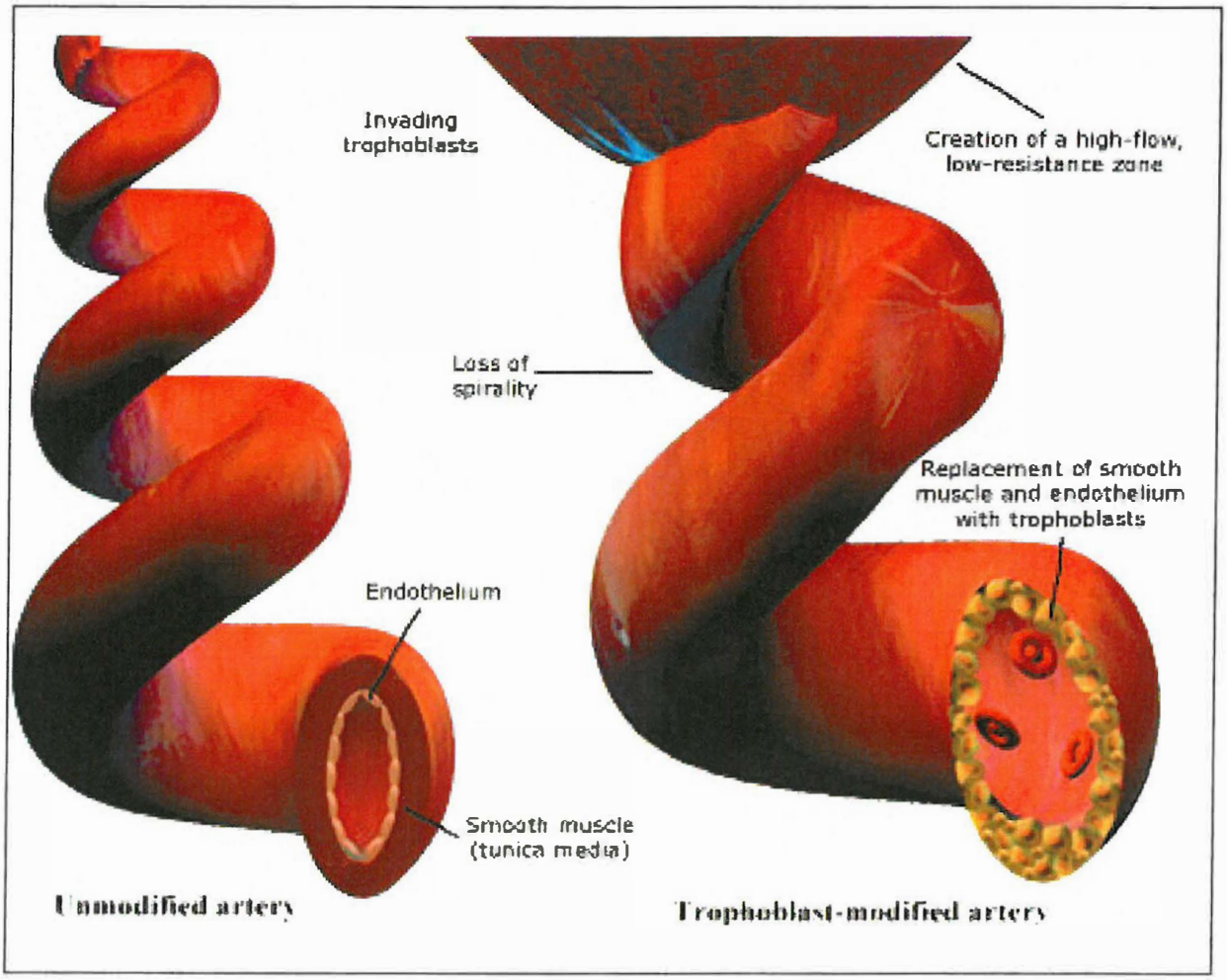

Fig 10: Schematic illustration of remodelling of Spiral Artery by Trophoblast cells (Reproductive and Cardiovascular Disease Research Group, 2005)

2.2 Apoptosis in Preeclampsia

Normal placental development involves constant tissue remodeling characterised by the functional loss of trophoblast cells by apoptosis. After proliferation and differentiation into specific cell subtypes, aging trophoblast cells are selectively removed and replaced by a younger population of trophoblasts without affecting neighboring cells (Mayhew, 2001). In complicated pregnancies such as preeclampsia, a greater incidence of trophoblast apoptosis has been observed (Allaire *et al.*, 2000), suggesting that alterations in the regulation of trophoblast apoptosis may contribute to the pathophysiology of this disease (Smith *et al*, 2002).

Cells undergoing apoptosis are quickly removed by phagocytosis. Macrophages present at the maternal-fetal interface quickly remove apoptotic cells to promote trophoblast survival and facilitate invasion and transformation of the spiral arteries (Mor and Abrahams, 2003). In placentas from complicated pregnancies, shallow trophoblast invasion and inefficient spiral artery transformation have been observed which may be partly due to the distribution and activation state of infiltrating macrophages (Brosens et al., 1972). The increase in trophoblast apoptosis may be attributed to placental oxidative stress which may be triggered by hypoxia (Kilani *et al.*, 2003).

3.0 Normal Cell cycle

Cell proliferation is a biological process of fundamental importance controlled by highly coordinated mechanisms (Schulter *et al.*, 1993). Apotosis is a process of the normal cell cycle events. The cell cycle can be defined as an ordered set of events culminating in cell growth and division into two identical daughter cells. In normal cells this complex process is initiated only in the presence of a mitogenic stimulus (Norbury and Nurse, 1992).

The cell cycle consists of several phases (Figure 11). In the first phase (G1) the cell grows and becomes larger. When a cell has reached a certain size it enters the next phase (S), in which DNA-synthesis takes place. The cell duplicates its hereditary material (DNA-replication) and a copy of each chromosome is formed. During the next phase (G2) the cell checks that DNA-replication is completed and prepares for cell division. The chromosomes are separated (mitosis, M) and the cell divides into two daughter cells. Through this mechanism the daughter cells receive identical chromosome set ups. After division, the cells are back in G1 and the cell cycle is completed (Norbury and Nurse, 1992).

Although placental development depends on careful coordination of trophoblast proliferation and differentiation, little is known about the mitotic regulators that are the key to synchronizing these events. Alterations in trophoblast expression of cell cycle markers may provide the basis for understanding factors that lead to abnormal placentation in diseases such as preeclampsia.

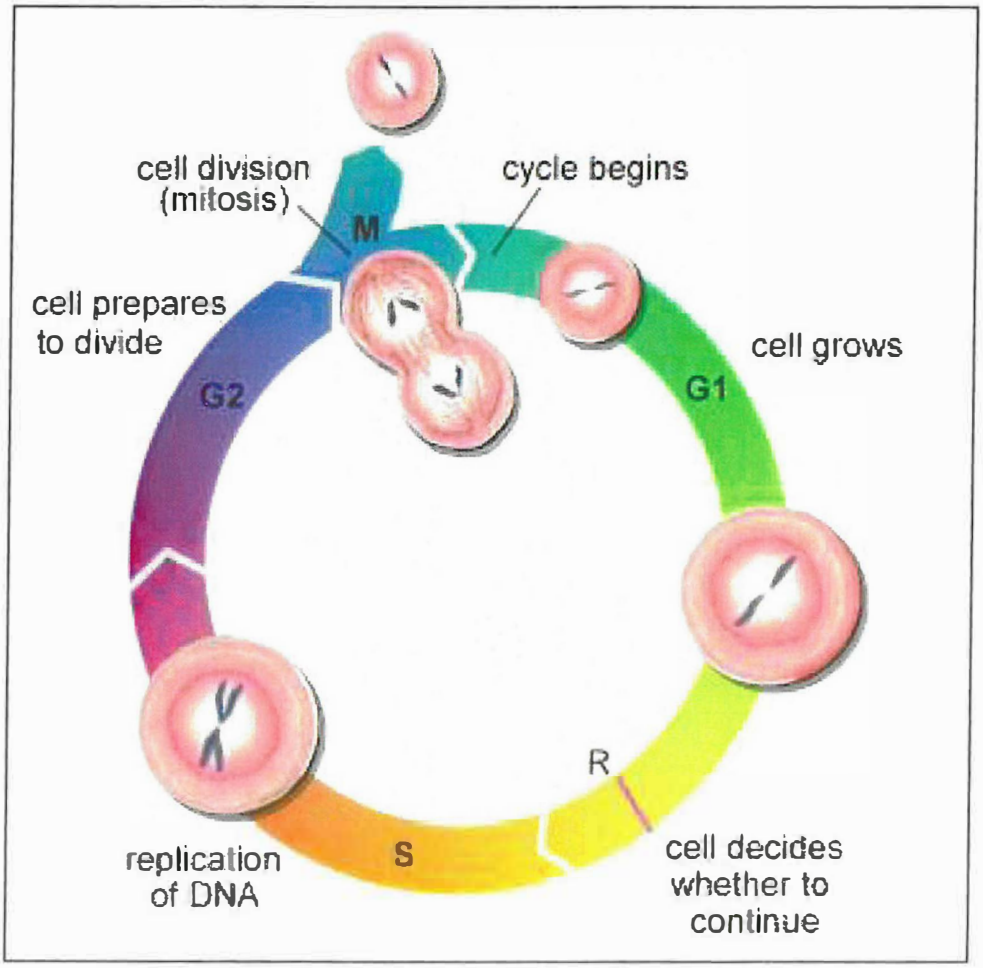

Fig 11: Cell cycle (From Learning Lab) [online image] Available at http://learninglab.co.uk/headstart/cycle3.htm accessed on the 17 December 2005

3.1 Ki67

The Ki67 protein was originally identified as an antigen which was recognised by the prototype antibody Ki67 (Gerdes *et al.*, 1983). The name was derived from the city of origin, Kiel, and the number of original clones in a 96-well plate. The unique feature found in the Ki67 primary structure is the occurrence of 16 repeated elements, each with a size of approximately 122 amino acid residues (Scholzen *et al.*, 1997). There is a highly conserved region present within the repetitive elements called the Ki67 motif which houses the epitope recognised by the Ki67 antibody (Scholzen and Gerdes, 2000).

In contrast to many other cell cycle-associated proteins the Ki-67 antigen is consistently absent in quiescent cells and is not detectable during DNA repair processes (Hall *et al.*, 1993). It is a constituent of compact chromatin (Kreitz *et al.*, 2000) and is vital for cell proliferation, since removal of Ki67 protein using antisense nucleotides prevents cell proliferation (Schluter *et al.*, 1993). Recent studies have showed that the C terminus of Ki67 interacts with heterochromatin protein 1 family and potentially plays a role in higher-order chromatin organization (Schlozen *et al.*, 2002). These data suggest that Ki67 protein is involved in the protein interaction network that drives cell division cycles. It is evident that Ki67 can be used as a tool to estimate the growth fraction of any human cell population as it has been detected during all active phases of the cell cycle (Sholzen and Gerdes, 2000). This stringent feature has made Ki67 a popular prognostic and diagnostic tool (Brown *et al.*, 2002).

The topographical distribution of the Ki-67 antigen is cell cycle dependent (Braun *et al.*, 1988; Guillaud *et al.*, 1989; du Manoir *et al.*, 1991). In the G1 phase the Ki-67 antigen is predominantly localised in the perinucleolar region, whilst in the later phases of the cell cycle the antigen is also detected throughout the nuclear interior, being predominantly localised in the nuclear matrix (Verheijen *et al.*, 1989a). In the S-phase, Ki-67 immunostaining was restricted to the nucleoli (Kill *et al.*, 1996) and in the nucleoplasm (Braun *et al.*, 1988). During the G2-phase cells Ki67 was detected in the nucleus (du Manoir *et al.*, 1991) foci in addition to a diffuse neoplasm distribution (Braun *et al.*, 1988).

In mitosis, there is a prominent redistribution of Ki-67 antigen. During prophase the Ki67 protein is reorganised and is detectable as a fine meshwork associated with condensing chromatin (Verheijen *et al.*, 1989b). In metaphase, a bright Ki67 antigen staining is visible covering the surface of the individual chromosome (Verheijen *et al.*, 1989b). During anaphase and telophase the Ki67 protein has been detected distributed diffusely in the cytoplasm (Braun *et al.*, 1988). The biological half-life of Ki67 has been estimated to be one hour as the immunostaining of Ki-67 rapidly decreases towards the end of mitosis (Bruno and Darzynkiewics, 1992).

3.2 Cytokeratin 18 (CK18)

Cytokeratins (CK) are a family of intermediate filament proteins comprising an essential component of the cytoskeleton of epithelial cells (Anderton *et al.*, 1981). There are over 20 different polypeptides of CK expressed by human epithelia that have been defined on the basis of their molecular weights and isoelectric points (Moll *et al.*, 1982a). Cytokeratins are expressed in a tissue-specific and a differentiation-dependent manner and are present in both keratinizing tissue and non-keratinizing tissue. Biochemically, cytokeratins are usually expressed in pairs comprising a type I (acidic polypeptide, CK9-20) and a type II (basic polypeptides, CK1-8) cytokeratins (Eichner *et al.*, 1986). At present, cytokeratins act as resilient yet pliable scaffolds that endow epithelial cells with the ability to sustain mechanical and non-mechanical stresses (Coulombe *et al.*, 2002). Cytokeratins play a critical role in differentiation and tissue specialization and function to maintain the overall structural integrity of epithelial cells (Moll *et al.*, 1982a). Together with actin microfilaments and microtubules, keratin filaments make up the cytoskeletons of vertebrate epithelial cells, forming alpha-helical coiled-coil dimers which associate laterally, and end-to-end to form 10-nm diameter filaments (Coulombe *et al.*, 2002).

Cytokeratin 18 has a widespread distribution and is co-expressed with cytokeratin 8 (CK8/18). It is an acidic keratin and is expressed in simple nonstratified, ductular and pseudostratified epithelia (Leers *et al.*, 1999).

These two cytokeratins are the first intermediate filaments to be expressed during mammalian development being associated with the differentiation to the trophectodermal layer of the blastocyst (Leers *et al.*, 1999).

Trophoblasts are of epithelial origin, and CK18 is a component of their cytoskeleton. Recently, cytokeratins have been observed to aggregate in apoptotic cells, this is mediated by hyperphosphorylation (Liao and Omary, 1996). Apart from hyperphosphorylation, CK18 undergoes a dramatic re-organization as it is cleaved by caspases 3 and 7, generating an apoptosis-specific neo-epitope, which is a specific formalin-resistant caspase cleavage site (Caulin *et al.*, 1997). This site is not present in normal cytokeratin 18 or cleavage sites not related to caspase proteolytic cleavage. This specific proteolytic cleavage occurs before the disruption of membrane asymmetry and DNA strand breaks (Leers *et al.*, 1999). The release of this neo-epitope occurs early in the apoptotic cascade and is recognised by the M30 antibody. This monoclonal antibody has been used successfully for analyzing apoptosis especially in epithelial cells, which placental villious trophoblasts are one type (Kadyrov *et al.*, 2001). The M30 antibody identifies early changes in the cytoskeleton related to action of caspases in apoptosis

Studies have suggested that the detection of cleaved CK18 could be a promising specific assay for apoptosis identification (Kusama *et al.*, 2000). The M30 monoclonal antibody has been used successfully for analyzing apoptosis especially in epithelial cells, of which placental villous trophoblasts are one type (Kadyrov *et al.*, 2001).

The TUNEL test has been established (Gavrieli *et al.*, 1992) to detect cells that have reached a final stage of the apoptosis cascade and that will die soon. However, studies have shown that the number of apoptotic cells stained by M30 is higher than that stained by TUNEL, due to the longer period of cytokeratin cleavage within the apoptosis cascade, as compared to the short period of endonuclease activation (Huppertz *et al.*, 1999; Robertson *et al.*, 2000). Furthermore, within complex tissues such as the placental bed, evaluation of the TUNEL test is often limited by difficulties in distinguishing apoptotic trophoblast from other apoptotic cell types.

4.0 Summation and Aims

During normal pregnancies extravillous trophoblast invade the myometrium via two pathways viz. interstitial and endovascular pathways. The spiral arteries are physiologically converted into large bore conduits. In preeclampsia, however, the endovascular pathway is compromised within the myometrium hence the arteries do not undergo conversion with a resultant inadquate supply of nutrients and oxygen to the developing foetus. Studies have shown that there is also an inadequate invasion of interstitial trophoblasts. This deficient invasion may be attributed to an increase in trophoblast apoptosis triggered by hypoxia due to the lack of spiral artery conversion. (Kilani *et al.*, 2003). Alternatively, alterations in trophoblast expression of cell cycle markers may lead to abnormal placentation. The balance between trophoblast apoptosis and proliferation may represent a mechanism to control trophoblast invasion.

Therefore, the aim of this study was to determine the immunoexpression profiles between trophoblast apoptosis (M30), and proliferation (Ki-67) in the placental bed of pre-eclamptic compared to normal pregnancies in an attempt to understand the imbalance that occurs in abnormal placentation.

CHAPTER TWO

MATERIALS AND METHODS

2.1 ETHICAL APPROVAL AND PATIENT CONSENT

This retrospective study was conducted on placental bed biopsies that were obtained at the Obstetric Unit of King Edward VIII Hospital (KEH), Durban, South Africa (Reference Number R092/97). For this study, ethical approval was obtained from the Ethics Committee (Reference Number R120/02), Nelson R. Mandela School of Medicine, University of Kwa-Zulu Natal. The placental bed biopsies were obtained as a non-routine procedure specifically as part of another study.

2.2 MATERIALS

The study group (n = 24) consisted of true placental bed wax embedded blocks obtained at caesarean section from normotensive (n = 12) and hypertensive (n = 12) pregnant women. The normotensive group (BP $\leq$ 120/80 mmHg) was matched for maternal age with the hypertensive group (90 $\leq$ DBP $\leq$ 100 mmHg- DBP $\geq$ 110 mmHg). Reasons for caesarean sections were previous caesarean section, fetal compromise and cephalo-pelvic disproportion. Patients' demographics were obtained. Parity ranged from 0 - 4. Retroviral status of these patients was unknown.

2.3 HISTOLOGY PREPARATION

Three µm sections were cut from archived wax blocks on a Leica Jung microtome (RM2035). Sections were floated in a water bath and collected onto uncoated slides for histology.

2.3.1 Haematoxylin & Eosin (H &E); Periodic acid Schiff reaction (PAS) and von Gieson elastic staining

For each patient three sections (3 µm thick) were cut and stained for screening of the placental bed biopsy with the following stains:

1. Haematoxylin and eosin staining (H & E): Mayer's Haematoxylin (Sigma Chemicals, St Louis; Mayer, 1903) and 0.5% alcoholic eosin (BDH, England);
2. Periodic acid-Schiff reaction (PAS; Pearse, 1953);
3. Von Gieson Elastic (EVG) staining.

The procedures used for the H & E and PAS and EVG are outlined in Table I, II and III respectively. Examination of the tissue was essential for the confirmation of a true placental bed biopsy.

Table I: Procedure for H & E staining

STEP	SOLUTION	TIME
1	Dewax - xylene	2 x 5 min
2	Rehydrate – absolute ethanol	2 x 1 min
3	Rehydrate – 90% ethanol	1 min
4	Rehydrate – 70% ethanol	1 min
5	Rehydrate – water	1 min
6	Mayer's Haematoxylin	5 min
7	Blue – rinse in running tap water	5 min
8	0.5% alcoholic eosin	2 min
9	Rinse quickly by immersing slides in 95% ethanol	30 sec
10	Dehydrate - Absolute Alcohol	2 x 1 min
11	Dehydrate - Xylene	1 min
12	Mount in DPX	

Table II: Procedure for PAS staining

STEP	SOLUTION	TIME
1	Dewax - xylene	2 x 5 min
2	Rehydrate – absolute ethanol	2 x 1 min
3	Rehydrate – 90% ethanol	1 min
4	Rehydrate – 70% ethanol	1 min
5	Rehydrate – water	1 min
6	1% Periodic Acid	10 min
7	Rinse in running water	30 sec
8	Schiff reagents (BDH, England)	15 min
9	Running tap water	5 min
10	Mayer's Haematoxylin	2 min
11	Blue in running tap water	2 min
12	2% Orange-G (KGaA 64271, Merck, Germany) in 5% Phosphotungstic acid	1 dip
13	Rinse in running tap water	2 min
14	Dehydrate - Absolute alcohol	2 x 1 min
15	Dehydrate - Xylene	1 min
16	Mount in DPX	

Table III: Procedure for von Gieson elastic staining

STEP	METHOD	TIME
1	Dewax and bring to 95% alcohol	
2	Miller's solution (BDH, England)	60 min
3	Rinse well	
4	Differentiate in 70% alcohol	
5	Wash well	
6	Van Gieson solution*	5 min
7	Blot dry	
8	Dehydrate through alcohol	
9	Clear in xylene	2 min
10	Mount in DPX	

2.4 TISSUE PROCESSING FOR IMMUNOHISTOCHEMICAL STUDIES

Tissue sections were cut at 2 μm thickness using sterile disposable blades on a rotary microtome (Leica Jung, RM2035). They were floated in a water bath and picked on poly-L-lysine (0.1%) coated glass slides (Sigma Chemicals, St Louis) for immunohistochemical staining procedures. The sections were then baked on a hotplate at 60°C for 10 min before dewaxing and bringing to water.

2.4.1 Mouse anti-human cytokeratin antibody (Clone MNF 116) isolation and specificity

Cytokeratin is the most sensitive marker for all types of trophoblastic elements (cytotrophoblasts, syncytiotrophoblast and intermediate trophoblast cells from day 12 to full term placenta (Daya and Sabet, 1991). Monoclonal mouse anti-human cytokeratin, Clone MNF 116 (M821; Dako, USA) was initially utilised for the identification of the trophoblast cell population; however we progressed to cytokeratin 18 as it is affected in early apoptosis.

Clone MNF 116 antibody reacts with an epitope that is present in a wide range of cytokeratins. Immunoblotting reveals a number of discrete 45 to 56.5 kDa keratin polypeptides. These include keratin numbers 6,8,17 and 19 (Moll *et al.*, 1982). This antibody shows a broad pattern of reactivity with human epithelial tissues from simple glandular to stratified squamous epithelium (Moll *et al.*, 1982; Earl *et al.*, 1987). Epithelial cells are labelled whether they are ectodermal, mesodermal or endodermal in origin. Occasionally, the antibody shows cross-reactivity with uterine

myometrial muscle cells but this is a non-specific reaction occurring in cells that are clearly morphologically distinguishable from the trophoblast cell.

2.4.1.1 Immunostaining schedule for anti-MNF 116 antibody

Antigen retrieval using pepsin (0.01% in HCl; 0.01M at 37°C for 10 min) was performed prior to commencement of an indirect immunoperoxidase staining schedule utilising diaminobenzidine as the chromogen. Tris buffered saline (0.01% tris, 0.9% sodium chloride, pH 7.6) was used throughout the procedure, except in the chromogen step where Tris-HCl buffer (0.05 M) was used. Bovine serum albumin was used as a blocking agent (Fraction V, Sigma A4503). The primary antibody dilution was 1:1000. The secondary antibody, a biotinylated rabbit anti-mouse immunoglobulin (1:400) was linked to streptavidin peroxidase conjugate (1:1000) and detection of peroxidase activity was performed with 3, 3'-diaminobenzidine (Sigma D4418). Nuclear (Mayer's haematoxylin) and cytoplasmic (0.5% alcoholic eosin) staining was subsequently performed. This procedure is outlined in Table IV.

Table IV: Procedure for immunohistochemical localisation of anti-MNF 116

STEP	TREATMENT	SOLUTION	TIME
1	**Pretreatment**	pepsin (0.01%) in HCl (0.01M)	10 min (37°C)
2	**Blocking endogenous peroxidase**	H_2O_2 (0.5%) + sodium azide (0.1%) in methanol	30 min
3	**Blocking**	BSA (2%)	15 min
4	**Primary antibody**	Mouse anti-human cytokeratin (clone MNF 116) (1/1000)	120 min
5	**Blocking**	BSA (2%)	15 min
6	**Secondary antibody**	Biotinylated rabbit anti-mouse immunoglobulin (1/400) + normal human serum (1/25)	30 min
7	**Linking**	Streptavidin peroxidase conjugate (1/1000)	30 min
8	**Detection of peroxidase activity**	DAB	10 min
9	**Nuclear staining**	Mayer's haematoxylin	1 min
10	**Counter staining**	Alcoholic Eosin (0.5%)	10 sec

2.4.2 Immunohistochemical procedure for anti-Ki67 antibody

2.4.2.1 Rabbit Anti-Human Ki67 antibody

Rabbit Anti-Human Ki67 antibody (Clone: Ki-67, Isotype: IgG1) is a polyclonal antibody that reacts with an antigen present in the nucleus of proliferating human cells. Ki-67 expression occurs during the phase of the cell cycle designated as late G1, S, M and G2. However during the G0 phase, the antigen cannot be detected.

The assessment of cell proliferation by the detection of Ki67 antigen in neoplastic cell populations has been shown to be of prognostic value. The polyclonal antibody (NCL-Ki67p) labels Ki67 antigen in the granular components of the nucleolus during late G1, S, G2 and M phases (Gerdes *et al.*, 1984). There is a strong correlation between low or high Ki67 index and low or high grade histopathology of neoplasms (Gerdes *et al.*, 1987).

2.4.2.2 Immunostaining schedule for anti-Ki67 antibody

The immunostaining schedule utilised is outlined in Table V; however, the following steps varied;

a. Serum Blocking: normal goat serum blocking solution
b. Primary Antibody: Rabbit Anti-Human Ki67 (NCL-Ki67-P, Novocastra) diluted 1:3000 in PBS and incubated for 1 hour at room temperature.

c. Secondary Antibody: biotinylated Goat Anti-Rabbit IgG (BA1000, Vector Laboratories) diluted 1:500 in PBS and incubated for 30 minutes at room temperature.

d. Detection: HRP-Streptavidin (SA-5004, Vector Laboratories) diluted 1:500 in PBS for 30 minutes at room temperature.

Table V: Procedure for immunohistochemical localisation of anti-Ki67 antibody

STEP	TREATMENT	SOLUTION	TIME
1	**Pre-treatment**	Citrate buffer	20 min
2	**Blocking endogenous peroxidase activity**	H_2O_2 (0.5%) + sodium azide (0.1%) in methanol	10 min
3	**Blocking**	BSA (2%)	15 min
4	**Primary antibody**	Rabbit Anti-Human Ki67 (1:3000)	60 min
5	**Secondary antibody**	biotinylated Goat Anti-Rabbit IgG (1:500)	30 min
6	**Linking**	HRP-Streptavidin (1:500)	15 min
7	**Detection of peroxidase activity**	Diaminobenzidine	10 min
8	**Nuclear staining**	Harris haematoxylin	1 min

* Tris buffered saline used throughout

2.4.3 Cytokeratin 18 antibody isolation and specificity

Monoclonal Mouse Anti-Human Cytokeratin 18, Clone DC10 (M7010 DakoCytomation) labels epithelial expressing Cytokeratin 18 (Lane and Alexander, 1990). CK18 belongs to intermediate filaments which create a cytoskeleton in almost all cells. In contrast to other intermediate filaments Cytokeratins are made up of a highly multigene family of polypeptides with molecular masses ranging from 40-68 kDA (Moll *et al.*, 1982)

2.4.3.1 Immunostaining schedule for anti-Cytokeratin 18 antibody

The immunostaining schedule utilised is outlined in Table VI.

a. Antigen retrieval : Citrate Buffer
b. Serum Blocking: normal horse serum blocking solution
c. Primary Antibody: Mouse Anti-Human Cytokeratin 18 (Clone DC10) (DakoCytomation, M7010). Optimal dilution 1:100.
d. Secondary Antibody: Horse Anti-Mouse IgG (H+L), biotinylated (Vector Laboratories, BA-2000). Optimal dilution 1:500.
e. Detection: HRP-Streptavidin (SA-5004, Vector Laboratories) diluted 1:500 in PBS for 30 minutes at room temperature.

Table VI: Procedure for immunohistochemical localisation of Cytokeratin 18 antibody

STEP	TREATMENT	SOLUTION	TIME
1	**Pre-treatment**	Citrate buffer	20 min
2	**Blocking endogenous peroxidase activity**	H_2O_2 (3%)	10 min
3	**Blocking**	Horse serum (5%)	15 min
4	**Primary antibody**	Mouse Anti-Human Cytokeratin 18 (1:100)	overnight
5	**Secondary antibody**	Horse Anti-Mouse IgG (H+L), biotinylated (1:500)	60 min
6	**Linking**	HRP-Streptavidin (1:500)	30min
7	**Detection of peroxidase activity**	Diaminobenzidine	10 min
8	**Nuclear staining**	Mayer's haematoxylin	1 min

2.4.4 Clone M30, Cytodeath mouse IgG_{2b} antibody isolation and specificity

Clone M30, Cytodeath mouse IgG_{2b} antibody (214322/150, Roche) is obtained from Balb-c-mice. It recognises a specific caspase cleaved formalin-resistant epitope of the human cytokeratin 18 (CK 18) cytoskeletal proteins that is not detectable in native CK 18 of normal cells (Leers *et al.*, 1999). Cytokeratins, in particular cytokeratin 18 are affected in early apoptosis (Caulin *et al.*, 1997). Consequently, it is a unique tool for reliable determination of early apoptosis in tissue sections where it is specifically located cytoplasmically; however, non specific reactivity with nuclear antigens of highly proliferating cells can occur (Kronberger *et al.*, 2000; Chen *et al.*, 2001; Bantel *et al.*, 2001).

2.4.4.1 Immunostaining schedule for anti-M30 antibody

Endogenous peroxidase was blocked by incubation of sections in aqueous hydrogen peroxidase (3%). After a 10 minute wash in running tap water, antigen retrieval was performed. For this process, sections were incubated in Citric acid buffer (0.01M, pH 6.0) in a pressure cooker placed within a 570W microwave. The sections were allowed to incubate for 1-2 minute once the valve escaped. The solution was thereafter cooled in running tap water for 10 minutes and transferred to TBS-TT for 20 minutes.

This process was followed by a final rinse in TBS and the sections were then ringed with a PAP pen to create an incubation chamber. Blocking was performed with BSA (2%) and incubated for 30 minutes.

Primary antibody was diluted in 5% horse serum in TBS and incubated overnight at 4 ^{0}C (dilution 1:50; Roche). Sections were washed 3X 5 minutes in TBS-TT. The secondary antibody, a biotinylated horse anti-mouse immunoglobulin (1:200 in 5% horse serum in TBS; BA 2000-Vector) was linked to a pre-formed Avidin and biotinylated horseradish peroxidase macromolecular Complex for 45 minutes at room temperature (Vectastain *Elite* ABC Kit; PK 6100 - Vector). Detection of peroxidase activity was performed with diaminobenzidine. Nuclear (Mayer's haematoxylin) staining was subsequently performed followed by dehydration and mounting of sections with DPX. This procedure is outlined in Table VII.

2.4.5 Control

For method controls, the primary antibody was replaced with a non-immune serum of the same IgG class.

Table VII: Procedure for immunohistochemical localisation of M30 antibody

STEP	TREATMENT	SOLUTION	TIME
1	**Pre-treatment**	Citrate buffer	1-2 min
2	**Blocking endogenous peroxidase activity**	H_2O_2 (3%) in water	15 min
3	**Blocking**	BSA (2%)	30 min
4	**Primary antibody**	Clone M30, Cytodeath mouse IgG_{2b} (1:50)	Overnight
5	**Secondary antibody**	biotinylated horse anti-mouse immunoglobulin (1:200)	60 min
6	**Linking**	Avidin and biotinylated horseradish peroxidase Complex	45 min
7	**Detection of peroxidase activity**	Diaminobenzidine	10 min
8	**Nuclear staining**	Harris haematoxylin	1 min

2.5 IMAGE ANALYSIS

Image analysis is the process that extracts quantitative data from images.

2.5.1 Measurement Strategy

Initially, tissue sections were examined and areas of interest were photographed with a Nikon binocular Optiphot photomicroscope using 160 ASA colour film (Eastman-Kodak, USA). Subsequently, all fields of interest were digitised with a 3CCD Sony colour video camera interfaced with the Nikon Optiphot microscope that was linked to the Kontron Systems 300 image analysis system. For every specimen, 3 areas of the myometrium that did not contain a vein or any artery were also selected and stored. All cross sections of the spiral artery appearing on a particular slide were also included.

Areas of interest were viewed at an initial magnification of X40 prior to storage as a digital image (Fig 12a). A scale bar was then inserted on a graphics overlay and merged onto the image plane prior to storage as a 24 bit tagged image format. Due to the unavailability of a true colour densitometric setting on the KS 300 system used, all images were converted into grey images (Fig 12b). A true colour densitometric system would enable one to read the intensity of the DAB reaction as a range of brown on a colour scale. However, in the system used the intensity of the grey image is represented as numbers ranging from black (0) to white (255).

Automatic contrast adjustment of the grey image was performed on all digitised images (Fig 12c). All results reflect this uniform contrast enhancement.

The immunoreactive areas were easily detected, appearing dark grey to black on the image. These regions were segmented from the image on the basis of their grey scale. This process created a binary image (containing only 2 grey values - 0 and 255; Fig 12d) which defined the immunoreactive areas (white) to be analysed. Sometimes, filling of holes in certain selected regions or deletion of regions in a specified size range was necessary (deletion is illustrated in Fig 12e). Regions consisting of nuclei were routinely scrapped as their grey value often overlapped with that of the chromogen (DAB).

For quantitation purpose, the image was geometrically calibrated according to the initial magnification. Immunoreactive regions were expressed as a percentage of the frame area. A record of measurements was extracted from the binary image according to predefined specific features. To validate the regions measured, a draw mask (segmented areas) of the binary image was superimposed onto the original image plane (Fig 12f). Measurement values consisted of the defined measurement parameters as a data list and were stored in a database file. For vessel assessment, the area of the spiral artery wall was calculated by subtracting the area of the lumen from the area of the outer adventitial boundary (Fig 13). Trophoblast cells were expressed as a percentage of the wall area. The predefined measurement parameters and their definitions are listed below:

1. FLD COUNT :	Number of measured regions
2. FLDAREA :	Area of all regions
3. FLDAREAP (%)	Percentage area of all regions in measurement frames
4. FRAME AREA (μm^2)	Area of measurement frame
5. FRAME AREA1 ($pixels^2$)	Unscaled area of the measurement frame
6. FLDMEAND	Mean grey value of all regions
7. FLDSTDD	Grey value standard deviation in all regions
8. FLDMIND	Minimum grey value in all regions
9. FLDMAXD	Maximum grey value in all regions

Table VIII shows steps formulated in the macro drawn-up for image analysis. The macro is pictorially illustrated in Fig 12a-f. Database files were created for the myometrium and myometrial spiral arteries immunostained with MNF 116, CK18, M30 and Ki67 antibodies in both the normal and hypertensive groups. Descriptive statistics were also used and presented as FLDAREAP(%) ± SD (FLDMIND-FLDMAXD). T-tests were done in Epicalc software to make pairwise comparisons (Epicalc 2000, version 1.02). Values were considered statistically significant at a p value<0.05.

Table VIII: Steps formulated in the macro utilised for image analysis of antibody distribution

Step	Macro command
1	Tvselect"WVFG METEOR"
2	Imgdelete 1
3	Imgdelete 2
4	Imgdelete 3
5	Imgdelete 4
6	Imgdelete 5
7	Gclear 0
8	Tvlive
9	Tvinput 1
10	Imgload"d:\enbavani\masters\5600CK18x10.tif,1
11	imgRGB2grey1,2
12	Normalise2,3,5
13	Dislev 3,4,52,197,1
14	Binscrap 4,5,0,30,0
15	MSsetgeom
16	MSsetframe
17	MSsetfeat"Drawfeat"
18	MSsetfeat"FIELDFEAT"
19	MSmeasmask 5,1,"methods",1,2,10
20	MSdrawmask 5,1
21	Imgdisplay 1

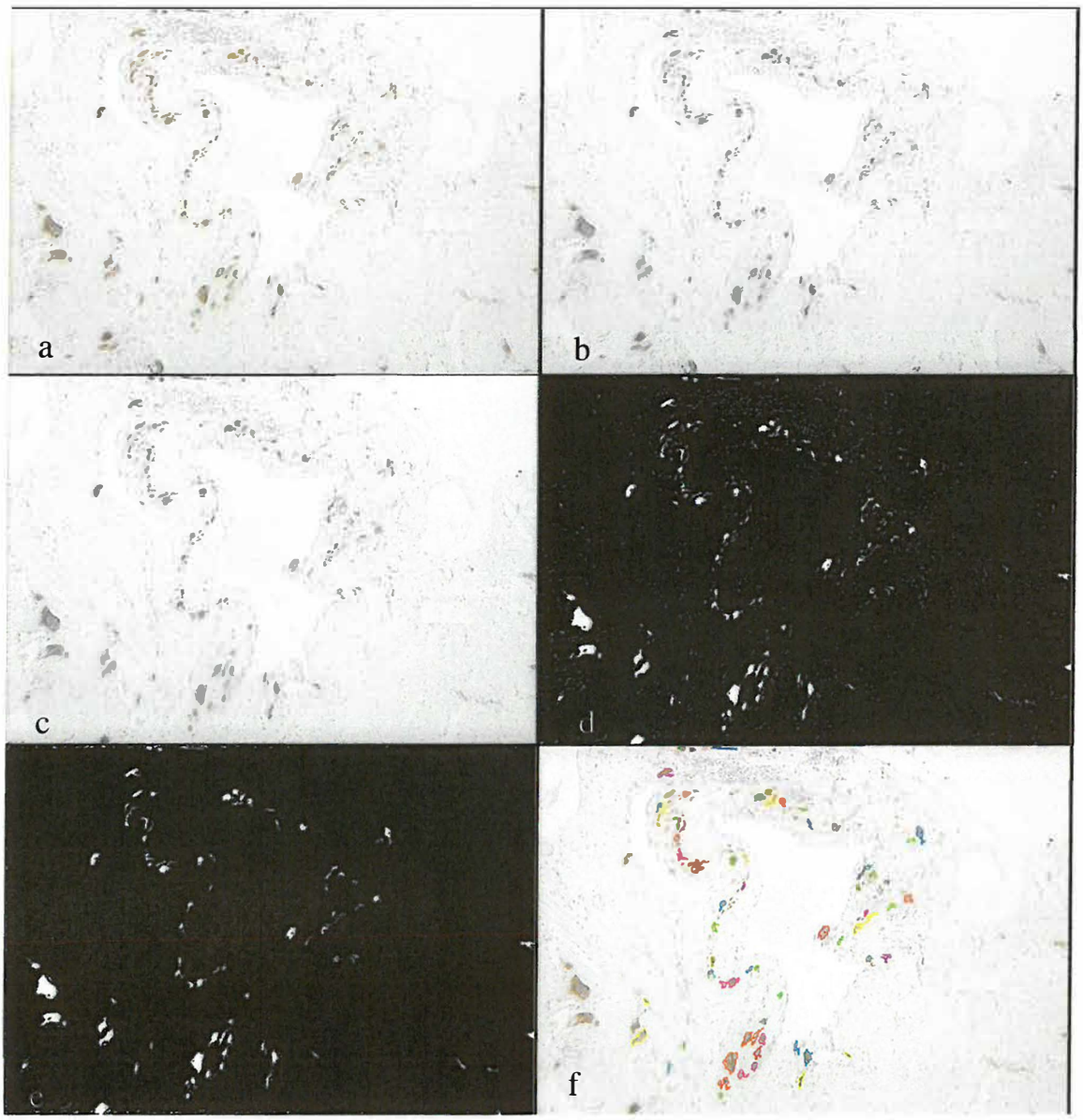

Fig 12a-f: Gallery of images of selected field for spiral artery analysis.

a-colour image of spiral artery immunoreactive CK18

b-black and white image of (a)

c-contrast enhanced black and white image of (b)

d-CK18 segmented image

e-scrapping of CK18 non-specific regions

f-image (e) overlay on image (a)

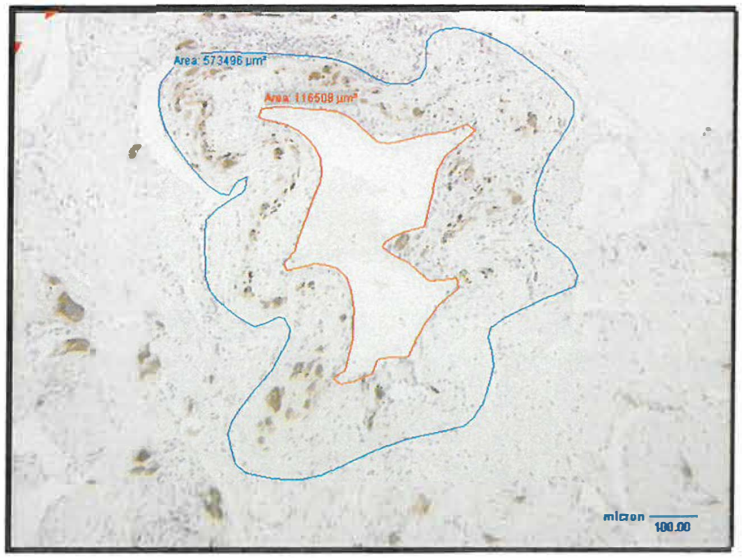

Fig 13: Computed light micrograph of spiral artery depicting segmented lumen and outer vessel wall. The area of the spiral artery wall was calculated by subtracting the area of the lumen from the area of the outer adventitial boundary.

CHAPTER 3

RESULTS

3.1 Patient Population

This retrospective study examined true placental bed biopsies obtained at caesarean section from a study population consisting of 12 women with normal pregnancies and 12 women with hypertensive pregnancies.

3.1.1 Demographic and clinical data of normotensive pregnant group

Twelve women with parity ranging 0 – 4 (mean: 2), mean age of 26 (range: 18 - 35) yrs, gestational age ≥ 30 weeks (mean: 39; range: 30 - 41 weeks) and mean gravida of 2 (range: 1 - 5) and a mean DBP of 80 ± 6 (95%CI: 74 - 79) mmHg had successful placental bed biopsies. The mean infant birth weight was 2.9 ± 0.50kg.

3.1.2 Demographic and clinical data of Pre-eclamptic group

Twelve patients with preeclampsia had a mean systolic blood pressure of 183 (95%CI: 168 - 198) mmHg and mean DBP of 115 (95%CI: 110 - 120) mmHg. The mean age of these patients were 25 (range: 17 - 33) yrs, parity ranged from 0 - 4 (mean: 1), mean gravida of 2 (range: 1 - 5) and gestational age ≥ 29 (mean: 35; range: 29 - 41) weeks.

The mean birthweight of the newborns was 2.22 ± 0.62 kg. All patients demonstrated an elevation of urinary protein (> 0.3 g/d).

Gestational ages at delivery in the pre-eclamptic group were significantly lower compared to the normotensive pregnant group ($p<0.001$). addition, all babies were born alive except for one stillbirth in the pre-eclamptic group. The clinical classification, demographic characteristics and peri-natal outcome of the two groups of patients are listed in Table IX.

Table IX: Clinical Classification of Two Groups of Patients in the study

	NORMOTENSIVE PREGNANT (n=12)	HYPERTENSIVE PREGNANT (n=12)
Age (yr)	26 (18-35)	25 (17-33)
Gestation (weeks)	39 (30-41)	35 (29-41)
Parity	2 (0-4)	1 (0-4)
Gravidity	2 (1-5)	2 (1-5)
Blood Pressure (mmHg)		
Systolic	120 ± 9*	183 ± 22
95%CI	(115 -123)	(168-198)
Diastolic	80 ± 6**	115 ± 7
95%CI	(74 - 79)	(110 -120)
Mean Birth weight (kg)	2.9 ± 0.50***	2.22 ± 0.62

* normotensive *vs* hypertensive group p< 0.0001;

** normotensive *vs* hypertensive group p< 0.0001;

*** normotensive *vs* hypertensive group p< 0.001

Results are given as mean and range

3.2 Histology of true placental bed biopsies

Histopathological examinations of tissue samples were carried out on Haematoxylin and Eosin (H&E), Periodic Acid-Schiff Reaction (PAS) and Elastic Von Gieson (EVG) stained sections. For recognition of trophoblast cell populations, an immunocytochemical staining protocol using either anti-MNF 116 or anti-Cytokeratin 18 as the primary antibody was examined.

Inclusion criteria used for histological identification of true placental bed biopsies were the presence of:

i) myometrial interstitial mononuclear cytotrophoblast,

ii) myometrial interstitial multinucleate giant cells,

iii) spiral arteries within the myometrial segment were the most striking feature used in confirming true placental bed biopsies in normal and hypertensive pregnancies.

3.2.1 Normotensive Group

All twelve placental bed biopsies contained the inclusion criteria for their classification as true placental bed biopsies. Distributed within the myometrium were spiral arteries displaying total physiological change as shown in H&E (Fig 14), PAS (Fig 15) and EVG (Fig 16) stained sections. The spiral arteries resembled sinusoids with large lumens. The walls of the spiral artery were fibrinoid in nature and lacking the typical muscular

elastic tunica media (Fig 14-16). Serial staining of sections were routinely performed (Figures 14-16).

Von Gieson's Elastic stained sections revealed the elastic content of the arterial wall to be reduced in the normotensive group compared to the hypertensive groups (Fig 16). Invading trophoblast cells as identified by MNF116 were found embedded within the fibrinoid wall of the spiral artery (Fig 17 and 18). These cells had long spider-like cytoplasmic projections (Fig 18). Sub-intimal thickening of the vessel was noted (Fig 18). The lumen was lined by endothelial cells. Endovascular trophoblasts were only observed within the lumen of one spiral artery.

Mononuclear invading trophoblast cells were observed in the myometrial interstitium occurring singly (Fig 19) or in streams (Fig 19). Multinucleated interstitial trophoblast cells often referred to as giant cells were observed in the vicinity of vessels and also occurred free within the myometrial interstitium (Fig 20 and 21). Large arcuate and small basal arteries were observed traversing the myometrium (Fig 22). Myometrial glands were also noted in some of the biopsies (Fig 23). The glandular epithelium appeared typically as cuboidal cells that displayed reactivity to the anti-cytokeratin antibody.

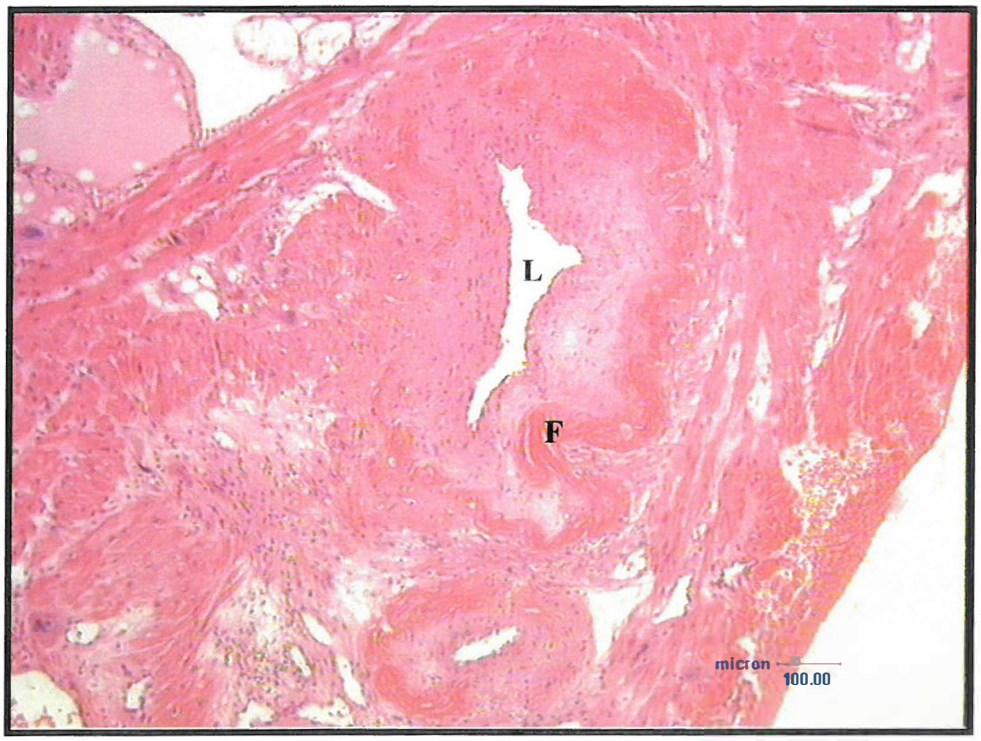

Fig 14: Micrograph showing physiologically converted myometrial spiral artery stained with H & E. Lumen (L), Fibrinoid wall (F).

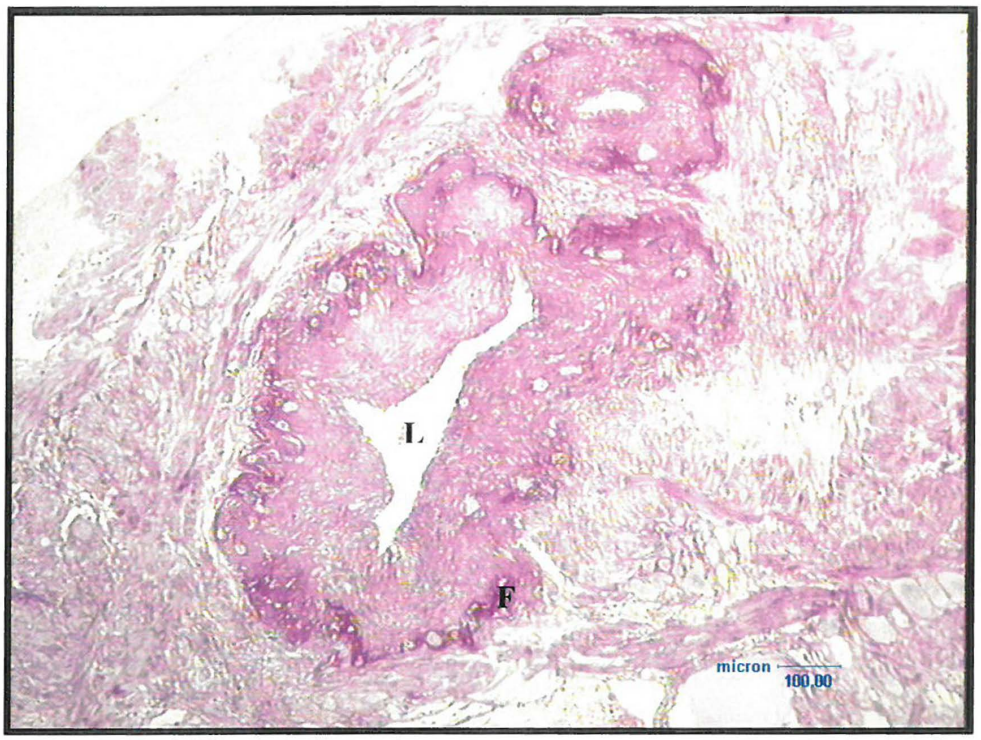

Fig 15: Micrograph showing physiologically converted myometrial spiral artery stained with PAS. Note that the orientation of section is reversed. Lumen (L), Fibrinoid wall (F).

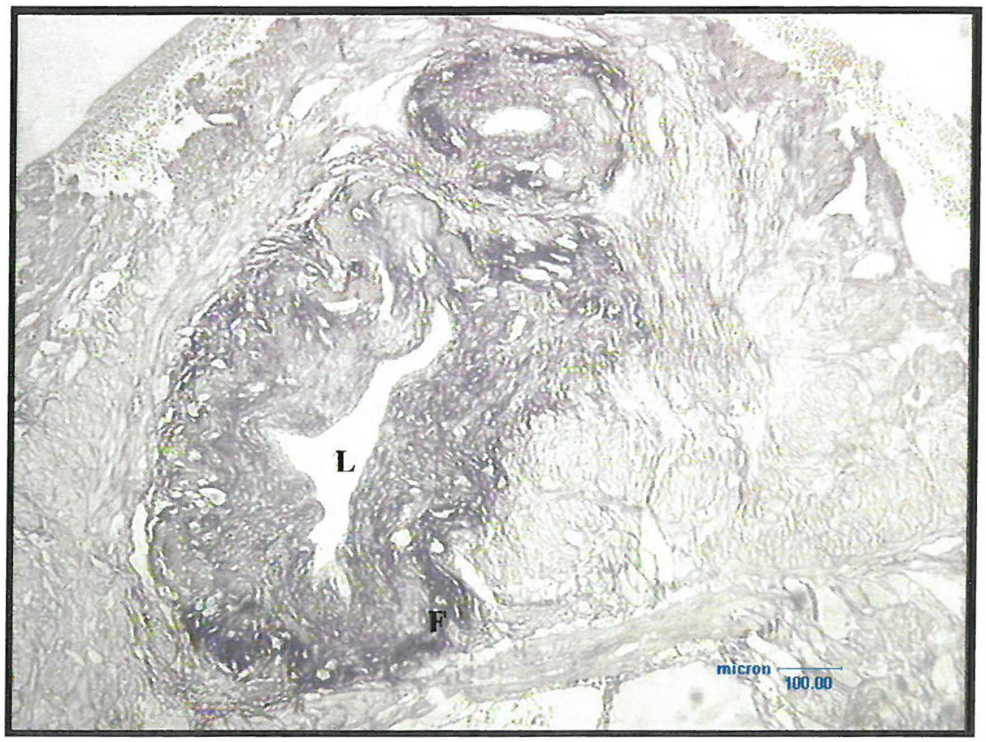

Fig 16: Micrograph showing physiologically converted myometrial spiral artery stained with EVG. Lumen (L), Fibrinoid wall (F)

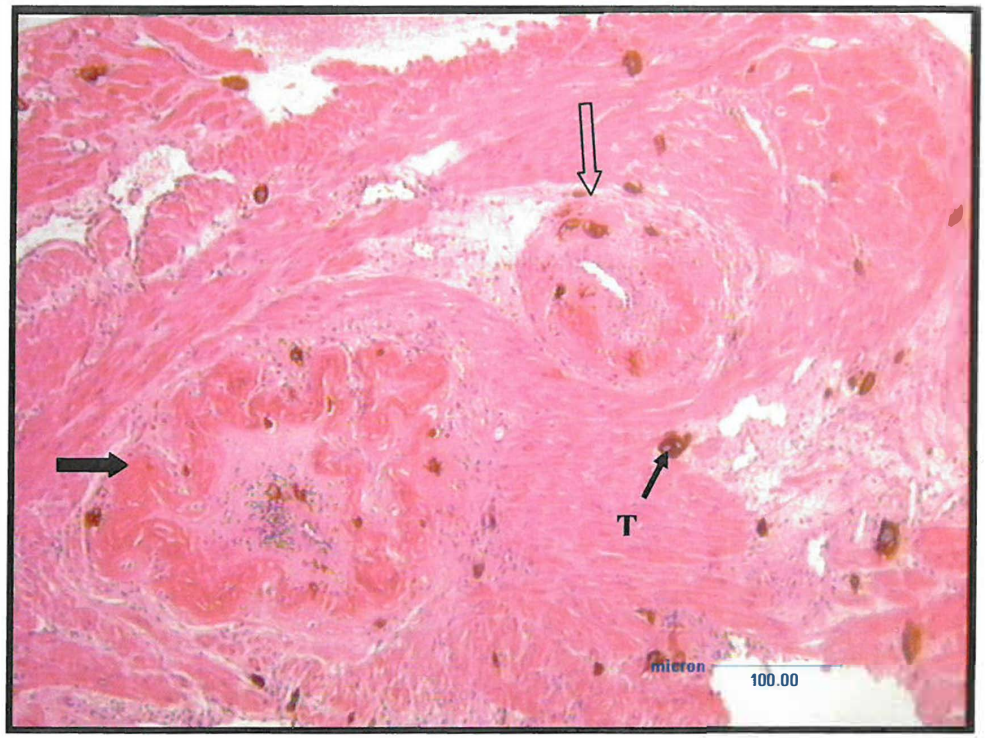

Fig 17: Micrograph immunostained with anti-MNF 116 showing total physiological conversion of spiral artery (arrow) whilst adjacent c/s of artery shows partial physiological conversion (clear arrow). Note also trophoblast cells (T).

Fig 18: High power micrograph illustrating cytoplasmic extensions (arrow) of the trophoblast cells embedded in the fibrinoid wall (F) of the spiral artery. Note lumen (L) and intimal cushion (I).

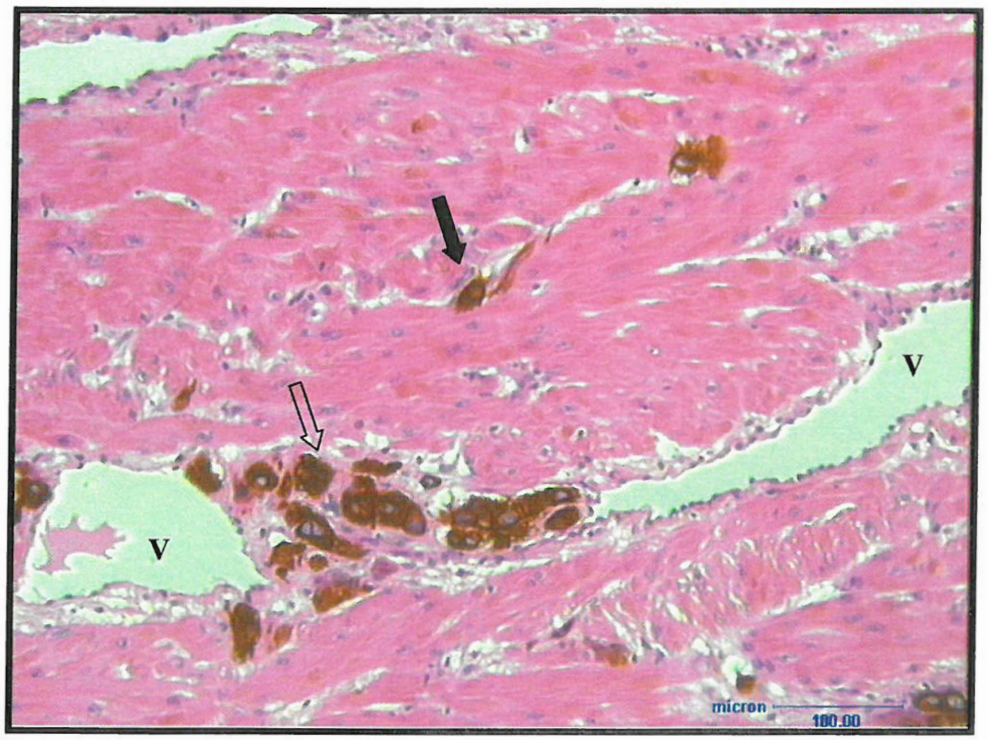

Fig 19: Micrograph immunostained with anti-MNF 116 depicting interstitial invasion of myometrium - singly (arrow) or in streams (clear arrow). Vein (V).

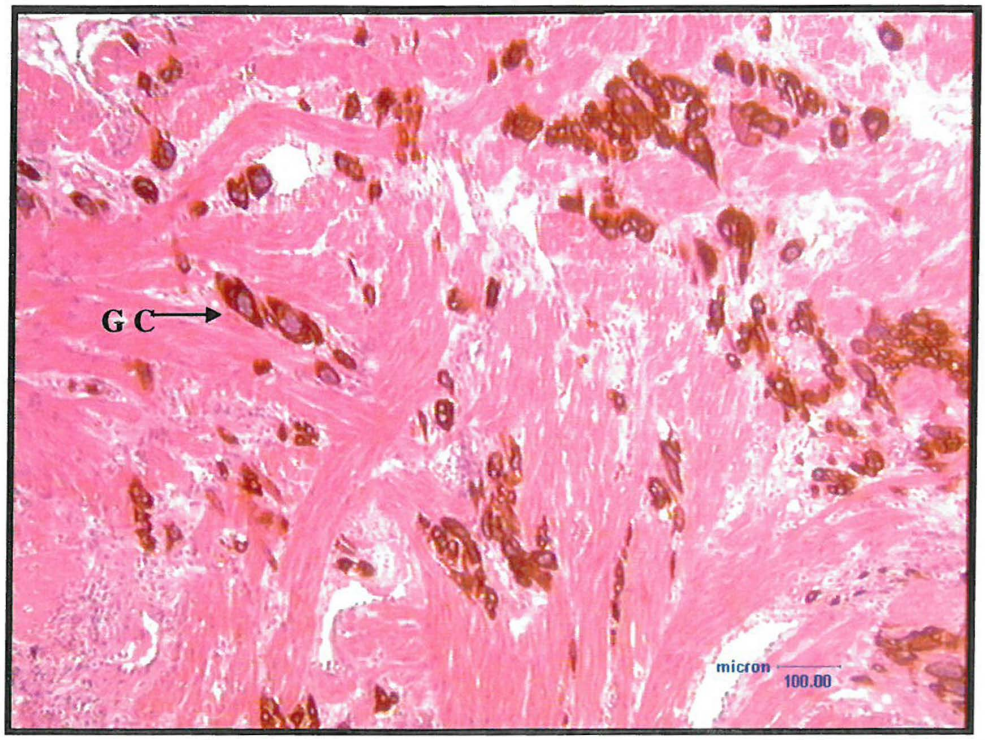

Fig 20: Micrograph immunostained with anti-MNF 116 showing myometrial interstitial invasion by trophoblast cells. Note also giant cells (GC).

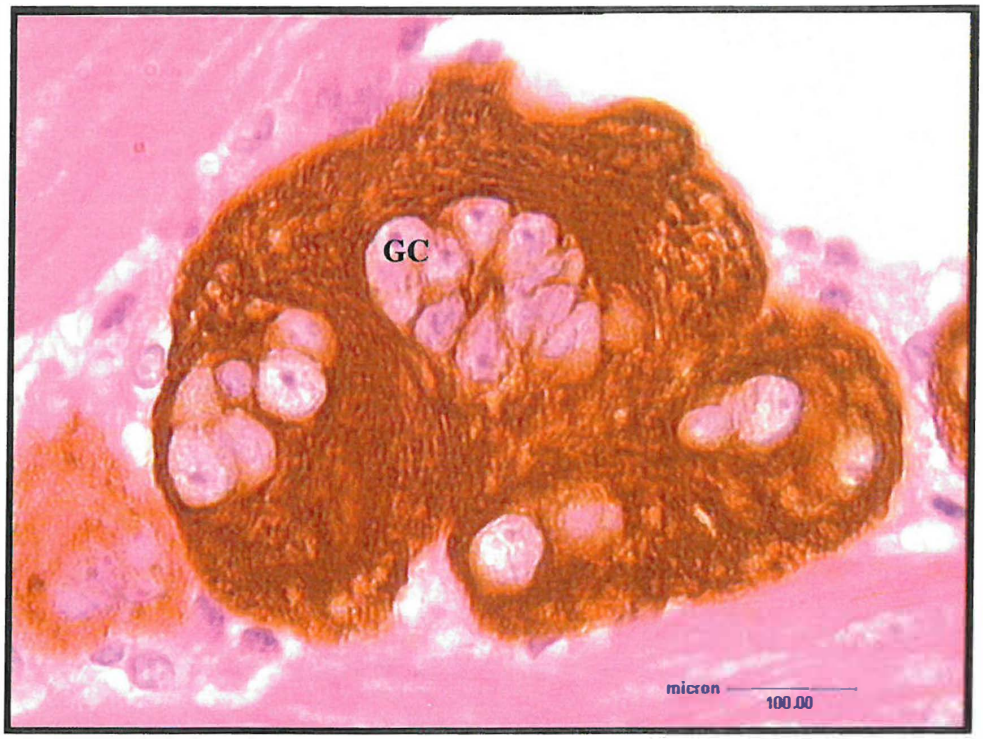

Fig 21: High power micrograph of multinucleated giant cell (GC) within myometrium immunostained with anti-MNF 116.

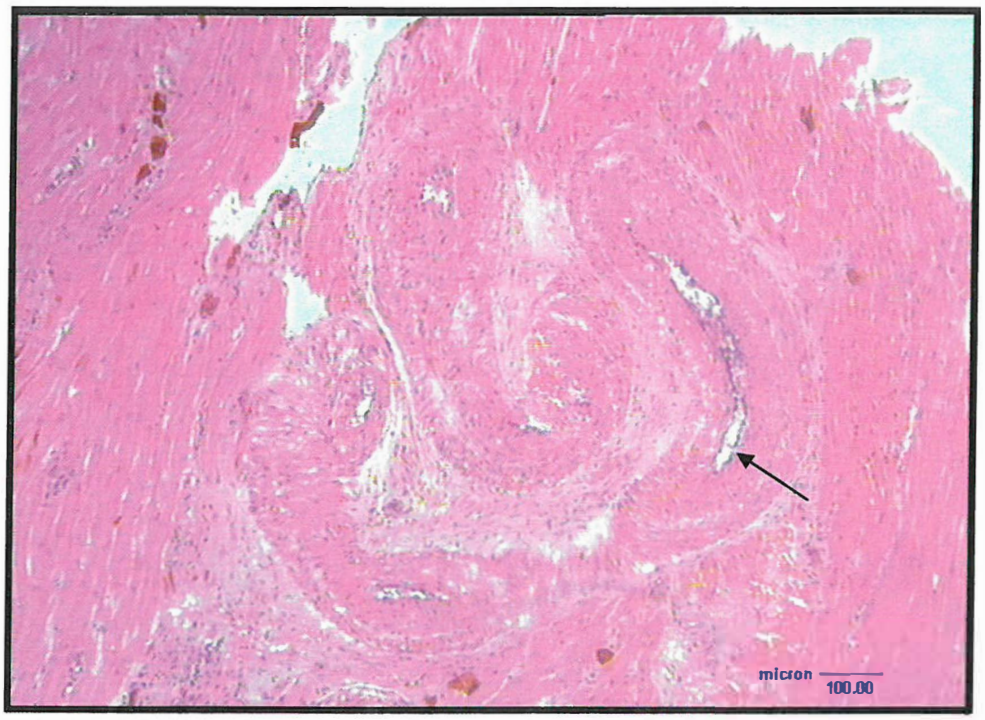

Fig 22: Micrograph immunostained with anti-MNF 116 illustrating large arcuate artery (arrow) occurring in preeclamptic group.

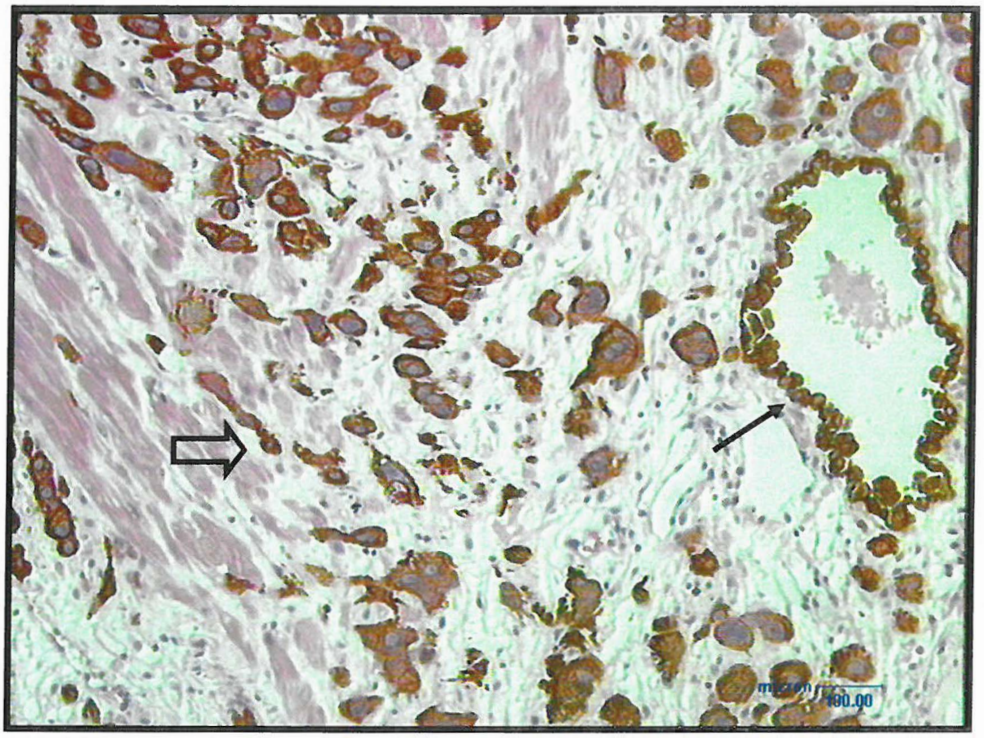

Fig 23: Micrograph immunostained with anti-MNF 116 depicting cross reactivity of primary antibody. The myometrial glandular epithelium (arrow) as well as the trophoblast cells (clear arrow) appears immunopositive.

3.2.2 Pre-eclamptic Group

All biopsies from this group that were adequate for assessment confirmed previous reports of lack of extravillous trophoblastic invasion of the spiral artery within the myometrial segment of the placental bed, that is there was an absence of physiological conversion of the spiral arteries (Fig 24) . Extensive reduction of lumen diameter was noted in these non-converted spiral arteries. Hyperplastic media of these non-converted arteries were clearly noted in H&E and PAS stained sections (Fig 25-26). Marked hyperplasia was associated with narrowing of the lumen (Fig 24-25). Perivascular mononuclear lymphocyte cell infiltrate were observed (Fig 25). Reduplication of the elastic lamina was noted in EVG stained sections (Fig 27). Endothelial vacuolation (Fig 28), intimal thickening and disorganization and hyperplasia of the media (Fig 29) were observed.

Invasive trophoblast cells as immunostained by MNF 116 were observed within the interstium of the myometrium occurring both mono and multi–nucleated (Fig 30 & 31). Other pathological features noted were acute atherosis as well as perivascular trophoblast cells (Fig 28-29). No intraluminal trophoblast cells were noted within spiral arteries. Qualitatively, it was noted that there was a decrease in interstial trophoblast cells with a concomitant increase in giant cell numbers.

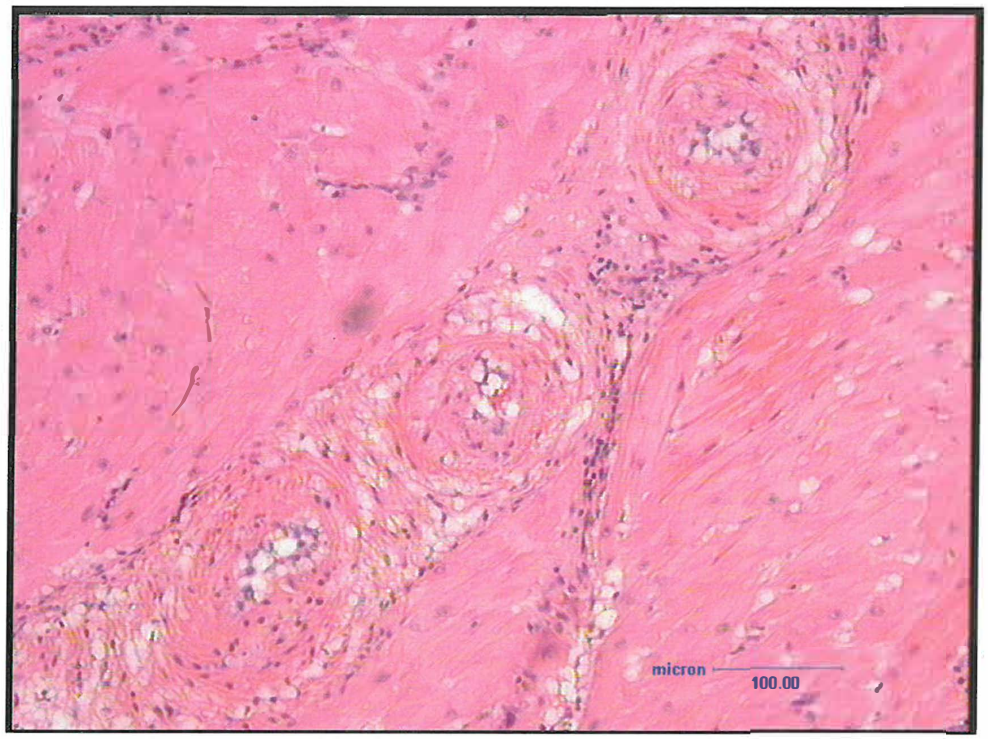

Fig 24: H&E stained section showing cluster of three myometrial spiral arteries occurring within the preeclamptic group.

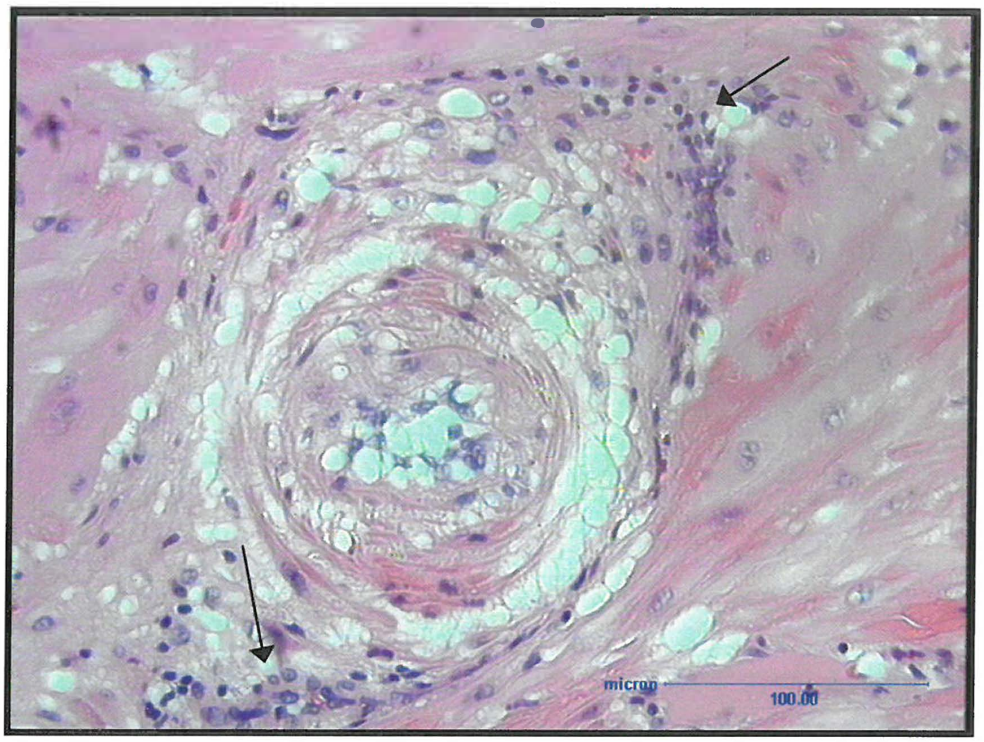

Fig 25: High power micrograph of figure above illustrating small lumen of artery, endothelial cell vacuolation and perivascular aggregation of polymorphonuclear lymphocytes (arrow).

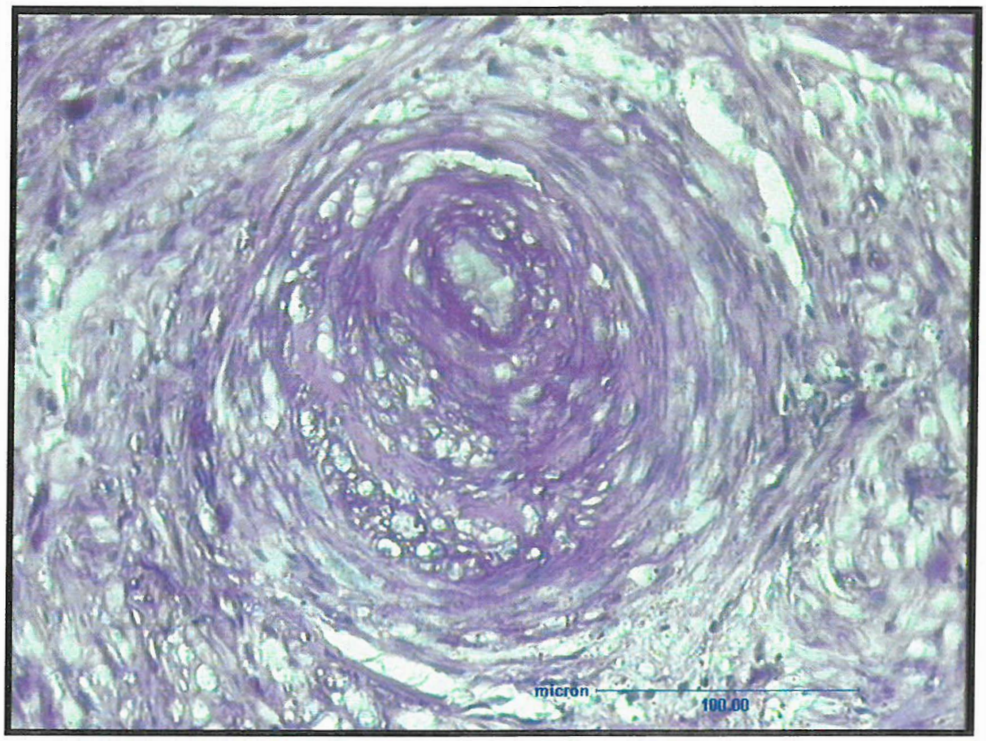

Fig 26: PAS stained section from preeclamptic group showing medial hyperplasia as well as medial disorganization of non converted spiral artery.

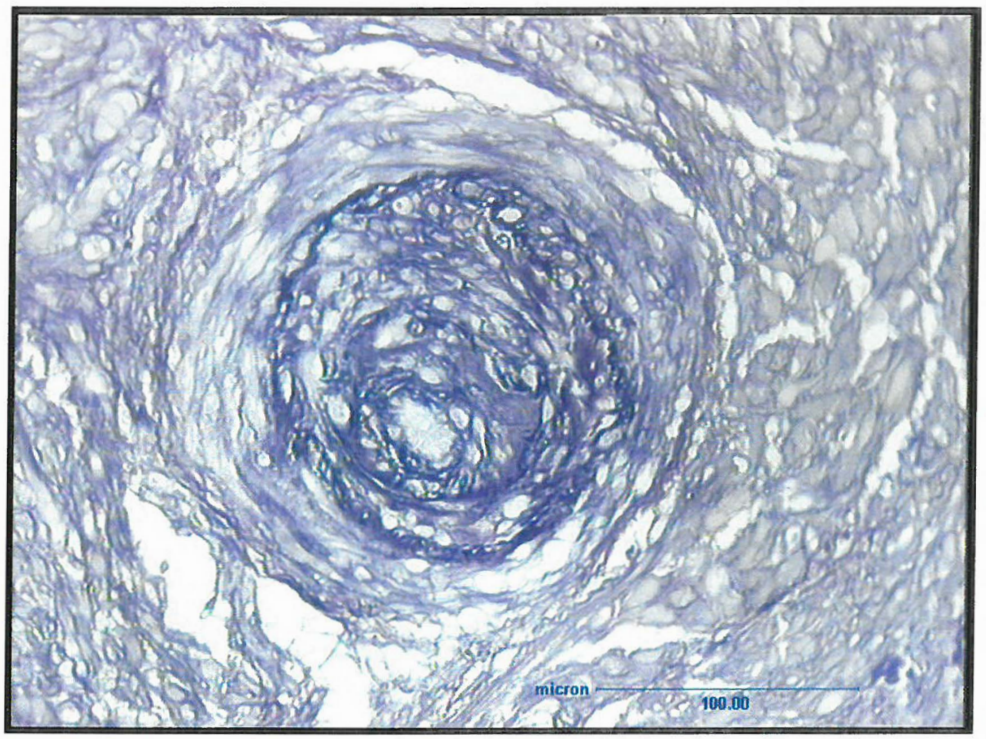

Fig 27: EVG stained section of spiral artery in pre-eclamptic group

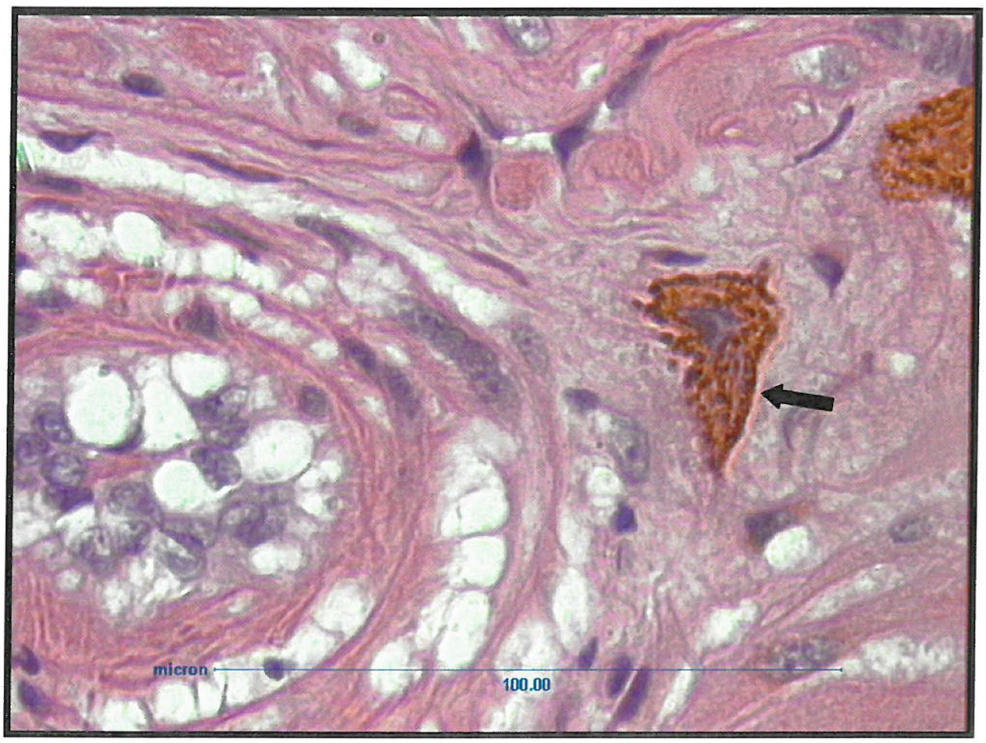

Fig 28: Micrograph immunostained with anti-MNF 116 showing perivascular localization of trophoblast cell (arrow).

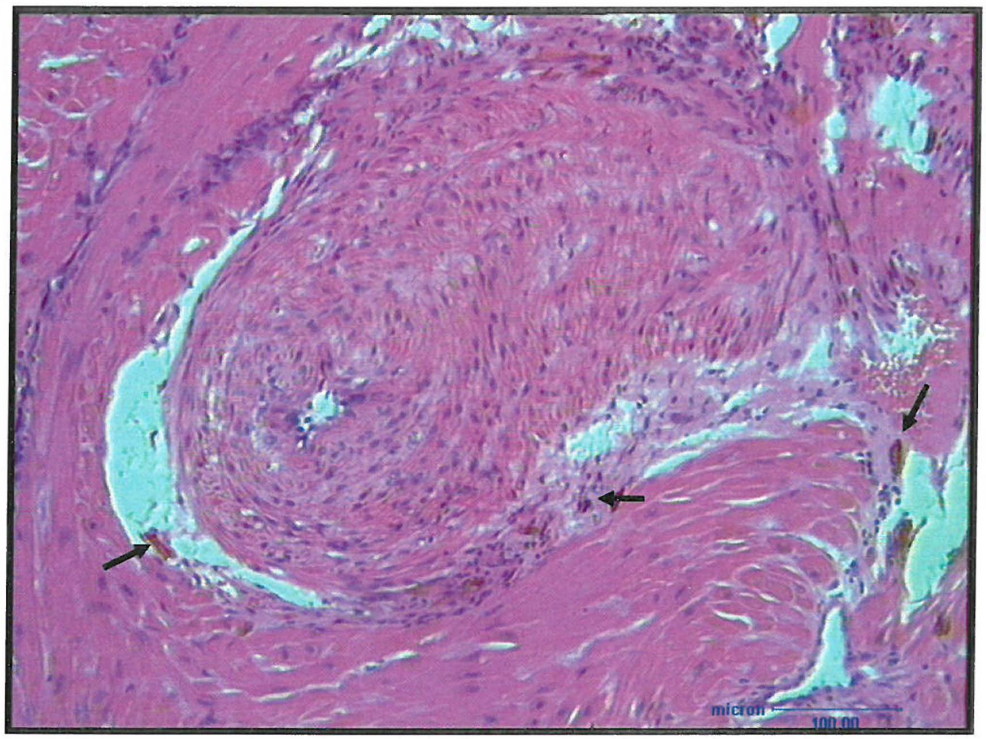

Fig 29: Micrograph immunostained with anti-MNF 116 from preeclamptic placental bed showing spiral artery with extensive hyperplasia of media and reduced lumen. Note also close peripheral proximity of trophoblast cells (arrows) to spiral artery.

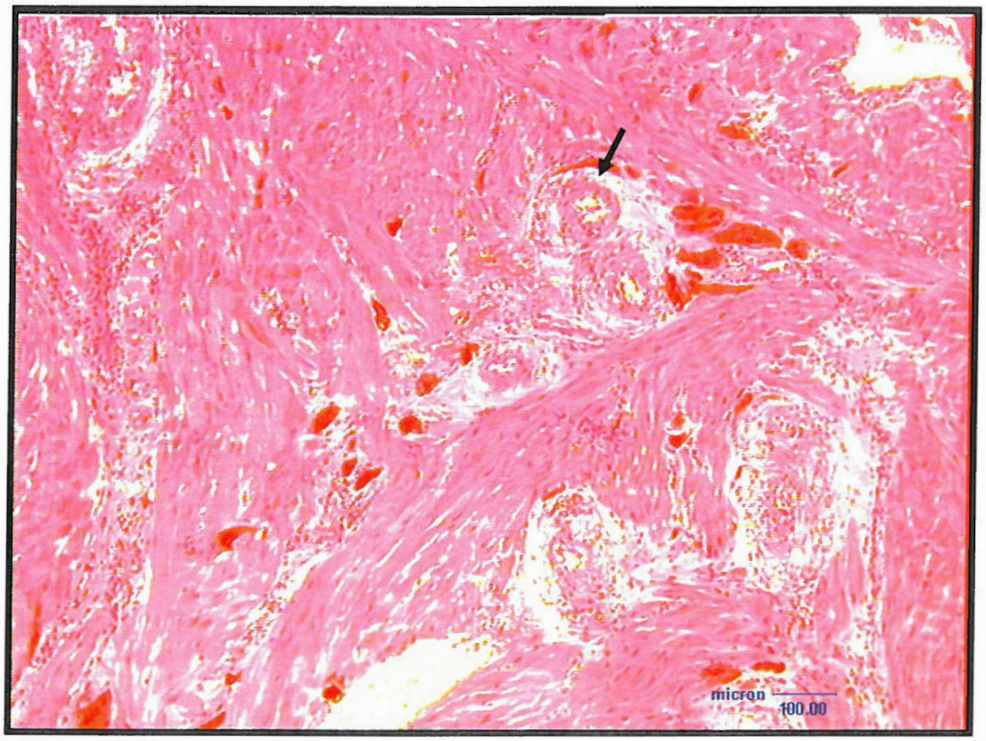

Fig 30: Micrograph immunostained with anti-MNF 116 showing basal arteries (arrow) and interstial trophoblast cells.

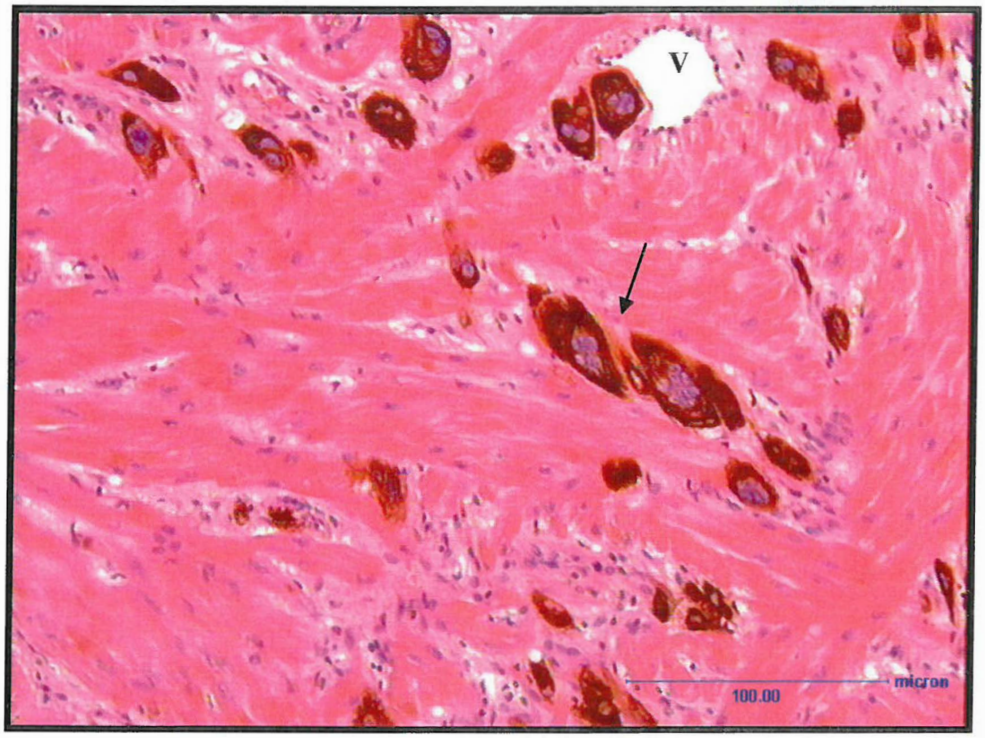

Fig 31: Micrograph immunostained with anti-MNF 116 illustrating myometrial interstitial trophoblast cells. Section shows large numbers of giant cells (arrows). Vein (V)

3.3 Anti-CK18 and anti-Ki67 Immunoreactivity

Serial sections immunostained for anti-CK18 and anti-Ki67 respectively were viewed concurrently for all samples. The anti-cytokeratin 18 *vs* anti-Ki67 immunoreactivity within placental bed of normotensive and hypertensive pregnant women is outlined in Table X.

In the normotensive pregnant group, spiral arteries that had undergone a total or partial physiological conversion displayed an intense anti-CK18 immunopositivity of intramural trophoblast cells embedded in the fibrinoid artery wall (Fig 32; 34; 36) with a concurrent total absence of immunoreactivity to Ki67 antibody (Fig 33; 35; 37). No immunoreactivity of the fibrinoid wall was observed for both antibodies.

Endothelial cells lining spiral arteries that had undergone a physiological change were non-reactive to anti-Ki67 (Fig 33; 35; 37) However in one specimen that displayed endovascular trophoblast cells within the lumen of a spiral artery (Fig 36), the endothelial cells displayed intense reactivity to anti-cytokeratin 18 (Fig 36). Both the endovascular trophoblast cells as well as the endothelial cells appeared non-reactive to anti-Ki67 (Fig 37). Perivascular cytotrophoblast cells were strongly immunoreactive to anti-CK18 but non-reactive to anti-Ki67 (Fig 38-39).

In the pre-eclamptic group, spiral arteries with extensive hyperplasia displayed absence of reactivity to anti-cytokeratin 18 (Fig 38 & 39). However, a nil to mild anti-Ki67 immunoreactivity was occasionally noted (Fig 40 & 41). Distinct immunoprecipitation

of anti-Ki67 were observed in smooth muscle cells of the microvasculature (Fig 42-45). In addition, the endothelial cells lining these small calibre lumens displayed an absence of immunoreactivity to anti-Ki67 (Fig 43 & 45).

Both mononuclear and multinucleated trophoblast giant cells, displayed intense immunostaining reaction to anti-CK18 with an absence of immuno-reactivity to anti-Ki67 (Fig 42-45).

For both antibodies, substitution of the primary antibody with non-immune sera of the same IgG species as the primary antibody produced an absence of reaction product (Fig 46 & 47).

In summary, immunocytochemical detection of anti-Ki-67 indicated no significant differences in the extravillous trophoblast proliferation within the myometrium of the placental beds of normal and pre-eclamptic beds. However, smooth muscle cells of the small caliber microvasculature were immunostained with Ki67, indicating proliferation of these cells. The multinucleated trophoblast cells in both groups demonstrated an absence of proliferation.

Table X: anti-Cytokeratin 18 *vs* anti-Ki67 Immunoreactivity within placental bed of normotensive and hypertensive pregnant women

	Normotensive		Hypertensive	
	Ck18	Ki67	Ck18	Ki67
Trophoblast cells in wall of converted spiral artery	+	-	+	-
Fibrinoid of converted spiral artery	-	-	-	-
Endothelial cell of spiral artery	+ *	-	-	-
Smooth muscle cell of non converted spiral artery	-	-	-	+
Perivascular trophoblast cell	+	-	+	-
Interstitial mononuclear trophoblast cells	+	-	+	-
Interstitial multinucleated trophoblast cells	+	-	+	-
Microvascualture- smooth muscle cells	-	+	-	+

* Feature noted in one spiral artery

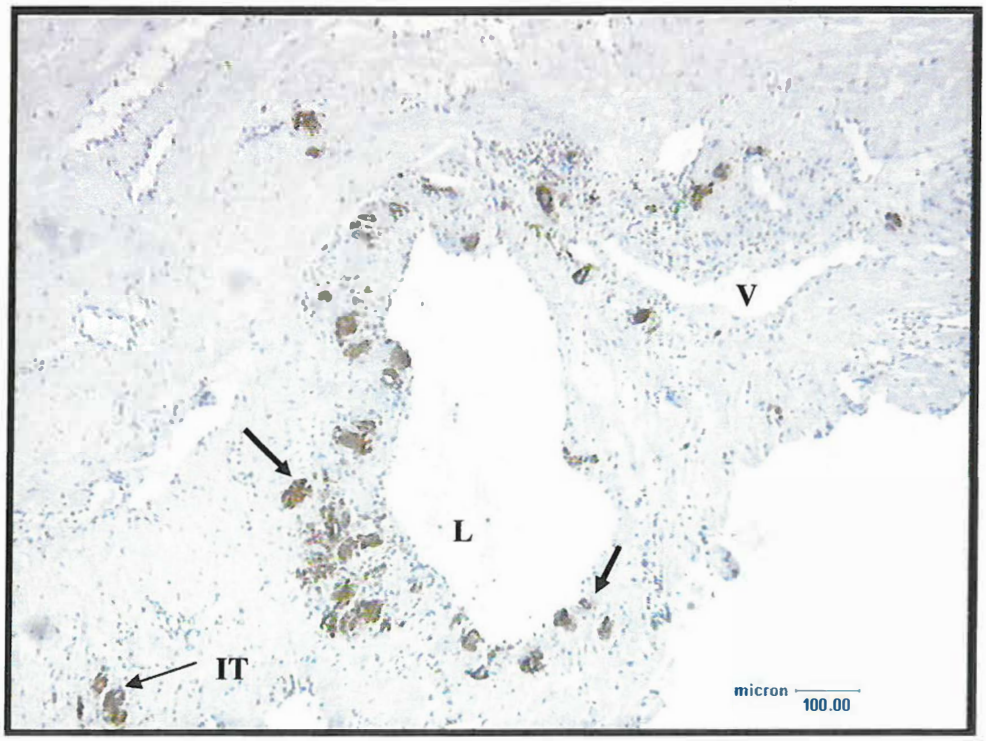

Fig 32: Physiologically converted spiral artery from placental bed of normotensive patient immunostained with anti-CK18. Note trophoblast cells (arrow) in fibrinoid wall as well as myometrial interstitial trophoblast cell (IT). Lumen (L), vein (V).

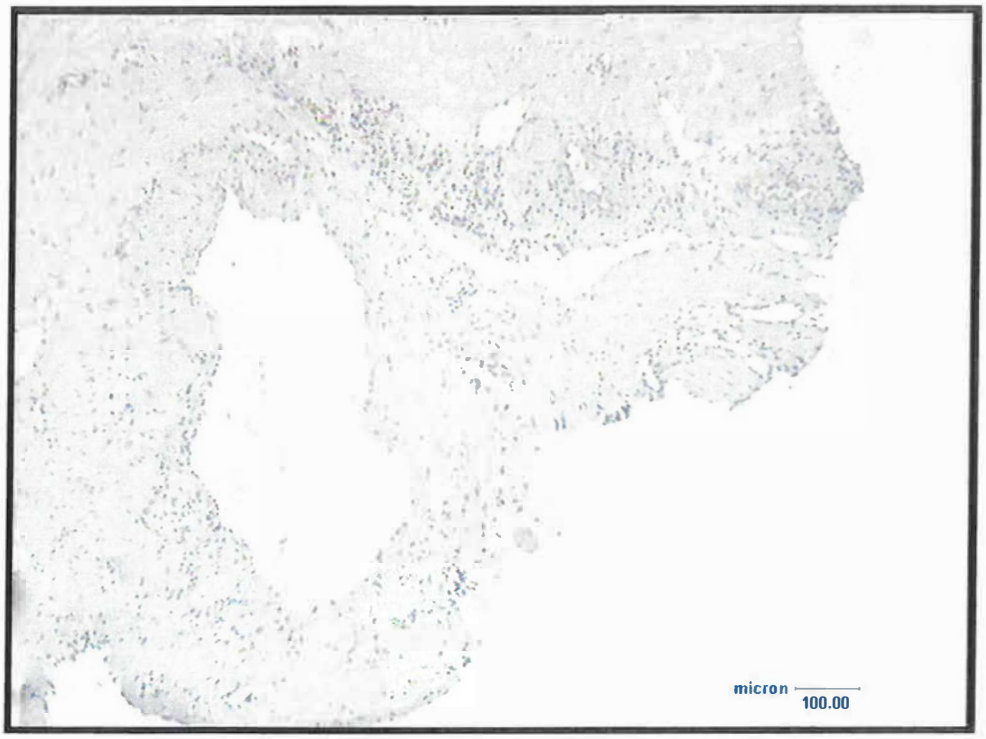

Fig 33: Serial section of Fig 32 immunostained with anti-Ki67 showing total absence of immunoreactivity in the trophoblast cell sub-populations.

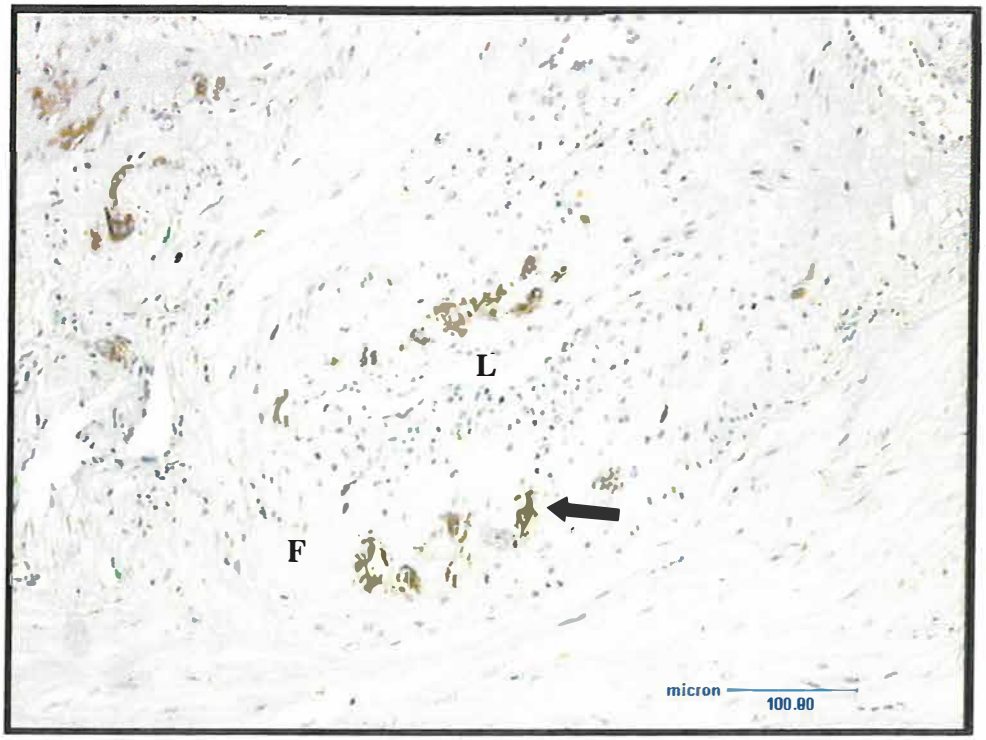

Fig 34: Spiral artery with partial physiological conversion immuno-stained with anti-CK18. Note immunoreactivity of trophoblast cells (arrow) in wall of spiral artery. Fibrinoid (F); lumen (L)

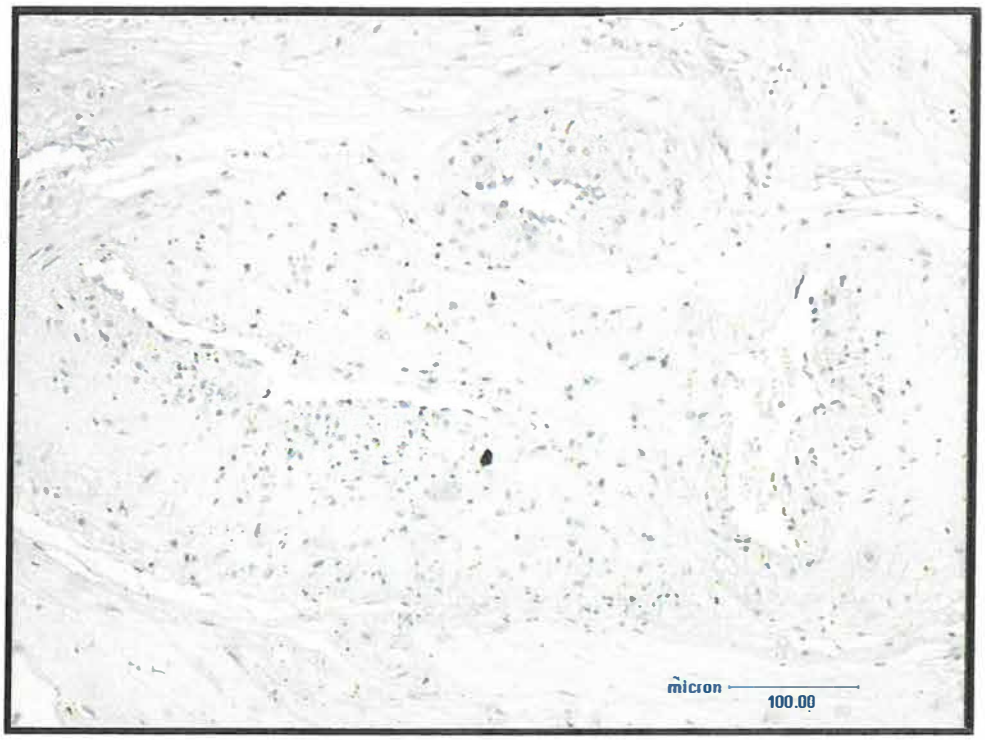

Fig 35: Serial section of Figure 34 illustrating non-reactivity of trophoblast cells in spiral artery to anti-Ki67.

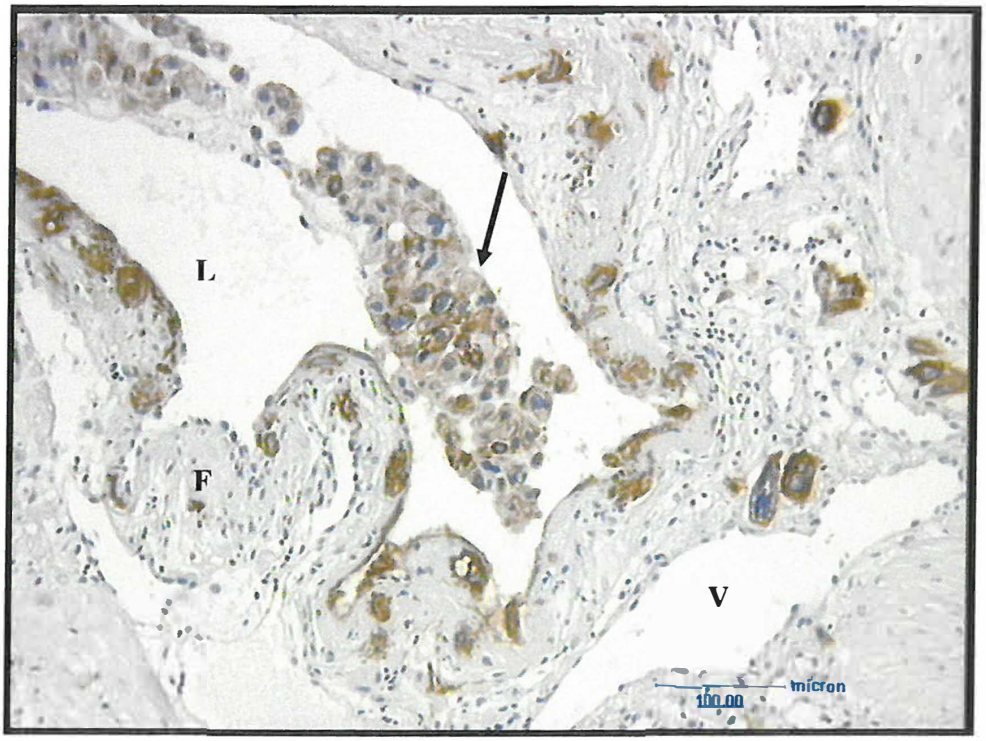

Fig 36: Cytokeratin positive section illustrating portion of physiologically converted spiral artery with Lumen (L) infiltrated by endovascular trophoblasts (arrow). Vein (V), fibrinoid wall (F)

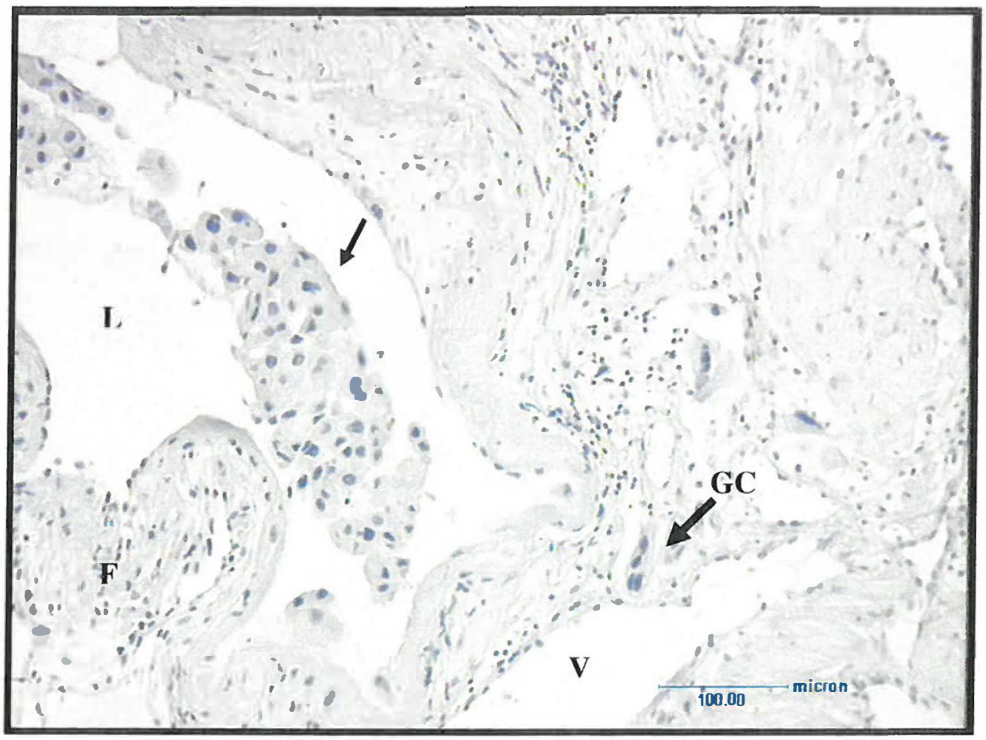

Fig 37: Serial section of Figure 36 illustrating non-reactivity of endovascular trophoblast (arrow) within lumen of spiral artery immunostained for Ki67. Note fibrinoid wall (F) and giant cell (GC). Lumen (L); vein (V)

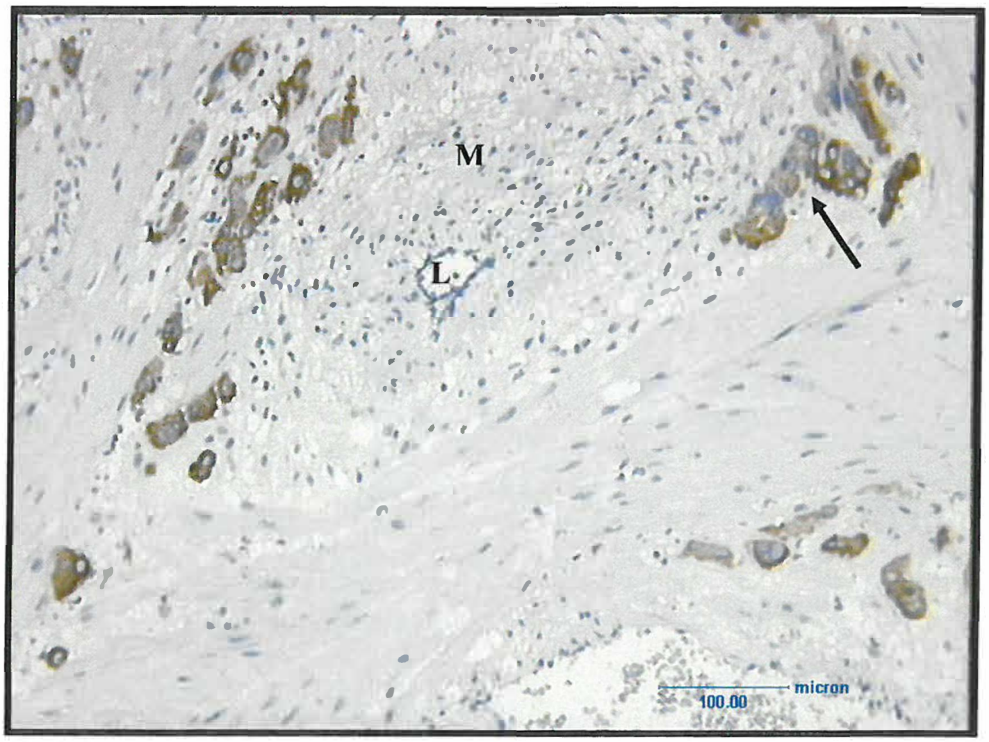

Fig 38: Cytokeratin positive section of non-physiologically converted artery from hypertensive patient illustrating reactivity of perivascular trophoblast (arrow), hyperplasia of media (M) and reduced lumen (L).

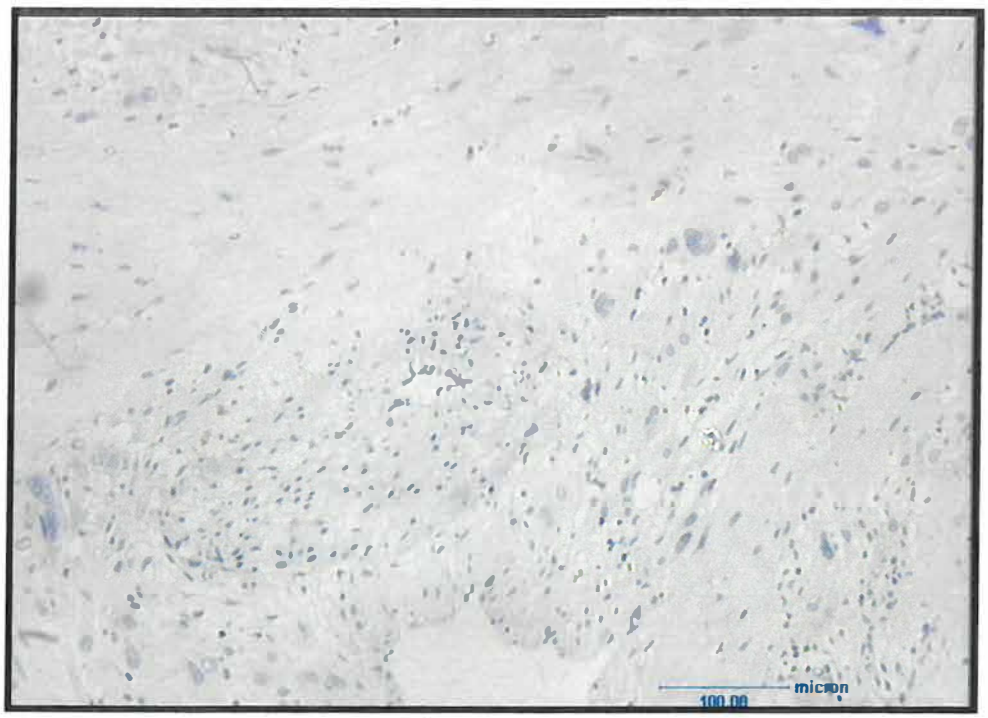

Fig 39: Deeper serial section of Figure 38 illustrating non-reactivity of anti-Ki67 within nonconverted spiral artery.

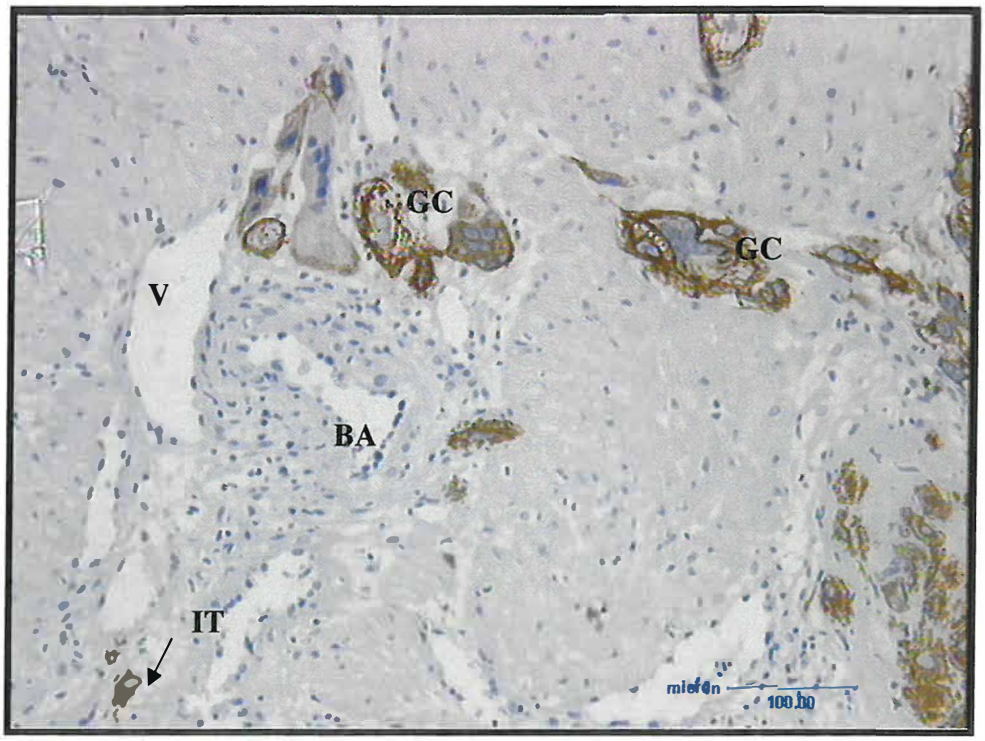

Fig 42: Section immunostained with anti-CK 18. Note giant cells (GC) as well as interstitial trophoblast cell (IT). Vein (V), basal artery (BA)

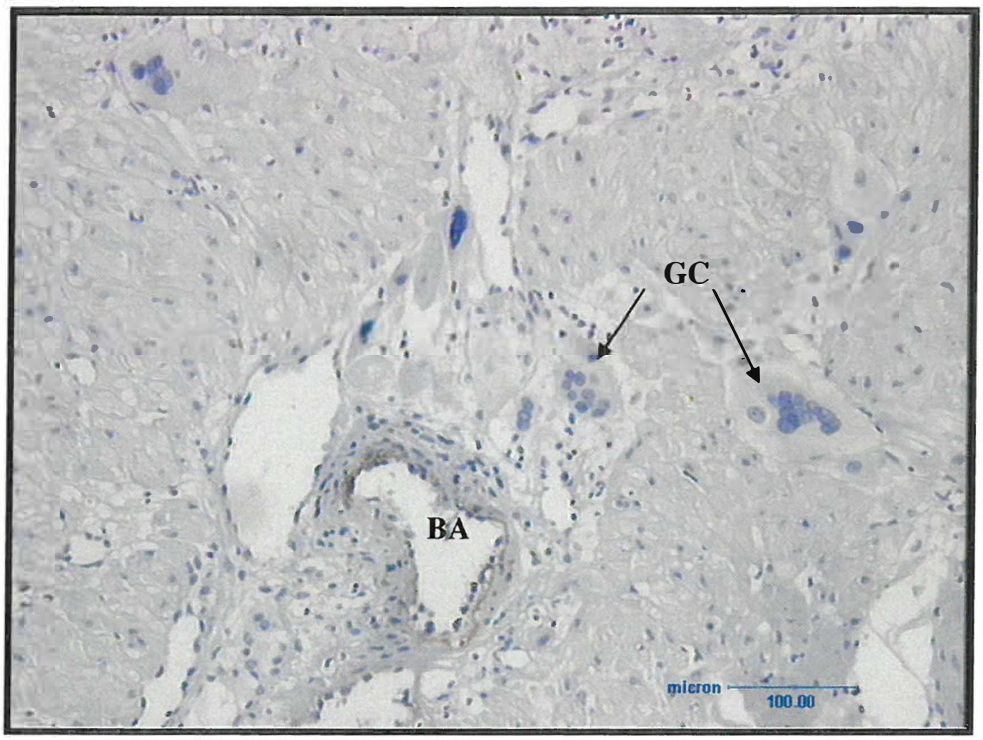

Fig 43: Serial section of Figure 42 immunostained with anti-Ki67. Note absence of immunoreactivity within non invasive trophoblast giant cells (GC) and moderate reaction product (arrow) in the smooth muscle cells of basal artery.

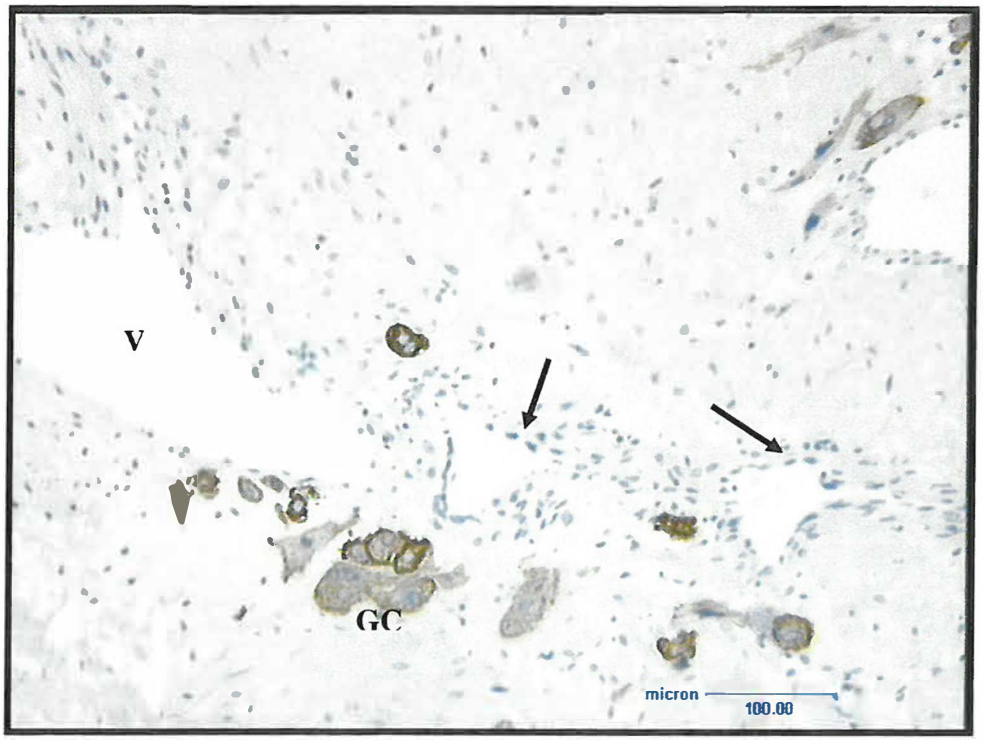

Fig 44: Micrograph of myometrium immunostained with anti-CK18. Note giant cells (GC) immunoreactive to anti-CK18. Vein (V), basal artery (arrow).

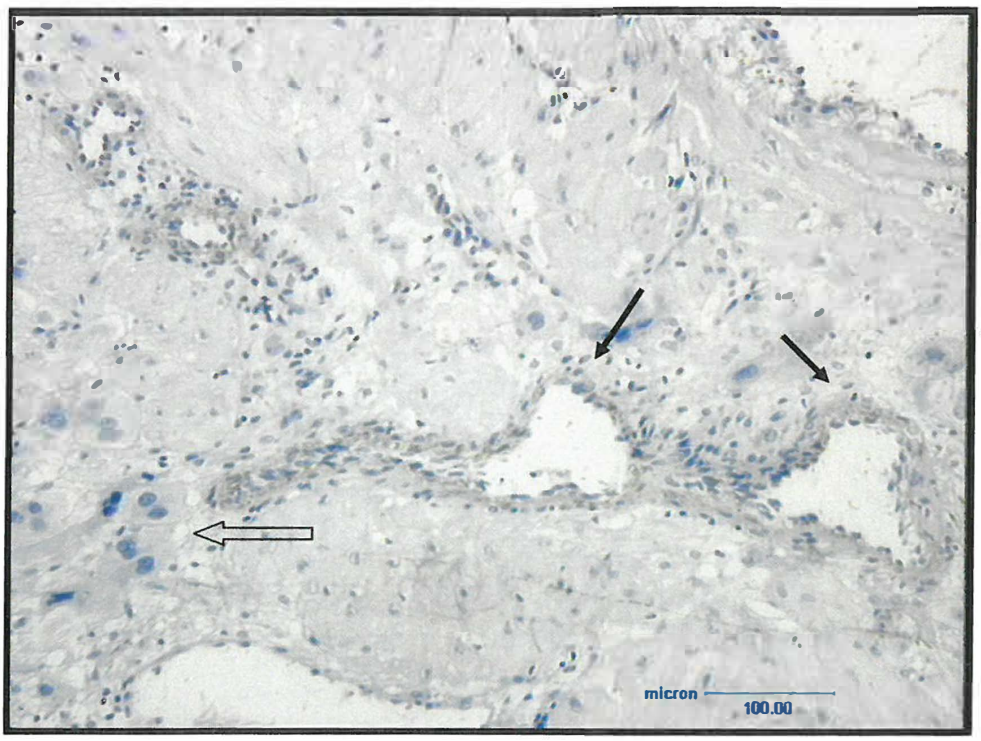

Fig 45: Serial section of Figure 44 showing non-reactive giant cells (clear arrow) with moderate Ki67 immunoreactivity (arrow) of smooth muscle cells of basal artery.

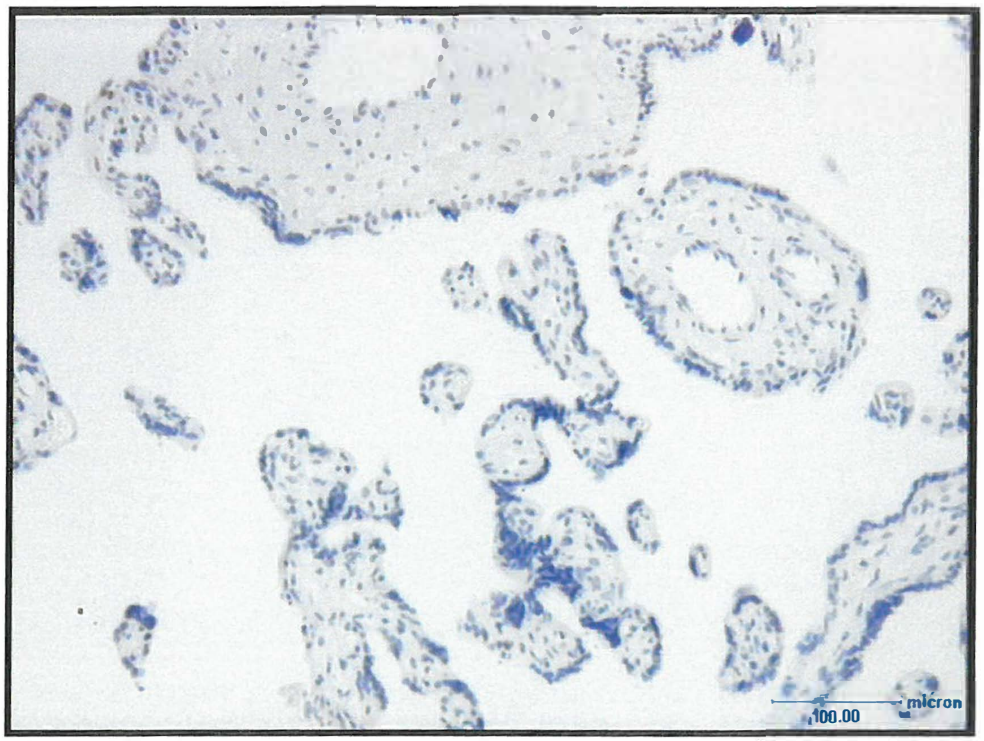

Fig 46 Method control for anti-CK18

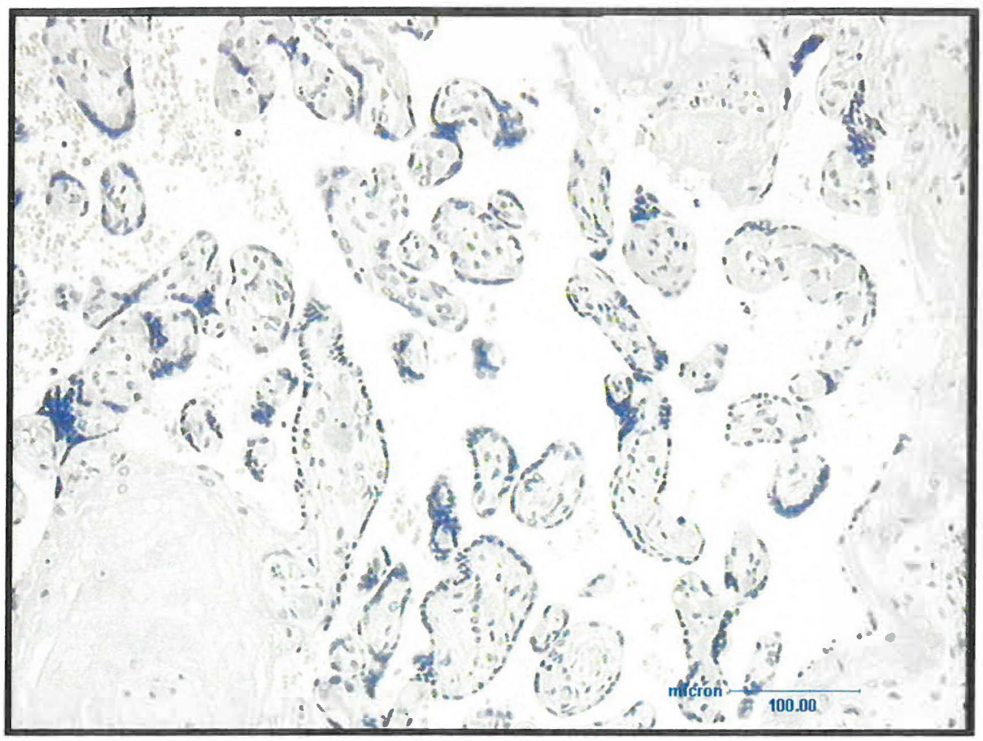

Fig 47: Method control for anti-Ki67

3.4 Anti-CK18 and anti-M30 Immunoreactivity

The distribution of anti-CK18 *vs* anti-M30 immunoprecipitation pattern within the placental bed of normotensive and hypertensive pregnant women is outlined in Table XI. On serial sections immunostained with anti-CK18 and anti-M30 (Figures 48-49 and 50-51 respectively), the profiles of spiral arteries were visualised and assessed. In both study groups, trophoblast cells were immunopositive for anti-CK18, but qualitatively reduced for anti-M30. Intramural trophoblast cells embedded within the fibrinoid wall of spiral arteries that are immunoreactive to M30 antibody is shown in Fig 49 and 51 compared to a non-reaction in the pre-eclamptic group (Fig 55).

In both study groups mononuclear and multinucleated interstitial trophoblast cell profiles were immunoreactive for anti-CK18 but varied for M30 (Fig 52-53 and 56-57 respectively).

Substitution of the primary antibody with non-immune sera of the same IgG class produced no reactivity (Fig 46 and 58).

3.4.1 Image analysis of anti-CK18 relative to M30 immunoexpression

Morphometric image analysis of anti-CK18 and M30 immunoexpression within trophoblast cells embedded in the fibrinoid wall of the spiral artery within normotensive groups was performed. The area of the wall of the spiral artery (C) was calculated by subtracting the lumen (B) area from the entire artery diameter using the outer adventitial vessel boundary (A). The area of the wall of the spiral artery of the normotensive group

was 311729 ± 51180 μm^2 compared to a significant decrease in area of 35795 ± 8045 μm^2 in the preeclamptic group ($p < 0.0001$). The lumen of the spiral artery was significantly decreased in the preeclamptic group compared to the normotensive (657 ± 106 μm^2 *vs* 102379 ± 60045 μm^2 respectively, p=0.000007; Table XII). The reduction in the area of spiral artery in the normotensive group compared to the pre-eclamptic group is illustrated in Fig 59.

The mean field area of trophoblast cells (anti-CK18) embedded within the fibrinoid wall of the spiral wall artery in the normotensive group was 13 ± 5 % compared to 0% in the non-converted spiral arteries of the preeclamptic group ($p < 0.0001$). The intensity profile varied from 0 - 230 DensUnit. M30 distribution on corresponding serial sections were 2.5 ± 0.7% with an intensity profile of 0 - 154 DensUnit for the normotensive group with an absence (0%) of reactivity in the non-converted spiral artery ($p < 0.0001$).

The mean field area of the interstitial trophoblast (anti-Ck18) invasion in the preeclamptic group was 2.87 ± 0.5% compared to 10.79 ± 4.2% in the normotensive group ($p < 0.0001$). However the serial sections immunostained with M30 showed elevation of apoptotic invasive interstial trophoblast in preeclamptic compared to the normotensive group (1.9 ± 0.5% *vs* 0.8 ± 0.3%; p=0.001). Figure 60 schematically illustrates the reduction of trophoblast cells in the normotensive group compared to the preeclamptic group. It also illustrates the elevation of apoptosis in the preeclamptic group.

Table XI: Cytokeratin 18 *vs* M30 Immunoreactivity within placental bed of normotensive and hypertensive pregnant women

	Normotensive n=12		Hypertensive n=12	
	Ck18	M30	Ck18	M30
Trophoblast cells in wall of spiral artery	+	+/-	-	-
Fibrinoid of spiral artery	-	-	-	-
Endothelial cell of spiral artery	-	-	-	-
Perivascular trophoblast cell	+	+/-	+	+/-
Interstitial mononuclear trophoblast cells	+	+/-	+	+/-
Interstitial multinucleated trophoblast cells	+	+/-	+	+/-

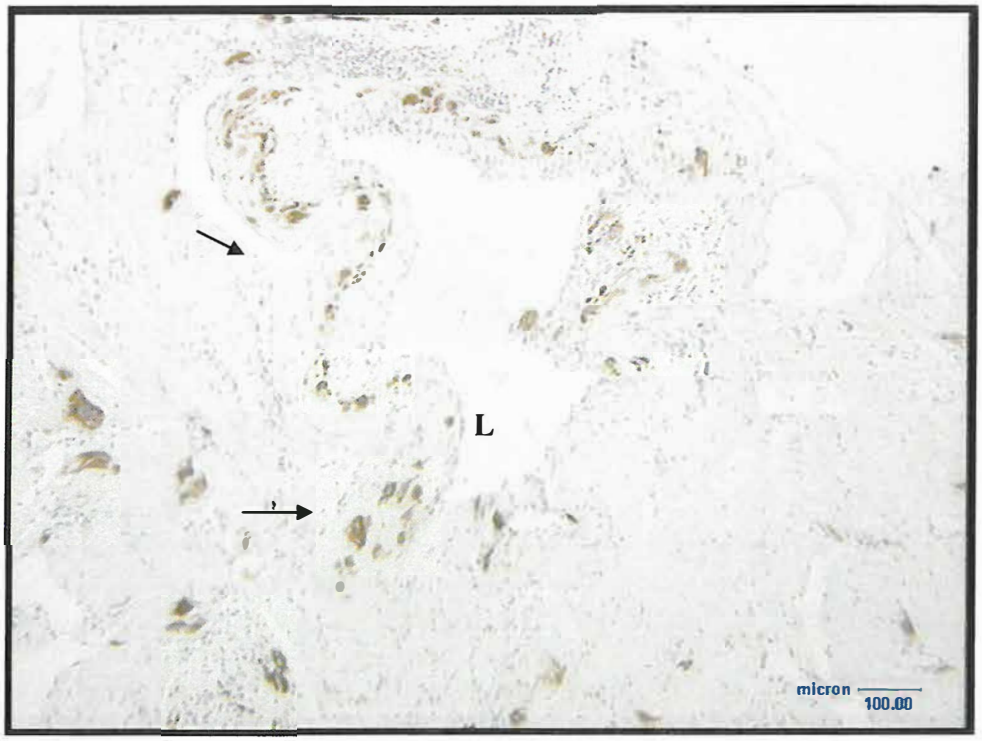

Fig 48: Micrograph illustrating anti-CK18 immunoreactivity within trophoblast cells (arrow) embedded in fibrinoid wall of spiral artery with total physiological conversion from normotensive placental bed. Lumen (L)

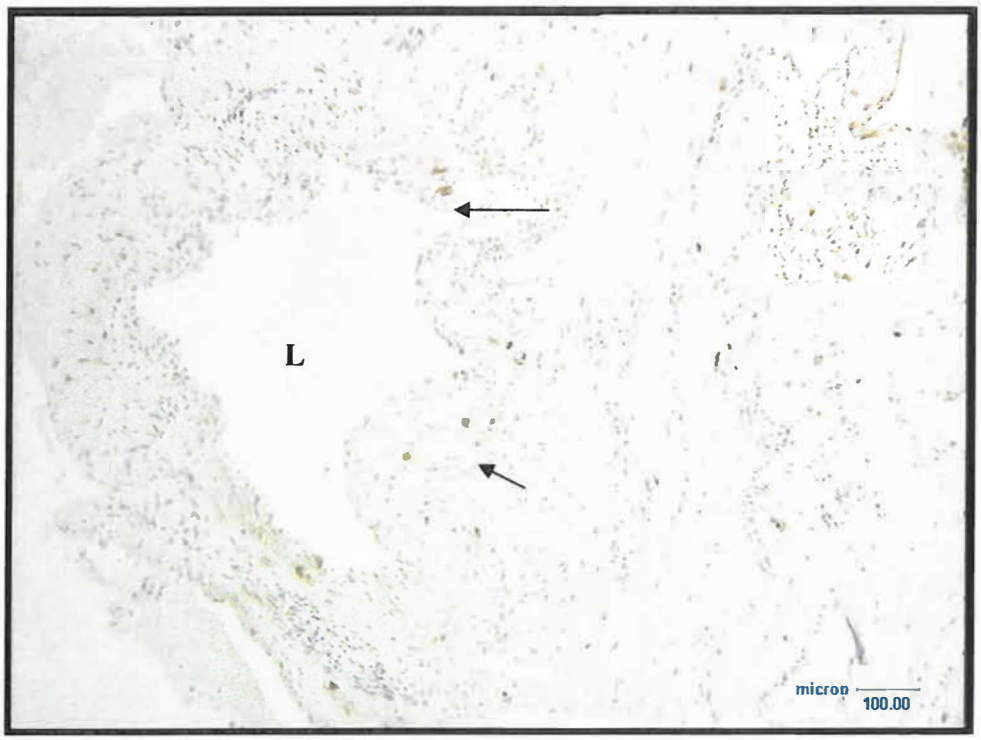

Fig 49: Serial section of Figure 48 immunostained with anti-M30. Few trophoblast cells (arrow) are immunoreactive to M30.

Fig 50: Micrograph of cross sections through loops of spiral arteries. Note immunoreactivity of trophoblast cells to anti anti-CK18 (arrow). Lumen (L).

Fig 51: Mild to moderate immunoreaction product within trophoblast cells embedded within fibrinoid wall of spiral artery of normotensive placental bed.

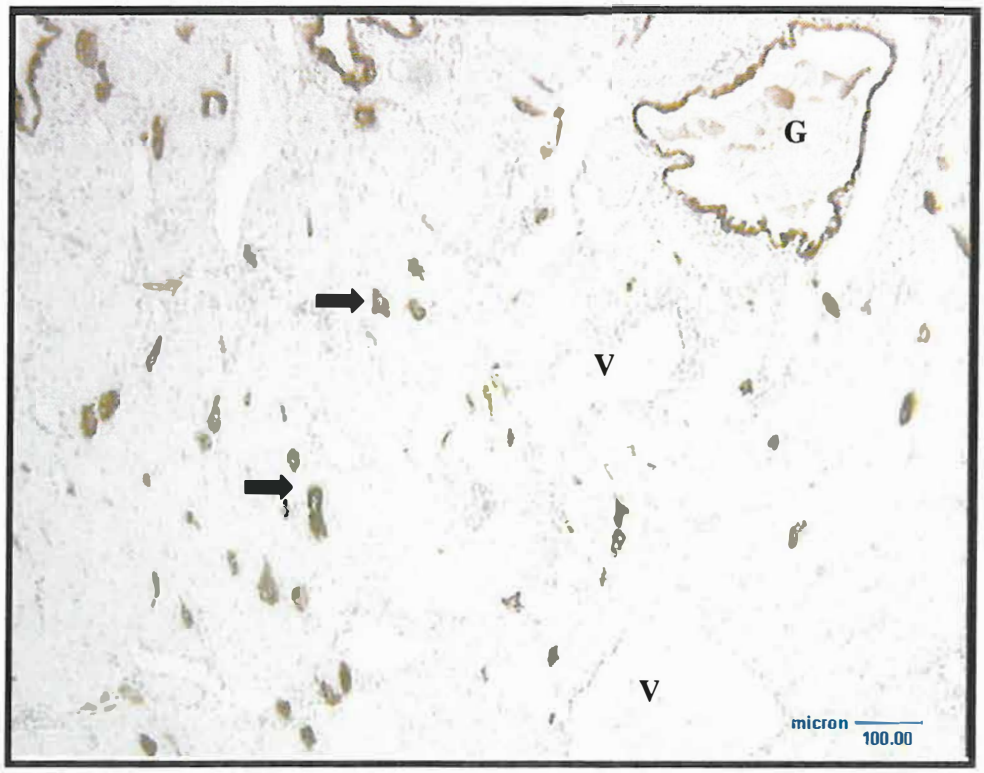

Fig 52: Myometrial interstitial trophoblast cells (arrow) immunoreactive to anti-anti-CK18 from the normotensive group. Note immunoreactivity of glandular epithelium (G). Vein (V).

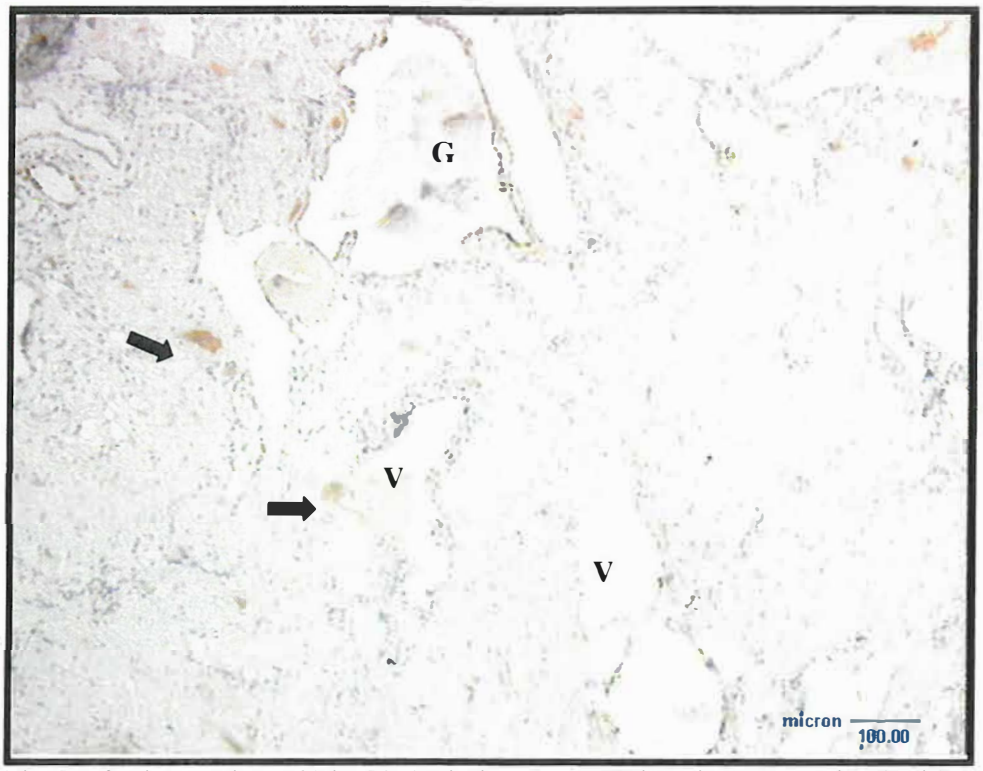

Fig 53: Serial section of Fig 52 depicting myometrium immunostained with anti-M30. Note absence of reaction product within glandular epithelial cells (G). Few interstitial trohoblast cells are reactive (arrow).

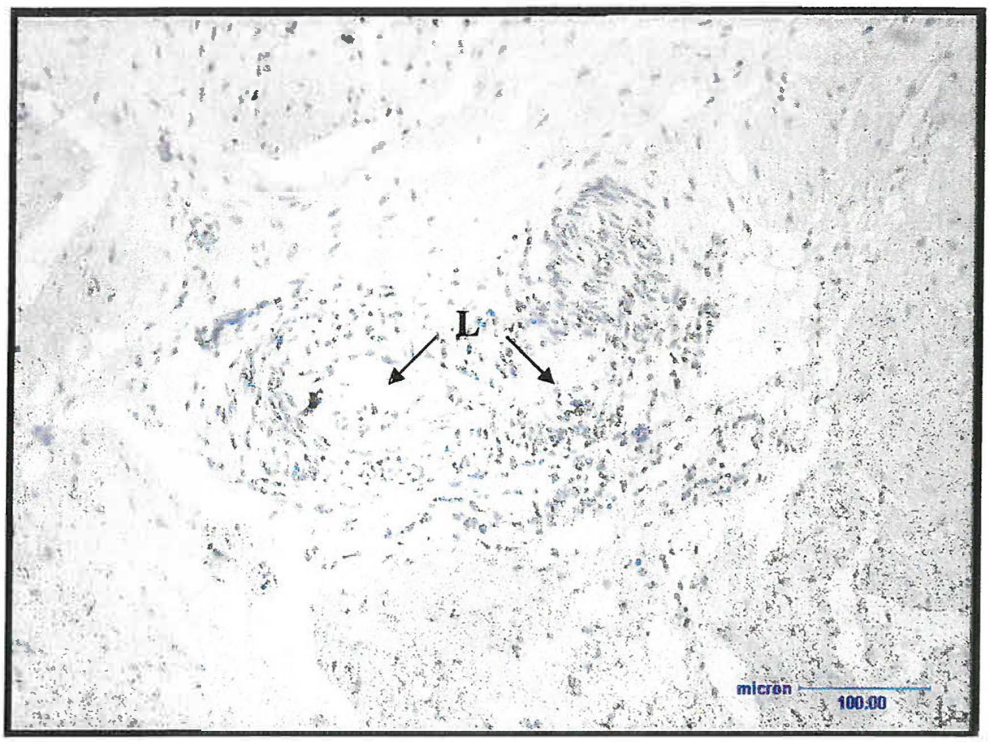

Fig 54: Micrograph of non physiologically converted spiral artery. Note absence of trophoblast cells and reduced lumen (L)

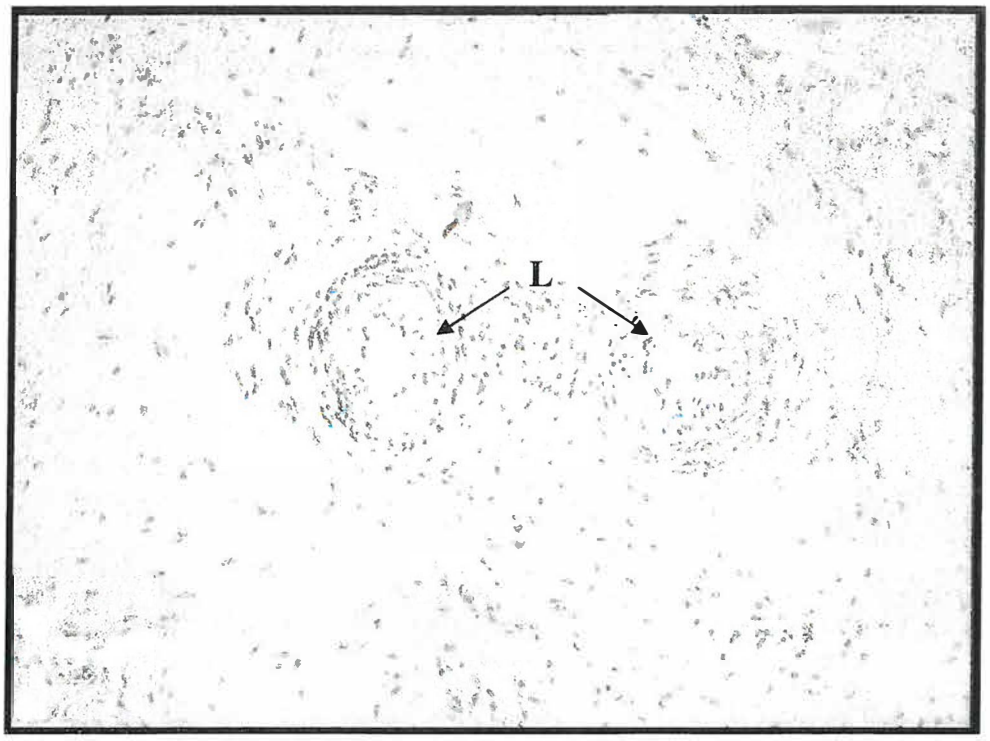

Fig 55: Serial section of non physiologically converted spiral artery immunostained for anti-M30. Note absence of trophoblast cells and reduced lumen (L)

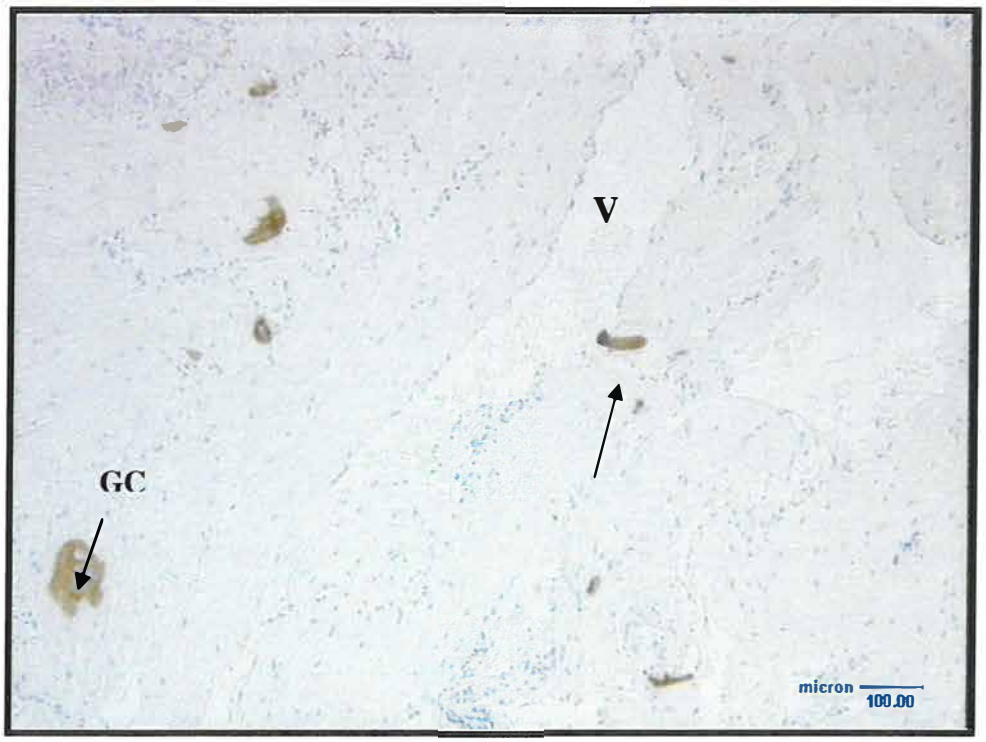

Fig 56: Micrograph illustrating interstitial trophoblast (arrow) population immunoreactivity anti-CK18 from the preeclamptic group. Note immunoreactive giant cell (GC). Vein (V).

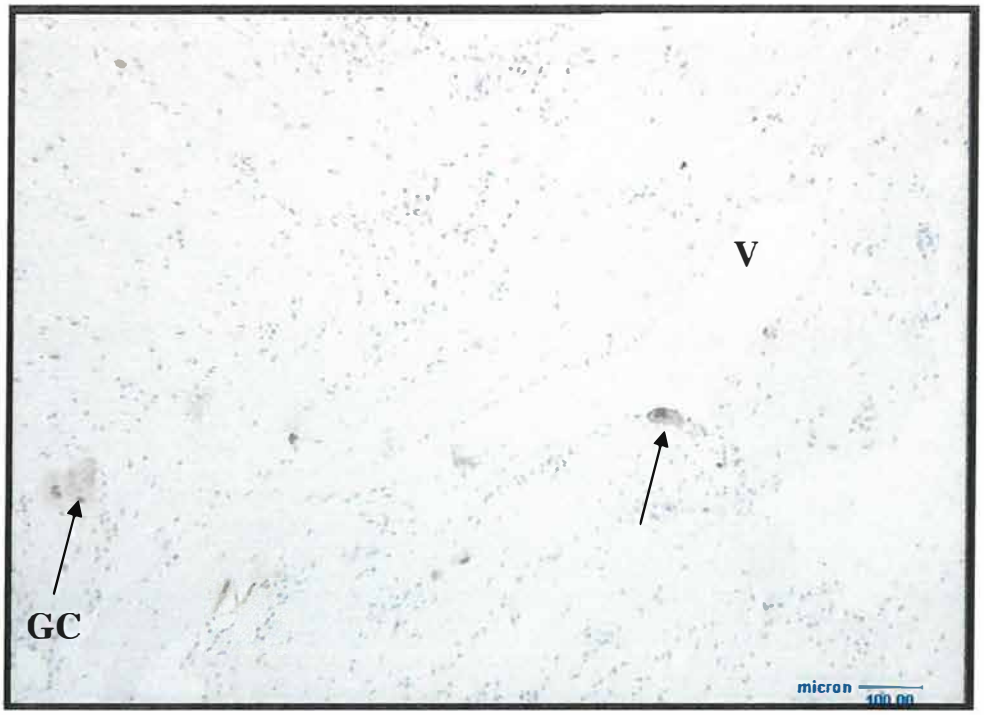

Fig 57: Serial section of Figure 56 illustrating interstitial trophoblast (arrow) and giant cell (GC) within myometrium. Vein (V).

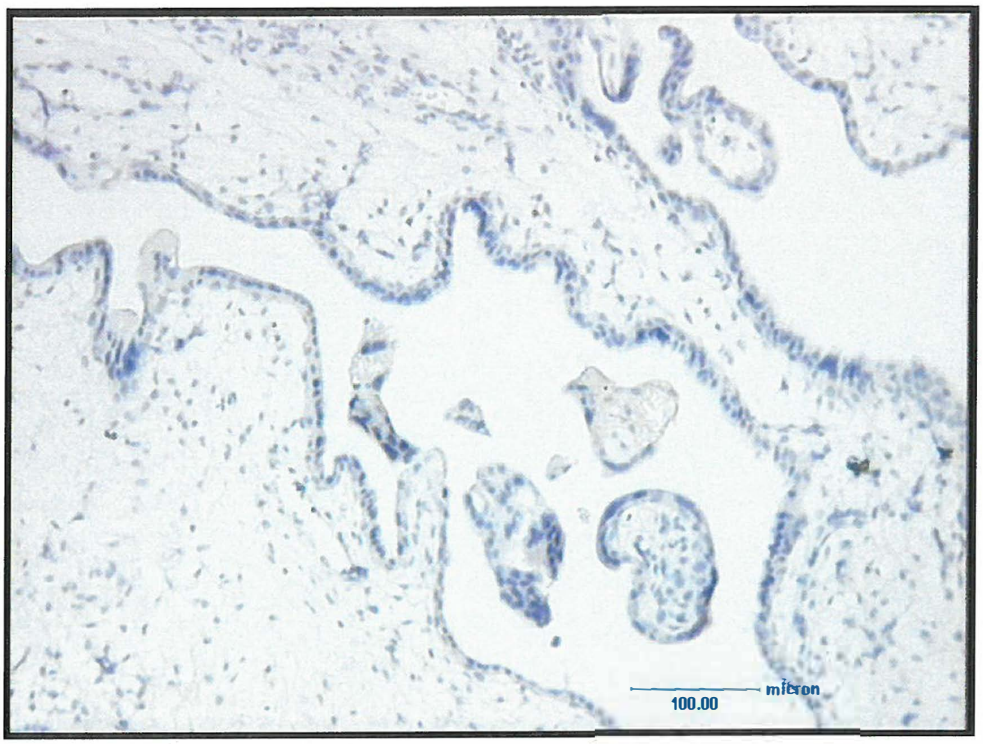

Fig 58: Method control for M30

Table XII: Mean area of spiral artery parameters in placental bed biopsies

	Mean Area μm^2		
	Artery inclusive of lumen (A)	Lumen (B)	Artery Wall (C) A – B = C
Normotensive n=12	414109 ± 57072	102379 ± 60045	311729 ± 51180
Preeclamptic n=12	36452 ± 9000	657 ± 106 p=0.000007	35795 ± 8045 p=0.000000

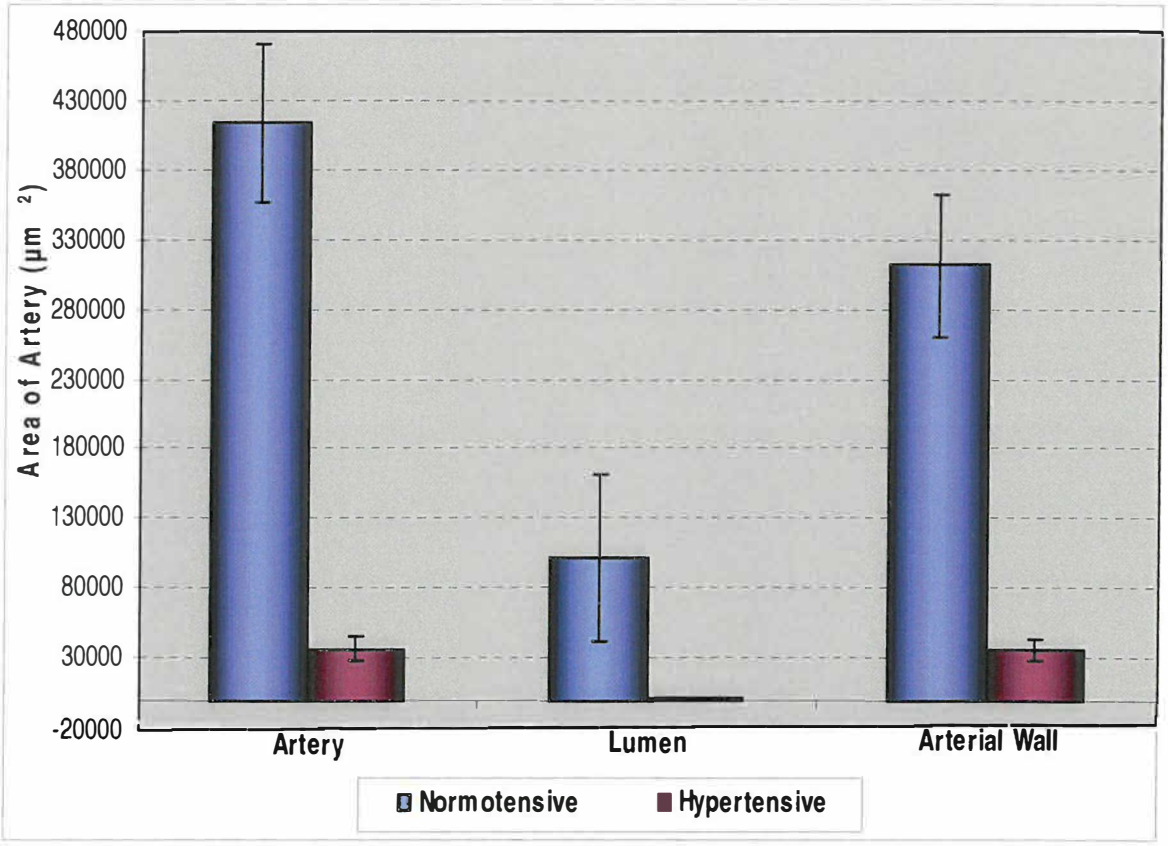

Fig 59: Histogram depicting area occupied by spiral artery, lumen and arterial wall

Table XIII: Image analysis of anti-CK18 *vs* M30 immunoexpression

		Normotensive	Preeclamptic
anti-CK18 Immunoreactivity %	Intramural trophoblast	13 ± 5	0 p < 0.0001
	Interstitial Trophoblast	10.79 ± 4.2	2.87 ± 0.5 p=0.000002
anti-M30 Immunoreactivity %	Intramural trophoblast	2.5 ± 0.7	0 p < 0.0001
	Interstitial Trophoblast	0.8 ± 0.3	1.9 ± 0. 8 p=0.001

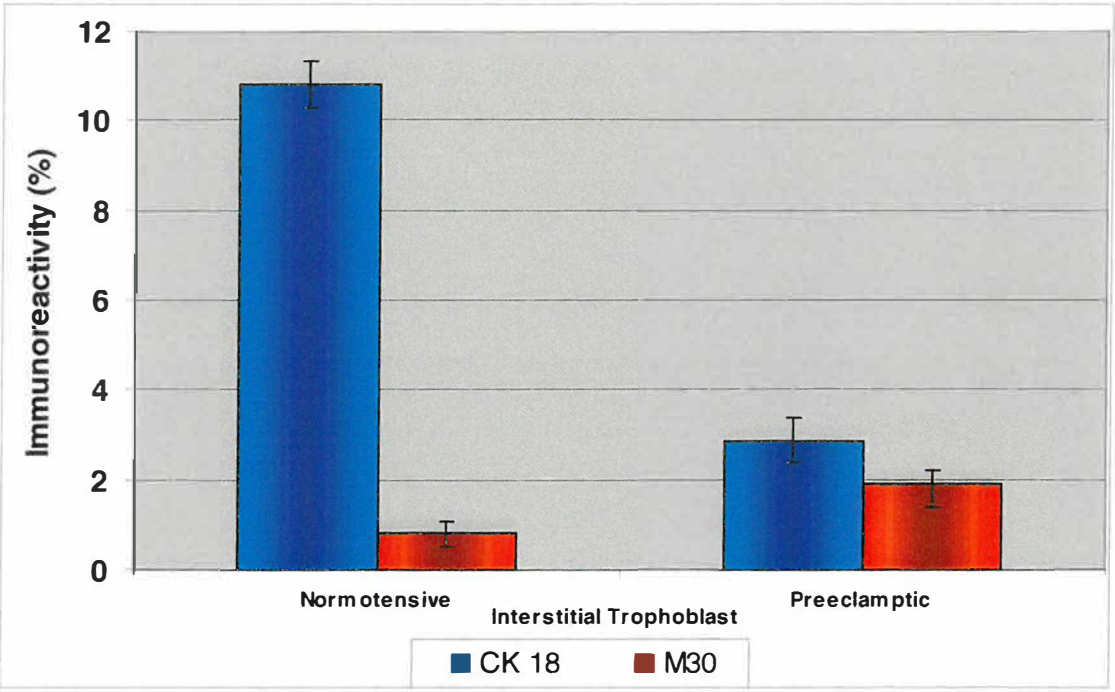

Fig 60: Histogram illustrating anti-CK and M30 immunoreactivity within interstititial trophoblast in both study groups.

CHAPTER FOUR

DISCUSSION

The placenta is a temporary organ that undergoes growth and development followed by senescence and death in nine months (Austgulen *et al.*, 2002). Placental growth depends on cytotrophoblast proliferation. A portion of cytotrophoblasts, which retain an undifferentiated phenotype throughout pregnancy, provide a reservoir of stem cells. The remaining cytotrophoblasts give rise to the two major trophoblasts subpopulations, syncytial trophoblasts and invasive cytotrophoblasts.

Controlled invasion by these cytotrophoblast stem cells of uterine decidua, myometrium and spiral arteries are essential for normal fetoplacental development. The interstitial trophoblast penetrates decidual tissues reaching the inner third of the myometrium. A subset of the trophoblast population, the endovascular trophoblast transforms uterine spiral arteries into large-bore conduits to enable the adequate supply of nutrients and oxygen to the placenta and thus the fetus. However, in the pregnancy disease preeclampsia, cytotrophoblast differentiation is abnormal and invasion is shallow. In recent years a number of studies have defined the molecular mechanisms, intrinsic to extravillous trophoblast, that appear to limit invasiveness of these cells into the uterine wall (Graham and McCrae, 1996; Zhou *et al.*, 1997).

Apoptosis is believed to play a role in the development, remodeling and aging of the placenta (Smith *et al.*, 1997). The balance between trophoblast differentiation, proliferation and apoptosis may represent a mechanism to control normal trophoblast invasion (Genbacev *et al.*, 1997). Alternatively, alterations in mitotic regulators of the trophoblast cell cycle may provide the basis for understanding factors that lead to abnormal placentation. Extravillous cytotrophoblast progression through and exit from the cell cycle as a function of differentiation is not well studied. Control of trophoblast invasion is still a mystery and therefore this study examines the imbalance between proliferation and apoptosis as possible mechanisms for the aberrant invasion that occurs in preeclampsia. The pathogenesis of preeclampsia may be due to an increase in apoptosis of trophoblast cells (Lyall and Myatt, 2002).

The use of immunohistochemical methods has become a widely accepted means of determining the state of cellular proliferation in histological material, because it allows architectural and cytological features to be preserved and avoids the *in vivo* administration of thymidine analogues (Hall and Wood., 1990). In recent years, evaluation of cell proliferation associated antigens by immunohistochemistry has evoked the interest of histopathologists. One of the most widely used reagents in this field is the Ki67 antibody which reacts with a nuclear non-histone protein of 395 and 345 kilodaltons present in active parts of the cell cycle, i.e. G1, S, G2, and mitosis but is absent in G0 (Sholzen and Gerdes, 2000). The diagnostic and prognostic value of Ki67 immunostaining in tumours has been well documented (Gerdes., 1990; Hall and Wood, 1990). Other proliferation cell markers, such as proliferation cell nuclear antigen, are expressed in non-cycling cells for example in association with DNA

repair, so that they tend to persist after the end of mitosis leading to an over-estimation of the degree of proliferative activity in a tissue, due to retention of staining in post-mitotic cells (Elston and Bagshawe, 1972).

The Ki67 immunoexpression seems to have a logical correlation with the proliferative activity in normal placentas being very active in first trimester placentas but diminished in term placenta (Suresh *et al.*, 1993). Interestingly, the prognosis of molar pregnancies cannot be determined using the Ki67 proliferative index (Cheung *et al.*, 1994). In this study, we demonstrate an absence of immunoexpression of Ki67 within the extravillous trophoblast population of the myometrium of both normal and pre-eclamptic placental bed biopsies by immunocytochemical techniques. As the presence of the Ki-67 antigen is strictly associated with the cell cycle and confined to the nucleus, this finding suggests an exit from the cell cycle. Ki-67 is a constituent of compact chromatin (Kreitz *et al.*, 2000) and hence is vital for the maintenance and/or regulation of the cell division cycle.

Bulmer and co-workers (1988) have used single and double immunohistochemical labelling to examine expression of apoptosis and cell cycle markers by villous and extravillous trophoblast in matched placentas and placental bed biopsies from normal pregnancies, 8-20 weeks gestational age and at term. Cytotrophoblast columns were positive for the proliferation marker anti-Ki67 even in the second trimester but interstitial and endovascular trophoblasts were always anti-Ki67 negative. In accordance with the latter study, this study, demonstrates non-reactivity of anti-Ki67

in both intramural/endovascular and interstitial trophoblast cell populations within normal and preeclamptic placental bed biopsies at term gestation.

In another study, immunostaining of first trimester placental bed biopsy specimens with an antibody against the Ki67 antigen, revealed that its expression abruptly stops at sites where cytotrophoblasts differentiate and attach to the uterine wall (Genbacev *et al.*, 1997). Our observations within the myometrial extravillous trophoblast population at term gestation conforms to this data further corroborating the fact that differentiation of invasive cytotrophoblast cells is coordinated with exit from the cell cycle. The expression patterns of G1 and G2 cyclins and of their cyclin-dependant kinases further supports this hypothesis (Genbacev *et al.*, 2000).

Multinucleated giant cells are regarded as degenerative non-invasive extravillous trophoblast cells. In this study, the multinucleated trophoblast cell population were usually scattered within the interstitium of the myometrium and were non-reactive to Ki67 antibody in both normotensive and pre-eclamptic groups. These findings suggest that these multinucleated trophoblast cells are non-proliferative and non-functional at term gestation. Interestingly, endoreduplication, the differentiation pathway that gives rise to trophoblast giant cells in the mouse, is also characterised by the expression of an unusual set of cell cycle regulators (MacAuley *et al.*, 1998).

Preeclampsia is characterised by hyperplasia of the smooth muscle cells of spiral arteries. In this study, there was an increase of proliferation of the smooth muscle cells of the hyperplastic spiral arteries in the preeclamptic group as they displayed a

mild degree of immunopositive staining to Ki67. This observation alludes to a slight increase in proliferation of the smooth muscle cells associated with the hypoxic microenvironment that occurs in preeclampsia. Furthermore, the additional observation of distinct immunoreactivity within smooth muscle cells of the myometrial microvasculature denotes proliferation. Hypoxia has been suggested as one of the micro-environmental factors that can modulate the phenotype of vascular smooth muscle cells *in vivo* and *in vitro*. It has also being shown to induce proliferation of vascular smooth muscle cells (Butler *et al.*, 1988; Dempsey *et al.*, 1991). In this study, the lumen of the spiral artery was significantly decreased in the preeclamptic group compared to the normotensive (657 ± 106 μm^2 *vs* 102379 ± 60045 μm^2 respectively) indicating reduced blood supply to the developing fetus. This data conforms to and adds to data of earlier investigators (Brosens *et al.*, 1967) who have demonstrated a positive correlation between trophoblast invasion and arterial dilation and a negative correlation between preeclampsia and arterial trophoblast invasion (Brosens *et al.*, 1972; Meekins *et al.*, 1994). Both these studies confirm that the microenviroment of the placental bed is relatively hypoxic. Ki67 has also being implicated in G1 arrest in a variety of tumor cell lines (Graeber *et al.*, 1994). Both these features has important implications as they suggest that ischemia can traumatize muscle tissues by killing cells and modulating differentiated cells to proliferate and thereby compromising the structural and functional integrity of the tissue. An alternate explanation may be attributed to the fact that hypoxia in proliferating cells can induce aberrant DNA replication patterns (Rice, 1984; Young *et al.*, 1989).

The present study also utilises immunoexpression of CK18 and its neo-epitope M30 for assessing trophoblast apoptosis in placental bed of normal and preclamptic pregnancies, at term. This immunohistologic method of detecting apoptosis has been developed using alterations of CK18 as it is widely distributed in epithelial cells. It has been suggested that the M30 antibody that recognises the CK18 epitope does not

react with necrotic and vital epithelial cells (Kadyrov *et al.*, 2001). As trophoblasts are epithelial in origin CK18 is a component of their cytoskeleton (Morsi *et al.*, 2000).

Apoptosis has being found in placentas throughout gestation using many techniques, including light microscopy, electron microscopy, and terminal deoxynucleotidyl transferase–mediated deoxyuridine triphosphate marker nick-end labeling (TUNEL) staining (Smith *et al.*, 1997). The TUNEL method, however, detects DNA fragmentation in all kinds of cells, whereas M30 staining can be expected only in CK18-containing cells. Furthermore, the TUNEL method and M30 staining recognise different aspects and steps of the apoptotic pathway. Since the neoepitope of CK18 is unmasked early in the apoptotic cascade, and DNA degradation occurs late in the process, one would expect that M30 antibody may be more sensitive for the detection of apoptosis. Smith *et al* (1997) reported that placental apoptosis occurs more frequently in pregnancies complicated by FGR. The latter authors found an apoptotic rate of 0.05% in normal term placenta, whereas Bulmer *et al* (1988) observed an apoptotic rate of approximately 0.03% in villous tissues. Recently, a report of M30 staining and extravillous trophoblast apoptosis has been published (Kadyrov *et al.*, 2001).

In this study, there was positive anti-CK18 immunoreactvity in all extravillous trophoblast cell populations within the placental bed of normotensive and preeclamptic placental bed biopsies. This reactivity was evident in the intramural

trophoblast cells embedded in the fibrinoid wall of the physiologically converted spiral artery and within the invasive interstitial trophoblast cells of the myometrium.

Morphometric image analysis in the present study indicates a reduction of intramural trophoblast invasion in the spiral artery to a non-invasion in the pre-eclamptic group (13% vs 0% for CK18 immunoreactivity for both groups respectively). In another study, Naicker *et al* (2003) demonstrated the mean field area percentage of intramural trophoblasts within the wall of myometrial spiral arteries to be 10.15% in the normotensive group compared to none in the severe hypertensive group. As expected the apoptotic (M30 positive) intramural trophoblast cells in the pre-eclamptic group was 0% due to the non-invasion of the artery walls. In contrast to the findings of this study, trophoblast apoptosis of spiral arteries has been reported to be similar in anemia and normal pregnancies but increased in preeclampsia (Kadyrov *et al.*, 2006). This increase of apoptosis of trophoblast cells in the wall of the spiral artery in the preeclampsia group is open to speculation. Trophoblastic invasion of spiral arteries has being reported to be absent in the majority placental bed biopsies with hypertension (Pijnenborg *et al.*, 1991). Similarly, Naicker *et al* (2003) reported a total absence of physiological conversion of the myometrial spiral arteries in the severe hypertensive disorder of preeclampsia. Both these studies demonstrate an absence of trophoblast cells embedded within the vessel wall. The morphometric data of elevated apoptosis of intramural trophoblast cells in the pre-eclamptic group by Kadyrov *et al* (2006) may possibly reflect a wide range of inclusion criteria in terms of severity of hypertension. Mild hypertension may for example, include a range of partial-total physiological conversion. Additionally, others have reported

increased apoptosis of syncytiotrophoblasts close to fibrinoid deposition (Nelson, 1996). The occurrence of M30-positive trophoblasts in the fibrinoid wall of the spiral artery of normotensive patients may be allied to the latter report.

In preeclampsia, the interstitial component of invasion is compromised, with an abnormally shallow trophoblast invasion (Brosens *et al.*, 1972). In this study, there was a marked elevation of apoptosis of the interstitial trophoblast population in the pre-eclamptic group compared to the normotensive group (1.9 % *vs* 0.8%). Although lower in value, the elevation of expression of apoptotis in the preeclamptic group conforms to the work carried out by Bulmer *et al* (1988).

This study further demonstrates variable distribution of anti-M30 immunoexpression within giant cells of both study groups. Studies have demonstrated that unlike the villous syncytiotrophoblast, these placental bed giant cells express HLA-G class I major histocompatibility complex antigens (Loke *et al.*, 1997). The HLA-G on giant cells may facilitate interaction with the maternal cells in the placental bed. This interaction may lead to some cells undergoing programmed cell death (apoptosis) (Al-Lamki *et al.*, 1998), while others may undergo terminal differentiation to giant cells.

DiFederico *et al* (1999) recently described an absence of apoptosis in normal uterine wall with 15-50% of invading cytotrophoblasts in preeclampsia being apoptotic. It is unknown whether the increase in the incidence of placental apoptosis seen in preeclampsia is a result of the pathologic process leading to or an etiologic component in the development of this disorder. Apoptosis is triggered by hypoxia (Kerr *et al.*, 1991). If a placenta is poorly perfused, it could account for preeclampsia

and apoptosis could simply be a marker for hypoxia and not a cause of preeclampsia. Similarly, poor placental perfusion and subsequent hypoxia associated with preeclampsia could explain the observed increase in interstitial trophoblast apoptosis in this study.

In the normotensive group of this study, dilated spiral artery segments that were invaded by trophoblast cells were largely void of macrophages. By contrast, in the preeclamptic group, the outer media of undilated spiral artery segments and the adventitial boundary were heavily infiltrated by macrophages and devoid of extravillous trophoblast. Maternal cells such as macrophages and endothelial cells may have a role on trophoblast invasion and apoptosis (Huppertz *et al*., 2005). In the pre-eclamptic group, we observed large numbers of macrophages around most of the spiral arterial walls in preeclampsia. It is possible that these cells have a role in apoptosis. Reister *et al* (1999; 2001) indicate that macrophages, residing in excess in the placental bed of pre-eclamptic women, are able to limit extravillous trophoblast invasion of spiral arterial segments through apoptosis mediated by the combination of TNFα secretion and tryptophan depletion. The latter study is supported by a report of Pijnenborg *et al* (1998), who found a higher incidence of cell clusters secreting TNFα, probably macrophages, in the placental bed of patients with severe forms of preeclampsia. There are two possible pathways by which macrophages could inhibit extravillous trophoblast invasion (a) passively, because apoptotic extravillous trophoblast cells may attract macrophages; (b) actively, because macrophages may prevent extravillous trophoblast invasion of the vessel walls by inducing apoptosis in the perivascular interstitial trophoblast.

In conclusion, the immunoexpression pattern of Ki67 antigen in this study suggests that differentiation of invasive cytotrophoblast cells in both normal and hypertensive pregnancies at term is coordinated with exit from the cell cycle. This study also demonstrates that immunoexpression of a neoepitope on cytokeratin 18, recognised by the monoclonal antibody M30, is an indicator of apoptosis in epithelial cells. The mean field area of the interstitial trophoblast (anti-Ck18) invasion in the preeclamptic group was 2.87 ± 0.5% compared to 10.79 ± 4.2% in the normotensive group. However the serial sections immunostained with CK18 and its neoepitope-M30 showed elevation of apoptosis of the invasive interstitial trophoblast cell population in the myometrium of the preeclamptic and the normotensive groups respectively (1.9 ± 0.5% *vs* 0.8 ± 0.3%).

The balance between trophoblast apoptosis and proliferation may represent a mechanism to control normal trophoblast invasion. A possibility exists that enhanced proliferation precedes apoptosis particularly in early gestation when invasion occurs. In a hypoxic environment, trophoblast cells continue to proliferate yet simultaneously differentiate abnormally in preeclampsia. In preeclampsia the invasive trophoblast cells probably exit the cell cycle in G1 phase, directing them towards apoptosis rather than passage in the S phase and mitosis. The absence of the compensatory increase in mitosis would result in the decrease in trophoblast invasion that occurs in preeclampsia.

REFERENCES

Adams, J. M. (2003). Ways of dying: multiple pathways to apoptosis. *Genes & development* **17**, 2481-2495.

Alison, M. R. (1999). Identifying and quantifying apoptosis: a growth industry in the face of death. *Pathol* **188**, 117-118.

Allaire, A. D., Ballenger, K. A., Wells, S. R., Mcmanhon, M. J., and Lessey, B. A. (2000). Placental Apoptosis in Preeclampsia. *Obstetrics & Gynecology* **96**, 271-276.

Al-Lamki, R. S., Skepper, J. N., Loke, Y. W., King, A., and J., B. G. (1998). Apoptosis in the early human placental bed and its discrimination from necrosis using the in-situ DNA ligation technique. *Human Reproduction* **13**, 3511-3519.

Almendral, J., Huebsch, M., Blundell, P. A., Macdonald-Bravo, H., and Bravo, R. (1987). Cloning and sequence of the human nuclear protein cyclin: homology with DNA-binding proteins. *Proceedings of the National Academy of Sciences USA* **84**, 1575–1579.

Anderton, B. H. (1981). Intermediate filaments: a family of homologous structures. *Muscle Res. Cell. Motil* **21**, 141–166.

Arngrímsson, R., Hayward, C., Nadaud, S., Baldursdóttir, A., Walker, J. J., Liston, W. A., Bjarnadóttir, R. I., Brock, D. J., Geirsson, R. T., Connor, J. M., and Soubrier, F. (1997). Evidence for a familial pregnancy-induced hypertension locus in the eNOS-gene region. *Am J Hum Genet.* **61**, 354–362.

Ashkenazi, A. (2002). Targeting death and decoy receptors of the tumour-necrosis factor superfamily. *Nat. Rev. Cancer* **2**, 420–430.

Austgulen, R., Chedwick, L., Vogt Isaksen, C., Vatten, L., and Craven, C. (2002). Trophoblast Apoptosis in Human Placenta at Term as Detected by Expression of a Cytokeratin 18 Degradation Product of Caspase. *Archives of Pathology and Laboratory Medicine* **126**, 1480–1486.

Barret, K. L., Willinghama, J. M., Garvina, J., and Willinghama, M. C. (2001). Advances in Cytochemical Methods for Detection of Apoptosis. *Histochemistry and Cytochemistry* **49**, 821-832.

Belizán, J. M., and Villar, J. (1980). The relationship between calcium intake and edema-proteinuria and hypertension-gestosis: a hypothesis. *American Journal of Clinical Nutrition* **33**, 2202-2210.

Braun, N., Papadopoulos, T., and Muller-Hermelink, H. (1988). Cell cycle dependent distribution of the proliferation-associated Ki-67 antigen in human embryonic lung cells.Virchows Arch B Cell Pathol Incl Mol Pathol. ;. *56:* (**1**), 25-33.

Brewer, T. (1976). Letter: Role of malnutrition in pre-eclampsia and eclampsia. *Am J Obstet Gynecol* **125**, 281-282.

Brosens, I., Robertson, W. B., and Dixon, H. G. (1967). The physiological response of the vessels of the placental bed to normal pregnancy. *Pathol Bacteriol* **93**, 569-579.

Brosens, I. A., Robertson, W. B., and Dixon, H. G. (1972). The role of the spiral arteries in the pathogenesis of pre-eclampsia. *Obstetrics and Gynecology* **1**.

Brown, D. C., and Gatter, K. C. (2002). Ki67 protein: the immaculate deception? *Histopathology* **40**, 2-11.

Brown, M. A., Zammit, V. C., Whitworth, J. A., Magoulas, T., and Penny, R. (1991). Endothelin production in pre-eclampsia. *Lancet* **338**, 261.

Bruno, S., and Darzynkiewicz, Z. (1992). Cell cycle dependent expression and stability of the nuclear protein detected by Ki-67 antibody in HL-60 cells. *cell prolif.* **25**, 31-40.

Bulmer, J. N., Morrison, L., and Johnson, P. M. (1988). Expression of the proliferation markers Ki67 and transferrin receptor by human trophoblast populations. *Reprod Immunol* **14**, 291–302.

Butler, A. J., Eagleton, M. J., Wang, D., Howell, R. L., Strauch, A. R., Khasgiwala, V., and C., S. H. (1991). Induction of the proliferative phenotype in differentiated myogenic cells by hypoxia. *Biol. Chem.* **266**, 18250-18258.

Caulin, C., Salvesen, G. S., and Oshima, R. G. (1997). Caspase cleavage of keratin 18 and reorganization of intermediate filaments during epithelial cell apoptosis. *Cell Biol* **22:**, 379–394.

Cheung, N., Ngan, H. Y., Collins, R. J., and Wong, Y. L. (1994). Assessment of cell proliferation in hydatidiform mole using monoclonal antibody MIB1 to Ki-67 antigen.A. *Clin Pathol* **47**, 601–604.

Chittenden, T., Harrington, E. A., O'Connor, R., Flemington, C., Lutz, R. J., Evan, G. I., and Guild, B. C. (1995). Induction of apoptosis by the Bcl-2 homologue Bak. *Nature* **374**, 733-736.

Coulombe, P. A., and Omary, M. B. (2002). 'Hard' and 'soft' principles defining the structure, function and regulation of keratin intermediate filaments. *Curr Opin Cell Biol* **14**, 110–122.

Crompton, M. (1999). The mitochondrial permeability transition pore and its role in cell death. *Biochem* **341**, 233–249.

Danial, N. N., and Korsmeyer, S. J. (2004). Cell death: critical control points. *Cell* **116**, 205–219.

Davey, D. A., and MacGillivray, I. (1988). The classification and definition of the hypertensive disorders of pregnancy. *Am J Obstet Gynecol* **158**, 892-898.

de Groot, C. J., and Taylor, R. N. (1993). New insights into the etiology of pre-eclampsia. *Ann Med* **25**, 243-249.

Dempsey, E. C., McMurtry, I. F., and O'Brien, R. F. (1991). Protein kinase C activation allows pulmonary artery smooth muscle cells to proliferate to hypoxia. *Am. J. Physiol* **260**, L136-L145.

DiFederico, E., Genbacev, O., and Fisher, S. J. (1999). Preeclampsia is associated with widespread apoptosis of placental cytotrophoblasts within the uterine wall. *Am J Pathol* **155**, 293–301.

Dizon-Townson, D. S., Nelson, L. M., Easton, K., and Ward, K. (1996). The factor V Leiden mutation may predispose women to severe preeclampsia. *Am J Obstet Gynecol* **175**, 902-905.

du Manoir, S., Gulllaud, P., Camus, E., Seigneurin, D., and Brugal, G. (1991). Ki-67 labeling in postmitotic cells defines different Ki-67 pathways within the 2c compartment. *Cytometry* **12**, 455-463.

Duckitt, K., and Harrington, D. (2005). Risk factors for preeclampsia at antenatal booking: systematic review of controlled studies. *BMJ* **330**, 565-557.

Easterling, T. R., Benedetti, T. J., Schmucker, B. C., and Millard, S. P. (1990). Maternal hemodynamics in normal and preeclamptic pregnancies: a longitudinal study. *Obstetrics & Gynecology* **76**, 1061-1069.

Eichner, R., Sun, T. T., and Aebi, U. (1986). The role of keratin subfamilies and keratin pairs in the formation of epidermal intermediate filaments. *Cell. Biol* **102**, 1767–1777.

Elston, C. W., and Bagshawe, K. D. (1972). The diagnosis of trophoblastic tumours from uterine curettings. *Clin Pathol* **25**, 111–118.

Fisher, K. A., Luger, A., Spargo, B. H., and Lindheimer, M. D. (1981). Hypertension in pregnancy: clinical-pathological correlations and remote prognosis. *Medicine* **60**, 267-276.

Gallery, E. D. M., and Brown, M. A. (1987). Volume homeostasis in normal and hypertensive human pregnancy. *Clin. Obstet. Gynnecol.* **49**, 555-562.

Gavrieli, Y., Sherman, Y., and Ben-Sasson, S. A. (1992). Identification of programmed cell death in situ via specific labeling of nuclear DNA fragmentation. *Cell Biol* **119**, 493-501.

Genbacev, O., McMaster, M. T., and Fisher, S. J. (2000). A Repertoire of Cell Cycle Regulators Whose Expression Is Coordinated with Human Cytotrophoblast Differentiation. *American Journal of Pathology* **157**, 1337-1351.

Genbacev, O., Zhou, Y., Ludlow, J. W., and Fisher, S. J. (1997). Regulation of human placental development by oxygen tension. *Science* **277**, 1669-1672.

Gerdes, J. (1990). Ki67 and other proliferation markers useful for immunohistological diagnostic and prognostic evaluations in human malignancies. *Osborn Med. Cancer biology* **1**, 99-206.

Gerdes, J., Lemke, H., Baisch, H., Wacker, H. H., Schwab, U., and Stein, H. (1984). Cell cycle analysis of 380 Structural Basis of Ki67 FHA Binding to hNIFK a cell proliferation-associated human nuclear antigen defined by the monoclonal antibody Ki-67. *Immunol* **133**, 1710-1715.

Gerdes, J., Schwab, U., Lemke, H., and Stein, H. (1983). Production of a mouse monoclonal antibody reactive with a human nuclear antigen associated with cell proliferation. *Int. J. Cancer* **31**, 13-20.

Ghidini, A., Salafia, C. M., and Pezzullo, J. C. (1997). Placental vascular lesions and likelihood of diagnosis of preeclampsia. *Obstetrics & Gynecology* **90**, 542-545.

GOPEC Consortium (2005). Disentangling Fetal and Maternal Susceptibility for Pre-Eclampsia: A British Multicenter Candidate-Gene Study. *American Journal of Human Genetics* **77**, 127–131.

Graeber, T. G., Peterson, J. F., Tsai, M., Monica, K., Fornace, A. J., and Giaccia, A. J. (1994). Hypoxia induces accumulation of p53 protein, but activation of a G1-phase checkpoint by low-oxygen conditions is independent of p53 status. *Mol. Cell. Biol.* **14**, 6264–6277.

Graham, C. H., and McCrae, K. R. (1996). Altered expression of gelatinase and surface-associated plasminogen activator activity by trophoblast cells isolated from placentas of preeclamptic patients. *Am J Obstet Gynecol* **175**, 555-562.

Green, D. R., and Kroemer, G. (2004). The Pathophysiology of Mitochondrial Cell Death. *Science* **305**, 626 - 629.

Gross, A., McDonnell, J. M., and Korsmeyer, S. J. (1999). BCL-2 family members and the mitochondria in apoptosis. *Genes Dev* **13**, 1899-1911.

Guillaud, P., du Manoir, S., and Seignenrin, D. (1989). Quantification and topographical description of Ki-67 antibody labelling during the cell cycle of normal fibroblastic (MRC-5) and mammary turnout cell lines (MCF-7). *Anal. Cell. Pathol* **1**, 25-39.

Gulbis, J. M., Kelman, Z., Hurwitz, J., O' Donnell, M., and Kuriyan, J. (1996). Structure of the C-terminal region of p21(WAF1/CIP1) complexed with human PCNA. *Cell* **87**, 297–306.

Guohua, P., Rourke, K., Chinnaiyan, A. M., Gentz, R., Ebner, R., and J., N. (1997). The Receptor for the Cytotoxic Ligand TRAIL. *Science* **276 (5309)**, 111 - 113.

Hall, P. A., McKec, P. H., H., d. P. M., Dover, R., and Lane, D. P. (1993). High levels of p53 protein in UV irradiated normal human skin. *Oncogene.* **8**, 203-207.

Hall, P. A., and Wood, A. L. (1990). Immunohistochemical markers of cellular proliferation: achievements, problems and prospects. *CeUl Tissue Kinet* **23**, 531-549.

Helewa, M. E., Burrows, R. F., Smith, J., Williams, K., Brain, P., and Rabkui, S. W. (1997). Definitions, evaluation, and classification of hypertensive disorders in pregnancy. *CMAJ* **157**, 715–725.

Higgins, J. R., and Swiet, M. (2001). Blood pressure measurement and classificationin pregnancy. *Lancet* **357**, 131-135.

Huppertz, B., Frank, H. G., and Kaufmann, P. (1999a). The apoptosis cascade morphological and immunohistochemical methods for its visualization. *Anat Embryol* **200**, 1–18.

Huppertz, B., and Herrler, A. (2005). Review:Regulation of proliferation and apoptosis during development of the preimplantation embryo and the placenta. *Birth Defects Research Part C: Embryo Today: Reviews* **75**, 249 - 261.

Kadyrov, M., Kaufmann, P., and Huppertz, B. (2001). Expression of Cytokeratin 18 Neo-epitope is a specific marker for trophoblast apoptosis in human placenta. *Placenta* **22**, 4-48.

Kadyrov, M., Kingdom, J. C. P., and Huppertz, B. (2006). Divergent trophoblast invasion and apoptosis in placental bed spiral arteries from pregnancies complicated by maternal anemia and early-onset preeclampsia/intrauterine growth restriction. *American Journal of Obstetrics and Gynecology* **194**, 557–563.

Kelman, Z. (1997). PCNA: structure, functions and interactions. *Oncogene* **14**, 629–640.

Kerr, J. F., Wyllie, A. H., and Currie, A. R. (1972). Apoptosis: a basic biological phenomenon with wide-ranging implications in tissue kinetics. *Br J Cancer* **26**, 239-257.

Khong, T. Y., De Wolf, F., Robertson, W. B., and Brosens, I. (1986). Inadequate maternal vascular response to placentation in pregnancies complicated by pre-eclampsia and by small-for-gestational age infants. *Br J Obstet Gynaecol* **93**, 1049–1059.

Kilani, R. T., Mackova, M., Davidge, S. T., and Guilbert, L. J. (2003). Effect of oxygen levels in villous trophoblast apoptosis. *Placenta* **24**, 826–834.

Kill, I. R. (1996). Localisation of the Ki-67 antigen within the nucleolus.Evidence forj a fibrillarin-deficient region of the dense fibrillar component. *Cell Science* **109**, 1253-1263.

Kingdom, J. C., Burrell, S. J., and Kaufmann, P. (1997). Pathology and clinical implications of abnormal umbilical artery Doppler waveforms. *Ultrasound Obstet Gynecol* **4)**, 271-286.

Klonoff-Cohen, H. S., Savitz, D. A., Cefalo, R. C., and McCann, M. F. (1989). An epidemiologic study of contraception and preeclampsia. *JAMA* **262**.

Kong, X. P., Onrust, R., O'Donnell, M., and Kuriyan, J. (1992). Three dimensional structure of the B subunit of E.coli DNA polymerases III holoenzyme:a sliding DNA clamp. *Cell* **69**, 425-437.

Krammer, P. H. (2000). CD95's Deadly Mission in the Immune System. *Nature* **407**, 789-795.

Kreitz, S., Fackelmayer, F. O., Gerdes, J., and Knippers, R. (2000). The proliferation-specific human Ki-67 protein is a constituent of compact chromatin. *Expt. Cell Res.* **261**, 284-292.

Krishna, T. S. R., Kong, X. P., Gary, S., Burger, P. M., and Kuriyan, J. (1994). Crystal structure of the eukaryotic DNA polymerase processivity factor PCNA. *Cell* **79**, 1233–1243.

Kroemer, G., Zamzami, N., and Susin, S. A. (1997). Mitochondrial control of apoptosis. *Immunol Today* **18**, 44-51.

Kupferminc, M. F., Eldor, A., Steinman, N., Many, A., Bar-Am, A., Jaffa, A., Fait, G., and Lessing, J. B. (1999). Increased Frequency of Genetic Thrombophilia in Women with Complications of Pregnancy. *N Engl J Med* **340**, 9-13.

Kusama, K., Jiang, Y., Toguchi, M., Ohno, J., Shikata, H., Sakashita, H., and Sakagami, H. (2000). Use of the monoclonal antibody M30 for detecting HSG cell apoptosis. *Anticancer Res.* **20**, 151-154.

Lachmeijer, A. M., Arngrimsson, R., Bastiaans, E. J., Frigge, M. L., Pals , G., Sigurdardottir, S., Stefansson, H., Palsson, B., Nicolae, D., Kong, A., Aarnoudse, J. G., Gulcher, J. R., Dekker, G. A., ten Kate, L. P., and Stefansson, K. (2001). A genome-wide scan for preeclampsia in the Netherlands. *Eur J Hum Genet* **9**, 758–764.

Laivuori, H., Lahermo, P., Ollikainen, V., Widen, E., Häivä-Mällinen, L., Sundström, H., Laitinen, T., Kaaja, R., Ylikorkala, O., and Kere, J. (2003). Susceptibility Loci for Preeclampsia on Chromosomes 2p25 and 9p13 in Finnish Families. *The American Journal of Human Genetics* **72**, 168–177.

Learning Lab [online image]. Available at http://learninglab.co.uk/headstart/cycle3.htm (accessed on the 17 December 2005)

Leers, M. P. G., Kölgen, W., Björklund, V., Bergman, T., Tribbick, G., and Persson, B. (1999). Immunocytochemical detection and mapping of cytokeratin 18 neo-epitope exposed during early apoptosis. *Pathol* **187**, 567-572.

Liao, J., and Omary, M. B. (1996). 4-3-3 proteins associate with phosphorylated simple epithelial keratins during cell cycle progression and act as a solubility cofactor. *Cell Biol* **133**, 345–357.

Liu, X., Kim, C. N., Yang, J., Jemmerson, R., and Wang, X. (1996). Induction of apoptotic program in cell-free extracts: requirement for dATP and cytochrome c. *Cell* **86**, 147–157.

Loke, Y. W., and King, A. (1997). Immunology of human placental implantation: clinical implications of our current understanding. *Mol. Med. Today* **3**, 153–159.

Loor, G., Zhang, S. J., Zhang, P., Toomey, N. L., and Lee, M. Y. W. T. (1997). Identification of DNA replicationand cell cycle proteins that interact with PCNA. *Nucleic Acids Research* **25**, 5041–5046.

López-Jaramillo, P., Casas, J. P., and Serrano, N. (2001). Preeclampsia: from epidemiological observations to molecular mechanisms. *Braz J Med Biol Res* **34**, 1227-1235.

Lyall, F. (2002). The Human Placental Bed Revisited. *Placenta* **23**, 555–562.

Lyall, F., and Myatt, L. (2002). The role of the placenta in pre-eclampsia - A Workshop Report. *Placenta* **23**, S142-S145.

MacAuley, A., Cross, J. C., and Werb, Z. (1998). Reprogramming the cell cycle for endoreduplication in rodent trophoblast cells. *Mol Biol Cell* **9**, 795-807.

Matsumiya, S., Ishino, Y., and Morikawa, K. (2001). Crystal structure of an archaeal DNA sliding clamp: proliferatingcell nuclear antigen from Pyrococcus furiosus. *Protein Science* **10**, 17–23.

Mayhew, T. M. (2001). Villous trophoblast of human placenta: a coherent view of its turnover, repair and contributions to villous development and maturation. *Histol Histopathol* **16**, 1213-1224.

McParland, P., Pearce, J. M., and Chamberlain, G. V. P. (1990). Doppler ultrasound and aspirin in recognition and prevention of pregnancy-induced hypertension. *Lancet* **335**, 1552-1555.

Mediscape: Pathophysiology of Preeclampsia [online]. Available from http://www.medscape.com/ ewarticle/495537_7 (accessed 7 May 2005)

Meekins, J. W., Pijnenborg, R., Hanssens, M., van Assche, A., and McFadyen, I. R. (1994). Immunohistochemical detection of lipoprotein(a) in the wall of placental bed spiral arteries in normal and severe preeclamptic pregnancies. *Placenta* **15**, 511-524.

Moll, R., Franke, W. W., Schiller, D. L., Geiger, B., and Krepler, R. (1982a). The catalog of human cytokeratin: Patterns of expression in normal epithelia, tumors and cultured cells. *Cell* **31**, 11–24.

Moodley, J. (2000). Saving Mothers in South Africa. *Soth African Medical Journal* **90**, 362-363.

Moodley, J. (2006). Women's Health, DDMRI, *Personal Communication*

Mor, G., and Abrahams, V. M. (2003). Potential role of macrophages as immunoregulators of pregnancy. *Reprod Biol Endocrinol* **1**, 119–126.

Mor, G., Straszewski, S., and Kamsteeg, M. (2002). Role of the Fas/Fas ligand system in female reproductive organs: survival and apoptosis. *Biochem Pharmacol* **64**, 1305–1315.

Morsi, H. M., Leers, M. P. G., Jager, W., Bjorklund, V., Radespiel-Troger, M., Kabarity, H. E., Nap, M., and Lang, N. (2000). The Patterns of Expression of an Apoptosis-Related CK18 Neoepitope, the bcl-2 Proto-Oncogene, and the Ki67 Proliferation Marker in Normal, Hyperplastic, and Malignant Endometrium. *International Journal of Gynecological Pathology* **19**, 118-126.

Moses, E. K., Lade, J. A., Guo, G., Wilton, A. N., Grehan, M., Freed, K., Borg, A., D., T. J., North, R., Cooper, D. W., and Brennecke, S. P. (2000). A genome scan in families from Australia and New Zealand confirms the presence of a maternal susceptibility locus for pre-eclampsia, on chromosome 2. *Am J Hum Genet* **67**, 1581–1585.

Naicker, T., Khedun, S. M., Moodley, J., and Pijnenborg, R. (2003). Quantitative analysis of trophoblast invasion in preeclampsia. *Acta Obstet Gynecol Scand* **82**, 722–729.

Nelson, D. M. (1996). Apoptotic changes occur in syncytiotrophoblast of human placental villi where fibrinoid type fibrinoid is deposited at discontinuities in the villous trophoblast. *Placenta* **17**, 387-391.

Ness, R. B., Markovic, N., Bass, D., Harger, G., and Roberts, J. M. (2003). Family History of Hypertension, Heart Disease, and Stroke Among Women Who Develop Hypertension in Pregnancy. *Obstet Gynecol* **102**, 1366-1371.

Nitric Oxide Research Group [online]. Available from www.sghms.ac.uk/depts/immunology/ ~dash/apoptosis/mito.html (accessed on the 17 December 2005)

Norbury, C., and Nurse, P. (1992). Animal Cell Cycles and Their Control. *Annual Review of Biochemistry* **61**, 441-468.

Oudejans, C. B. M., Mulders, J., Lachmeijer, A. M. A., van Dijk, M., Konst, A. A. M., Westerman, B. A., van Wijk, I. J., Leegwater, P. A. J., Kato, H. D., Matsuda, T., Wake, N., Dekker, G. A., Pals, G., ten Kate, L. P., and Blankenstein, M. A. (2004). The parent-of-origin effect of 10q22 in pre-eclamptic females coincides with two

regions clustered for genes with down-regulated expression in androgenetic placentas. *Mol. Hum. Reprod.* **10**, 589 - 598.

Panday, M., Mantel, G. D., and Moodley, J. (2004). Audit of Severe Acute Morbidity in hypertensive Pregnancies in a Developing Country. *Obstetrics & Gynecology* **24**, 387-391.

Perloff, D. (1998). Hypertension and pregnancy-related hypertension. *Cardiol Clin.* **16**, 79-101.

Pijnenborg, R. (1996). The placental bed. *Hypertens Preg* **15**, 7–23.

Pijnenborg, R., Anthony, J., Davey, D. A., Rees, A., Tiltman, A., Vercruysse, L., and Van Assche, F. A. (1991). Placental bed spiral arteries in the hypertensive disorders of pregnancy. *Br J Obstet Gynaecol* **98**, 648–655.

Pijnenborg, R., Dixon, G., Robertson, W. B., and Brosens, I. (1980). Trophoblastic invasion of human decidua from 8 to 18 weeks of pregnancy. *Placenta* **1**, 3-19.

Pijnenborg, R., Vercruysse, L., Verbist, L., and A., V. A. F. (1998). nteraction of interstitial trophoblast with placental bed capillaries and venules of normotensive and pre-eclamptic pregnancies. *Placenta* **19**, 569-575.

Red-Horse, K., Zhou, Y., Genbacev, O., Prakobphol, A., Foulk, R., McMaster, M., and Fisher, S. J. (2004). Trophoblast differentiation during embryo implantation and formation of the maternal-fetal interface. *J Clin Invest* **114:**, 744-754.

Redman, C. G. (1991). Pre-eclampsia and the placenta. *Placenta* **12**, 301–308.

Reed, J. C. (2000). Mechanisms of Apoptosis. *American Journal of Pathology* **157**, 1415-1430.

Reister, f., Frank, H. G., Heyl, W., Kosanke, G., Huppertz, B., and Schroder, W. (1999). The distribution of macrophages in spiral arteries of the placental bed in pre-eclampsia differs from that in healthy patients. *Placenta* **20**, 229-233.

Reister, F., Frank, H. G., Kingdom, J. C., Heyl, W., Kaufmann, P., and Rath, W. (2001). Macrophage-induced apoptosis limits endovascular trophoblast invasion in the uterine wall of preeclamptic women. *Lab Invest* **81**, 1143-1152.

Report of the National High Blood Pressure Education Program Working Group on High Blood Pressure in Pregnancy (2000). *Am J Obstet Gynecol* **183**,S1-22.

Rice, W. R. (1984). Sex chromosomes and the evolution of sexual dimorphism. *Evolution* **38**, 735–742.

Reproductive and Cardiovascular Disease Research Group) [online]. Available from http://www.sgul.ac.uk/depts/immunology/~dash/troph/artery.html (accessed 14 August 2005)

Roberston, W. B., Khong, T. Y., Brosens, I., De Wolf, F., Sheppard, B. L., and Bonnar, J. (1986). The placental bed biopsy: review from three European centres. *Am J Obstet Gynecol* **155**, 401–412.

Roberts, J. M., and Redman, C. W. (1993). Pre-eclampsia: more than pregnancy-induced hypertension. *Lancet* **341**, 1447-1451.

Robertson, J. D., Orrenius, S., and Zhivotovsky, B. (2000). Review: nuclear events in apoptosis. *Struct Biol* **129**, 346-358.

Robillard, P. Y., Hulsey, T. C., Périanin, J., Janky, E., Miri, E. H., and Papiernik, E. (1994). Association of pregnancy-induced hypertension with duration of sexual cohabitation before conception. *Lancet* **344**, 973–975.

Royburt, M., Seidman, D. S., Serr, D. M., and Mashiach, S. (1991). Neurologic involvement in hypertensive disease of pregnancy. *Obstet Gynecol Surv* **46**, 656-664.

Saftlas, A. F., Levine, R. J., Klebanoff, M. A., Martz, K. L., Ewell, M. G., Morris, C. D., and Sibai, B. M. (2003). Abortion, Changed Paternity, and Risk of Preeclampsia in Nulliparous Women. *Am. J. Epidemiol* **157**, 1108-1114.

Sahin, G. (2003). Incidence, morbidity and mortality of pre-eclampsia and eclampsia. *12th Postgraduate Course in Reproductive Medicine and Biology,* Geneva, Switzerland.

Salvesen, G. S., and Dixit, V. M. (1997). Caspases: intracellular signaling by proteolysis. *Cell* **91**, 443-446.

Schaafsma, H. E., and Ramaekers, F. C. S. (1994). Cytokeratin subtyping in normal and neoplastic epithelium: basic principles and diagnostic applications. *Pathol Annu Rev Biochem* **29**, 21–62.

Schluter, C., Duchrow, M., Wohlenberg, C., Becker, M. H., Key, G., Flad, H. D., and Gerdes, J. (1993). The cell proliferation-associated antigen of antibody Ki-67: a very large, ubiquitous nuclear protein with numerous repeated elements, representing a new kind of cell cycle-maintaining proteins. . *J. Cell Biol* **123**, 513-522.

Scholzen, T., Dimmler, C., Wohlenberg, C., Flad, H.-D., and Gerdes, J. (1997). Novel Splice Forms of the Ki-67 mRNA. *Eur.J Cell Biol* **72**, 40.

Scholzen, T., Endl, E., Wohlenberg, C., van der Sar, S., Cowell, I. G., Gerdes, J., and Singh, P. B. (2002). The Ki-67 protein interacts with members of the heterochromatin protein 1 (HP1) family: a potential role in the regulation of higher-order chromatin structure. *J. Pathol.* **196,**, 135-144.

Scholzen, T., and Gerdes, J. (2000). The Ki-67 protein: from the known and the unknown. *Cell Physiol.* **182**, 311-322.

Scott, A., and Owen, P. (1996). Recent advances in the aetiology and management of pre-eclampsia. *Br J Hosp Med* **8**, 476-478.

Shi, Y. (2002). Mechanisms of caspase activation and inhibition during apoptosis. *Mol Cell* **3**, 459-470.

Sibai, B. M. (2003). Diagnosis and Management of Gestational Hypertension and Preeclampsia. *Obstetrics & Gynecology* **102**, 181-192.

Slattery, M. A., Khong, T. Y., Dawkins, R. R., Pridmore, B. R., and Hague, W. M. (1993). Eclampsia in Association With Partial Molar Pregnancy and Congenital Abnormalities. *American Journal of Obstetrics & Gynecology* **169**, 1625-1627.

Smith, C. A., Farrah, T., and Goodwin, R. G. (1994). The TNF Receptor Superfamily of Cellular and Viral Proteins: Activation, Costimulation, and Death. *Cell* **76**, 959 - 962.

Smith, M. A. (1993). Preeclampsia. *Prim Care* **20**, 655-664.

Smith, S., Francis, R., Guilbert, L., and Baker, P. N. (2002). Growth factor rescue of cytokine mediated trophoblast apoptosis. *Placenta* **23**, 322–330.

Smith, S. C., Symonds, E. M., and Baker, P. N. (1997). Placental apoptosis in normal human pregnancy. *Am J Obstet Gynecol* **177**, 57–65.

Sohda, S., Arinami, T., Hamada, H., Yamada, N., Hamaguchi, H., and Kubo, T. (1997). Methylenetetrahydrofolate reductase polymorphism and pre-eclampsia. *Journal of Medical Genetics* **34**, 525-526.

Strasser, A., O'Connor, L., and Dixit, V. M. (2000). Apoptosis Signaling. *Annu Rev Biochem* **69**, 217-245.

Suliman, A., Lam, A., Datta, R., and Srivastava, R. K. (2001). Intracellular mechanism of TRAIL: apoptosis through mitochondrial-dependent and -independent pathways. *Oncogene* **20**, 2122–2133.

Suresh, U. R., Hale, R. J., Fox, H., and Buckley, C. H. (1993). Use of proliferating cell nuclear antigen immunoreactivity for distinguishing hydropic abortions from partial hydatidiform moles. *Y Clin Pathol* **46**, 48-50.

Susin, S. A., Lorenzo, H. K., Zamzami, N., Marzo, I., Snow, B. E., Brothers, G. M., Mangion, J., Jacotot, E., Costantini, P., Loeffler, M., Larochette, N., Goodlett, D. R., Aebersold, R., Siderovski, D. P., Penninger, J. M., and Kroemer, G. (1999). Molecular characterization of mitochondrial apoptosis-inducing factor. *Nature* **397**, 441-446.

Tsurimoto, T. (1999). PCNA binding proteins. *Frontiers of Biosciences* **4**, 849–858.

Vairapandi, M., Azam, N., Balliet, A. G., Hoffman, B., and Liebermann, D. A. (2000). Characterization of MyD118,Gadd45, and proliferating cell nuclear antigen (PCNA) interacting domains. PCNA impedes MyD118 and Gadd45-mediated negative growth control. *Journal of Biological Chemistry* **275**, 16 810–816 819.

Verheijen, N. R., Kuijpers, H. J., and R., v. D. (1989b). Ki-67 detects a nuclear matrix-associated proliferation-related antigen.II. Localization in mitotic cells and association with chromosomes. *Cell Science* **92**, 531-540.

Verheijen, R. H., H., K. J., Schlingemann R. O., Boehmer, A. L. M., van Driel R. , B. G. J., and S., R. F. C. (1989a). Ki-67 detects a nuclear matrix-associated proliferation-related antigen I. Intracellular localization during interphase. *Cell Science* **92**, 123-130.

Villar, J., and Belizán, J. M. (2000). Same nutrient, different hypotheses: disparities in trials of calcium supplementation during pregnancy. *American Journal of Clinical Nutrition* **71**, 1375S-1379.

Villar, J., Merialdi, M., Gulmezoglu, A. M., Abalos, E., Carroli, G., and Kulier, R. (2003). Nutritional interventions during pregnancy for the prevention or treatment of maternal morbidity and preterm delivery: an overview of randomized controlled trials. *Nutrition* **133**, 1S–20S.

Walker, J. (2000). Pre-eclampsia. *Lancet* **356**, 1260-1265.

Ward, K., Hata, A., Jeunemaitre, X., Helin, C., Nelson, L., Namikawa, C., Farrington, P. F., Ogasawara, M., Suzumori, K., Tomoda6S., Berrebi, S., Sasaki, M., Corvol, P., Lifton, R. P., and Lalouel, J. M. (1993). A molecular variant of angiotensinogen associated with preeclampsia. *Nature Genetics* **4**, 59 - 61.

Waterhouse, N. J., Ricci, J. E., and Green, D. R. (2002). And all of a sudden it's over: mitochondrial outer-membrane permeabilization in apoptosis. *Biochimie* **84**, 113–121.

Wolf, M., Sandler, L., Muñoz, K., Hsu, K., L., E. J., and Thadhani, R. (2002). First Trimester Insulin Resistance and Subsequent Preeclampsia: A Prospective Study. *Clinical Endocrinology & Metabolism* **87**, 1563-1568.

Yoder, B. L., and Burgers, P. M. J. (1991). Saccharomyces cerevisiae replication factor C. I. Purification and characterization of its ATPase activity. *J. Biol. Chem* **266**, 22689-22697.

Young, P. M., Rose, M. S., Sutton, J. R., Green, H. J., Cymerman, A., and Houston, C. S. (1989). Operation Everest II: plasma lipid and hormonal responses during a simulated ascent of Mt. Everest. *J. Appl. Physiol* **66**, 1430–1435.

Zhou, Y., Damsky, C. H., and Fisher, S. J. (1997). Preeclampsia is associated with failure of human cytotrophoblasts to mimic a vascular adhesion phenotype. One cause of defective endovascular invasion in this syndrome? *Clin. Invest.* **99**, 2152–2164.

Zuspan, F. P. (1988). The role of the uteroplacental bed in pregnancy-related hypertension. *Am J Hypertens* **1**, 186S-188S.

APPENDIX

1.0 SODIUM CITRATE BUFFER (0.1M; pH 6.0)

2.94 g Tri-sodium citrate (dihydrate)

1000 ml Distilled water

Mix to dissolve. Adjust pH to 6.0.

2.0 PHOSPHATE BUFFERED SALINE (PBS)

10X PBS (0.1M PBS, pH 7.2):

10.9 g Na2HPO4

3.2 g NaH2PO4

90 g NaCl

1000 ml Distilled water

Mix to dissolve.

Dilute 1:10 with distilled water before use and adjust pH if necessary.

3.0 TRIS BUFFERED SALINE (10X)

82g NaCl

6.0g Tris Base

1.0 l dH20

pH = 7.2-7.4

3.1 Tris Buffered Saline-TT

1X TBS

0.1% Triton

0.1% Tween 20

4.0 VON GIESON ELASTIC SOLUTION

900 ml saturated Picric acid solution

100 ml 1% acid fuchsin dissolved in 1*l* water.

Boil for 5 min and filter when cool.

5.0 MAYER'S HAEMOTOXYLIN

1g Haemotoxylin

0.2g Sodium Iodate

50g Potassium alum

1g Citric Acid

50g Choral hydrate

1000cm^3 Distilled water

Dissolve Haemotoxylin, alum and sodium iodate overnight. Add chloral and citric acid and bring to a boil for 5 minutes. Ready to use once cooled.

6.0 DAB

Dissolve DAB plus substrate tablets in 5 ml distilled water. Incubate tissue for 3-10 min. at room temperature whilst assessing chromagen reaction microscopically. Stop reaction by running under tap water.